Title	Separation and Purification of Rare Metals by Combination of Solvent Extraction and Chemical Reactions
Author(s)	平井, 隆之
Citation	大阪大学, 1992, 博士論文
Version Type	VoR
URL	https://doi.org/10.11501/3063617
rights	
Note	

Separation and Purification of Rare Metals by Combination of Solvent Extraction and Chemical Reactions

1992

Takayuki Hirai

Department of Chemical Engineering
Faculty of Engineering Science
Osaka University

Separation and Purification of Rare Metals by Combination of Solvent Extraction and Chemical Reactions

（溶媒抽出法と化学反応を組み合わせたレアメタルの分離・精製プロセス）

1992

Takayuki Hirai
平井隆之

Department of Chemical Engineering
Faculty of Engineering Science
Osaka University

Preface

The work of this dissertation was done under the guidance of Professor Isao Komasawa and many other members of his Laboratory at Department of Chemical Engineering, Faculty of Engineering Science, Osaka University from 1988 to 1992.

The objective of this dissertation is the development of novel process for separation and purification of rare metals by combination of solvent extraction and functional chemical reactions. The author hopes that the findings obtained in this work would give some suggestions for construction of effective separation process for rare metals.

Takayuki Hirai

Takayuki Hirai

Department of Chemical Engineering
Faculty of Engineering Science
Osaka University
Toyonaka, Osaka 560, Japan

Contents

General Introduction

Recently, much attention has been paid to rare metals as new industrial materials, especially the highly purified ones. Solvent extraction method is known to be one of the most effective methods for their separation and purification. This is a separation technique for separating the components of a solution by distribution between two liquid phases. It is in contrast to the other separation techniques, e.g., distillation, where heat is used to provide a vapor phase, or melt crystallization, which is a batch process. The solvent extraction technique was used initially for both the separation of uranium from its ore and then the treatment of spent reactor fuel to separate plutonium from uranium and its fission products in the 1940s. Now, the technique is widely used as industrial process for the separation of rare metals such as nickel/cobalt, tungsten/molybdenum, chromium/vanadium and rare-earth elements.30,41)

The general solvent extraction process consists of three stages; extraction, scrubbing and stripping. The metal-bearing aqueous feed solution and solvent are fed in a contactor in which the two phases are mixed. In the extraction stage, the metal of interest is transferred from the aqueous to the organic phase. Normally a metal ion exists in aqueous solution as a hydrated ion, with little or no tendency to transfer to an organic phase. To convert a metal ion to an organic-soluble species, its charge requires neutralization and some or all its hydration water has to be replaced by some other molecule or ion. These are done by compound formation by complexing the metal ion with a cation exchange extractant, by ion-pair formation with anion exchange extractant, or by solvation by solvating agent. After settling, the loaded solvent is separated and may go to another contactor where it is scrubbed with a suitable aqueous solution to remove small amounts of metals or impurities co-extracted in the extraction stage. After scrubbing, the loaded solvent passes to a third stage in which the metal is stripped from the organic phase by some suitable aqueous solution.40) Usually, separation is effected at the extraction stage on the basis of difference in distribution ratio between the metals in the feed solution.

There are many commercially available extractants used for the separation of rare metals.[30,40)] As the cation exchange extractants, tertiary carboxylic acid (Versatic Acid 10 or Versatic Acid 911), bis(2–ethylhexyl)phosphoric acid (D2EHPA), 2–ethylhexylphosphonic acid mono–2–ethylhexyl ester (EHPNA) and LIX64N, which is a mixture of 5,8–diethyl–7–hydroxy–6–dodecane oxime (LIX63) and 2–hydroxy–5–nonylbenzophenone oxime (LIX65N), are mainly employed. As the anion exchange extractants, tri–*n*–octylamine (TOA) and tri–*n*–octylmethylammonium chloride (TOMAC) are mainly used. The solvating extractant such as tri–*n*–butylphosphate (TBP) is also employed, especially in the Purex process for the recovery of plutonium and uranium from waste nuclear fuels.[7)]

Some metals such as rare–earth elements are, however, hardly separated into the individual ones by traditional extraction systems. In the rare–earth series, the chemical properties of adjacent members are very similar, making it very difficult to separate and purify the individual elements. Commercially available extractants for the elements are TBP, D2EHPA and EHPNA. The behavior of extraction of the series with these extractants is known to be divided into the four tetrads, such as La–Nd, Sm–Gd, Tb–Ho and Er–Lu. An inherent limitation is thus involved in the separation of the elements in each group into the individual ones. Separation factors are typically 1.5 ~ 2.5 for neighboring members of the series. The preparation of high–purity products requires 30 ~ 60 stages of separation.[30)] In order to improve the separation of rare metals by solvent extraction method, there may be two effective approaches. One is the modification of the aqueous–phase species by redox reaction or complexing reaction. The other is the modification of the extracted species by adding the second extractant, expecting a synergistic effect on extraction and separation.

The present study has been conducted to develop the novel processes for separation and purification of rare metals by combination of the solvent extraction and the chemical reactions to cope with and break through the limitation involved in the conventional technique as separation process. As the chemical reactions, (1) reduction of the target metal ions by adding reducing agent, by electrochemical or photochemical reduction method, (2) modification of the metal ions by adding water-soluble complexing agent, and (3) modification of the organic phase species by adding second extractant have been used.

This thesis composed of following 4 chapters.

In chapter 1, as the basic study, the extraction mechanism of rare metals without chemical reactions in the extraction systems used in the following chapters will be described. The extraction mechanisms of hydrochloric acid, cobalt and vanadium(V) by TOMAC diluted with benzene or chloroform, and that of the rare-earth elements by tri-*n*-octylmethylammonium nitrate (TOMAN) will be described, taking into account the association of the extractant in the organic phase. The extraction schemes and extraction equilibrium constants will be presented, which express the extraction of the acid and metals over a wide range of loading of the extractant.

In chapter 2, separation and purification of rare metals by solvent extraction and redox reactions will be described. As case studies, the separation of vanadium and molybdenum by chemical-reductive stripping using L-ascorbic acid as a reducing agent and electro-reductive stripping using a platinum electrode will be shown, together with the separation of europium from samarium and gadolinium by electroreduction using a titanium plate electrode and by photoreduction using a low-pressure mercury lamp. As the extractant, TOMAC and alkyl phosphoric acid such as D2EHPA or di-5-methyl-2-(1-methylneohexyl) neodecanoyl phosphoric acid (DP-18) have been used.

In chapter 3, the separation and purification of rare-earth elements by synergistic extraction will be described. The extraction of the elements in β-diketone (α-acetyl-*m*-dodecylacetophenone : LIX54)-TOMAN system and DP-18-TOMAN system will be described, together with that in the DP-18 alone system. The extraction schemes of the elements in the systems will be presented.

In chapter 4, the effect of addition of water–soluble complexing agent such as ethylenediaminetetraacetic acid (EDTA) on the separation of the rare–earth elements will be described. The system containing TOMAN as an extractant and ammonium nitrate as a salting–out agent has been mainly used, of which extractability of the elements decreases with the atomic number of the elements. The extraction equilibrium in the presence of the complexing agent will be presented. In order to examine the effect of complexing agent in mixer–settler batteries for extraction and scrubbing, the simulation of Nd/Pr separation by continuous countercurrent cascade has been carried out.

The results obtained in this work will be summarized in General Conclusions and the future work as an extension of the present thesis will be described.

Chapter 1　Extraction Mechanism of Rare Metals in Various Systems

1.1 Introduction

In this chapter, the extraction mechanism of rare metals in various extraction systems used in the following chapters has been investigated. The extractants used in this study are long–chain alkyl quaternary ammonium salt such as tri–*n*–octylmethylammonium chloride (TOMAC) and tri–*n*–octylmethylammonium nitrate (TOMAN), alkyl phosphoric acid extractant such as bis(2–ethylhexyl)phosphoric acid (D2EHPA) and di–5–methyl–2–(1–methylneohexyl) neodecanoyl phosphoric acid (DP–18), and β–diketone such as α–acetyl–*m*–dodecylacetophenone (LIX54). The extraction of vanadium and molybdenum by TOMAC from neutral solutions will be described in chapter 2. The extraction of rare–earth elements by DP–18 will be shown in chapter 3. The extraction of rare–earth elements by D2EHPA has already been studied widely.41) The extraction of rare–earth elements by TOMAN or by LIX54–TOMAN has already been reported,27,28) and will be summarized in section 1.3.3 and section 3.3.1, respectively.

The extraction of various metals with long–chain alkyl quaternary ammonium salts from halide media has been reported in a number of publications.18,40,48) However, knowledge of the extraction equilibrium formulation, or at least the composition of the extract entities, is rather fragmentary. The mechanism of cobalt extraction by TOMAC ($R_3R'NCl$, R) from hydrochloric acid was already studied.24,25) Water and acid were extracted by the extractant to a differing extent depending on the solvating nature of the diluents employed,23) and the water and acid actually were liberated from the salt hydration sphere of the extractant with the progress of loading with cobalt. Based on the behavior of water and acid, an extraction scheme of cobalt was presented, in which the extraction of cobalt was assumed to occur via reaction with the acid–complex of extractant, i.e., via replacement of water and acid in the salt hydration sphere by the cobalt chloride. This scheme was successfully applied to the cobalt extraction in benzene as a diluent to weakly solvate the extractant. This was, however, not applicable to the extraction in solvating-effect diluents such as chloroform and 2-ethylhexylalcohol, and the extraction was assumed to occur via reaction with all the extractant uncomplexed with cobalt. A problem concerning the active species of the extractant during the process of cobalt extraction might, therefore, have been implicitly involved.

In the first part of this chapter, as the basic study of the extraction of rare metals without chemical reactions, a further analysis of cobalt extraction has been carried out to obtain a reasonably complete picture of the extraction mechanism of the high-molecular weight quaternary ammonium salt in the presence of acid or salt as salting-out agent. Association of the extractant has been taken into account. The association state of TOMAC was studied by vapor-phase osmometry by Daud and Cattrall10) and Miyake *et al.*,34) and was found to be expressed by a simple association model of monomer and tetramer in benzene and monomer and dimer in chloroform. The cobalt extraction is assumed to occur via reaction with monomer of the extractant in competition with the formation of acid-complex in both diluent systems. The extraction of vanadium(V) by the same extractant have been also studied to corroborate with findings on the chemistry of cobalt extraction. Sato *et al.* reported the extraction of tetravalent vanadium (VO^{2+}) from hydrochloric acid by Aliquat 336.47) However, the extraction behavior and mechanism of pentavalent vanadium from hydrochloric acid has not been clarified. This is probably due to partial reduction of vanadium(V) to vanadium(IV) by HCl,2,51) which makes an interpretation of the extraction of vanadium(V) difficult. Thus, the partial reduction of vanadium(V) to vanadium(IV) in HCl solution has been taken into consideration in this study.

1.2 Experimental

Tri-*n*-octylmethylammonium chloride (TOMAC), marketed as KEX-L-84 by Koei Kagaku Kogyo Ltd., Osaka, was purified in accordance with the procedure developed for the purification of Aliquat 336(46) and was diluted with benzene or chloroform. Standardization of the extractant in diluent was carried out by a Volhardt titration method, assuming one chloride ion per extractant molecule. Stock solutions of cobalt and vanadium were prepared by dissolving cobalt chloride ($CoCl_2$) or sodium metavanadate ($NaVO_3$) in distilled water. Stock solutions of hydrochloric acid were also prepared, and working solutions were prepared volumetrically from these stocks. Equal volumes of the organic and aqueous solutions were shaken for 3 hours in a thermostat bath at 25°C. The two phases were separated and a weighed organic sample was stripped with 0.1 mol/*l* HCl solution. The chloride and water concentration in the organic phase was determined by a Volhardt method and Karl-Fisher titration, respectively. The hydrogen ion concentration in the organic phase was determined in accordance with Vieux *et al.*(54) The concentration of the metals in the aqueous solutions were determined using a Jarrell-Ash 702 atomic absorption spectrophotometer.

1.3 Results and Discussion

1.3.1 Extraction of Cobalt from Hydrochloric Acid by Tri-*n*-octylmethylammonium Chloride

1.3.1.1 Association of TOMAC in benzene and chloroform

The association of the present quaternary ammonium salt in benzene has been found by Miyake *et al.*(34) to be expressed by the following simple model.

$$4\overline{\mathrm{R}} = \overline{\mathrm{R}_4} \qquad K_T = [\overline{\mathrm{R}_4}] / [\overline{\mathrm{R}}]^4 \tag{1.1}$$
$$C_N = [\overline{\mathrm{R}}] + 4[\overline{\mathrm{R}_4}] \tag{1.2}$$

where R, R_4 and C_N denote, respectively, the monomer, tetramer and total salt molecules. The tetramerization constant, K_T, has been determined as $K_T = 10^8$ $(\mathrm{mol}/l)^{-3}$. In chloroform the association has also been found by Daud and Cattrall[10)] to be expressed by a dimerization model with $K_D = 3.9\ (\mathrm{mol}/l)^{-1}$, as follows.

$$2\overline{\mathrm{R}} = \overline{\mathrm{R}_2} \qquad K_D = [\overline{\mathrm{R}_2}] / [\overline{\mathrm{R}}]^2 \tag{1.3}$$
$$C_N = [\overline{\mathrm{R}}] + 2[\overline{\mathrm{R}_2}] \tag{1.4}$$

1.3.1.2 Extraction of water and hydrochloric acid by TOMAC

When equilibrated with pure water, the molecular ratios of water to TOMAC in the organic phase are about 5 for benzene and 1.2 for chloroform for the whole range of TOMAC concentration, as shown in Fig. 2 in ref. 23. The monomeric species is, therefore, considered to be associated with water and to form a salt hydration sphere as well as tetrameric or dimeric species.

$$4\overline{\mathrm{R\cdot 5H_2O}} = \overline{(\mathrm{R\cdot 5H_2O})_4}$$
$$K_T = [\overline{(\mathrm{R\cdot 5H_2O})_4}] / [\overline{\mathrm{R\cdot 5H_2O}}]^4 = 10^8\ (\mathrm{mol}/l)^{-3} \tag{1.1'}$$

$$2\overline{\mathrm{R\cdot H_2O}} = \overline{(\mathrm{R\cdot H_2O})_2}$$
$$K_D = [\overline{(\mathrm{R\cdot H_2O})_2}] / [\overline{\mathrm{R\cdot H_2O}}]^2 = 3.9\ (\mathrm{mol}/l)^{-1} \tag{1.3'}$$

Typical examples of the amount of hydrochloric acid extracted by TOMAC are shown in **Fig. 1.1**. Only the monomeric species of TOMAC is assumed to take part in the acid extraction. The extract entities of the acid complex are assumed to be identical to those already obtained.[23)] In benzene diluent, the species have been obtained as $\overline{\mathrm{R_2\cdot HCl\cdot 9H_2O}}$, $\overline{\mathrm{R\cdot HCl\cdot 4H_2O}}$ and $\overline{\mathrm{R\cdot (HCl)_2\cdot 3H_2O}}$, and thus the extraction equilibrium formulations are made as follows.

$$2\overline{R\cdot 5H_2O} + H^+ + Cl^- = \overline{R_2\cdot HCl\cdot 9H_2O} + H_2O$$
$$K_{A,1/2} = [\overline{R_2\cdot HCl\cdot 9H_2O}]a_W / [\overline{R\cdot 5H_2O}]^2 a_H{}^2 \qquad (1.5)$$

$$\overline{R_2\cdot HCl\cdot 9H_2O} + H^+ + Cl^- = 2\overline{R\cdot HCl\cdot 4H_2O} + H_2O$$
$$K_{A,1} = [\overline{R\cdot HCl\cdot 4H_2O}]^2 a_W / [\overline{R_2\cdot HCl\cdot 9H_2O}]a_H{}^2 \qquad (1.6)$$

$$\overline{R\cdot HCl\cdot 4H_2O} + H^+ + Cl^- = \overline{R\cdot (HCl)_2\cdot 3H_2O} + H_2O$$
$$K_{A,2} = [\overline{R\cdot (HCl)_2\cdot 3H_2O}]a_W / [\overline{R\cdot HCl\cdot 4H_2O}]a_H{}^2 \qquad (1.7)$$

The mean ionic activity of hydrochloric acid, a_H, and water activity, a_W, were obtained from acid concentration, using literature data.[31)] The material balance of TOMAC is expressed as follows, where C_N is the feed concentration of TOMAC and $[\overline{R}]$ is the concentration of the free TOMAC monomer.

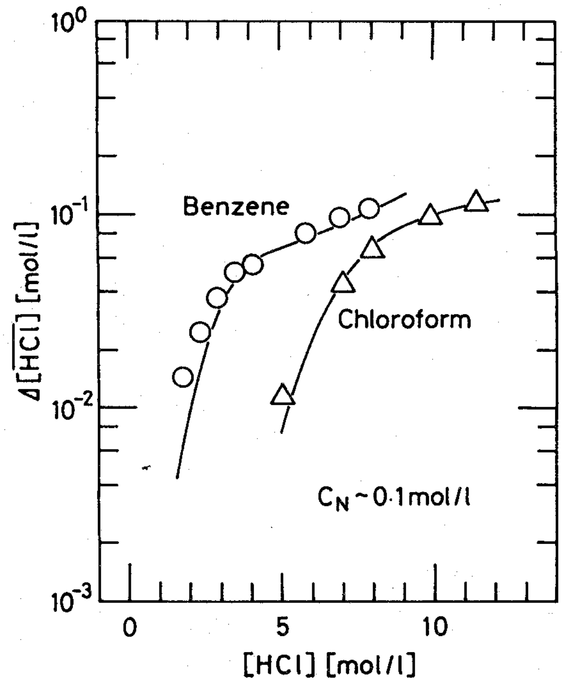

Fig. 1.1. Effect of hydrochloric acid concentration on amount of acid extracted. Comparison of observed data with prediction shown by solid lines.

$$
\begin{aligned}
C_N &= 4[\overline{(\mathrm{R\cdot 5H_2O})_4}] + 2[\overline{\mathrm{R_2\cdot HCl\cdot 9H_2O}}] + [\overline{\mathrm{R\cdot HCl\cdot 4H_2O}}] \\
&\quad + [\overline{\mathrm{R\cdot (HCl)_2\cdot 3H_2O}}] + [\overline{\mathrm{R\cdot 5H_2O}}] \\
&= 4K_T\,[\bar{\mathrm{R}}]^4 + 2\,K_{A,1/2}\,a_H^{\,2}\,[\bar{\mathrm{R}}]^2 / a_W + \{(K_{A,1/2}\,K_{A,1})^{1/2}\,a_H^{\,2} / a_W\} \\
&\quad \times (1 + K_{A,2}\,a_H^{\,2} / a_W)\,[\bar{\mathrm{R}}] + [\bar{\mathrm{R}}] \qquad (1.8)
\end{aligned}
$$

The most likely values of $K_{A,1/2}$, $K_{A,1}$ and $K_{A,2}$ were estimated by minimizing the sum of the squares of residuals based on Eqs. (1.5) ~ (1.7), using respective input concentrations for the acid of 1 ~ 8 mol/*l* and the extractant, 10^{-2} ~ 10^{-1} mol/*l*. The values thus obtained are shown in **Table 1.1**. With these constants by use of Eq. (1.8), the value of $[\bar{\mathrm{R}}]$ can then be calculated for each run, and enabling the value of $\Delta[\overline{\mathrm{HCl}}]$ to be calculated. The predicted values are shown by solid lines in Fig. 1.1 and show good agreement with the experimental data.

For the chloroform diluent system, the following extraction equilibrium formulations are made.

$$
\begin{aligned}
&2\overline{\mathrm{R\cdot H_2O}} + \mathrm{H^+} + \mathrm{Cl^-} = \overline{\mathrm{R_2\cdot HCl\cdot H_2O}} + \mathrm{H_2O} \\
&\quad K_{A,1/2} = [\overline{\mathrm{R_2\cdot HCl\cdot H_2O}}]a_W / [\overline{\mathrm{R\cdot H_2O}}]^2 a_H^{\,2} \qquad (1.9)
\end{aligned}
$$

$$
\begin{aligned}
&\overline{\mathrm{R_2\cdot HCl\cdot H_2O}} + \mathrm{H^+} + \mathrm{Cl^-} = 2\overline{\mathrm{R\cdot HCl}} + \mathrm{H_2O} \\
&\quad K_{A,1} = [\overline{\mathrm{R\cdot HCl}}]^2 a_W / [\overline{\mathrm{R_2\cdot HCl\cdot H_2O}}]a_H^{\,2} \qquad (1.10)
\end{aligned}
$$

$$
\begin{aligned}
&\overline{\mathrm{R\cdot HCl}} + \mathrm{H^+} + \mathrm{Cl^-} = \overline{\mathrm{R\cdot (HCl)_2}} \\
&\quad K_{A,2} = [\overline{\mathrm{R\cdot (HCl)_2}}] / [\overline{\mathrm{R\cdot HCl}}]a_H^{\,2} \qquad (1.11)
\end{aligned}
$$

Table 1.1. Extraction equilibrium constants for hydrochloric acid by TOMAC

	$K_{A,1/2}$	$K_{A,1}$	$K_{A,2}$
Benzene	$1.07 \times 10^{2}[(\mathrm{mol}/l)^{-2}]$	$3.55 \times 10^{-5}[-]$	$2.85 \times 10^{-6}[(\mathrm{mol}/l)^{-1}]$
Chloroform	$2.47 \times 10^{-3}[(\mathrm{mol}/l)^{-2}]$	$1.76 \times 10^{-5}[-]$	$1.07 \times 10^{-6}[(\mathrm{mol}/l)^{-2}]$

The most likely K_A values are shown in Table 1.1. The predicted $\Delta[\overline{HCl}]$ values are shown in Fig. 1.1 and show good agreement with the observed data.

1.3.1.3 Extraction of cobalt by TOMAC in benzene and chloroform diluents

In the present analysis, only the monomeric species of the extractant is assumed to take part in the cobalt extraction, in competition with the acid extraction in both diluent systems. The extract entities are assumed to be identical to those already obtained.[24,25] In benzene diluent formation of three extracts, $\overline{R \cdot CoCl_2}$, $\overline{R_2 \cdot CoCl_2}$ and $\overline{(R_2 \cdot CoCl_2)_2}$ have been assumed, since plot of D $(=[\overline{Co}]/[Co^{2+}])$ against $[\overline{R \cdot 5H_2O}]$ gave straight lines of slope 1 ~ 2, as shown in **Fig. 1.2.** The extraction equilibrium may, therefore, be formulated as follows.

$$\overline{R \cdot 5H_2O} + Co^{2+} + 2Cl^- = \overline{R \cdot CoCl_2} + 5H_2O$$

$$K_{ex,1} = [\overline{R \cdot CoCl_2}]a_w^{\,5} / [\overline{R \cdot 5H_2O}][Co^{2+}]a_H^{\,2} \tag{1.12}$$

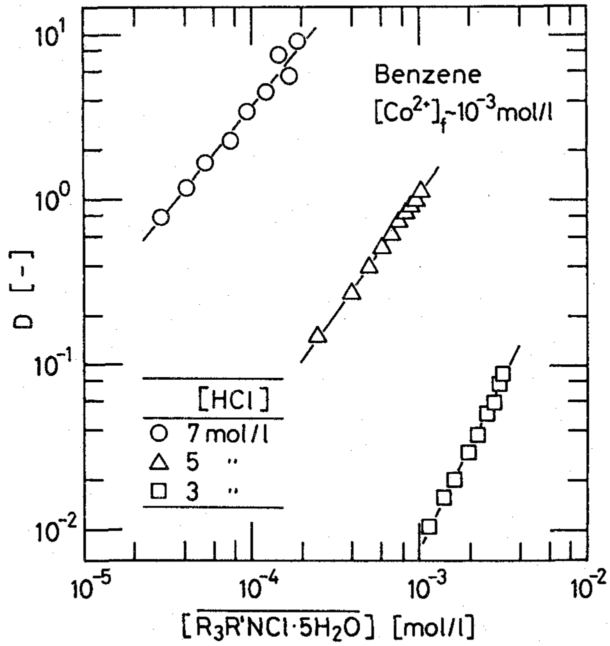

Fig. 1.2. Relationship between distribution ratio of cobalt and concentration of free TOMAC monomer in benzene diluent system.

$$\begin{aligned}&2\overline{\mathrm{R\cdot 5H_2O}} + \mathrm{Co}^{2+} + 2\mathrm{Cl}^- = \overline{\mathrm{R_2\cdot CoCl_2}} + 10\mathrm{H_2O}\\&\quad K_{ex,2} = [\overline{\mathrm{R_2\cdot CoCl_2}}]a_W^{10} / [\overline{\mathrm{R\cdot 5H_2O}}]^2[\mathrm{Co}^{2+}]a_H^2\end{aligned}\tag{1.13}$$

$$\begin{aligned}&2\overline{\mathrm{R_2\cdot CoCl_2}} = \overline{\mathrm{(R_2\cdot CoCl_2)_2}}\\&\quad K_2 = [\overline{\mathrm{(R_2\cdot CoCl_2)_2}}] / [\overline{\mathrm{R_2\cdot CoCl_2}}]^2\end{aligned}\tag{1.14}$$

The material balance for the extractant is expressed as follows.

$$\begin{aligned}C_N &= 4[\overline{\mathrm{(R\cdot 5H_2O)_4}}] + 2[\overline{\mathrm{R_2\cdot HCl\cdot 9H_2O}}] + [\overline{\mathrm{R\cdot HCl\cdot 4H_2O}}] + [\overline{\mathrm{R\cdot (HCl)_2\cdot 3H_2O}}]\\&\quad + [\overline{\mathrm{R\cdot 5H_2O}}] + [\overline{\mathrm{R\cdot CoCl_2}}] + 2[\overline{\mathrm{R_2\cdot CoCl_2}}] + 4[\overline{\mathrm{(R_2\cdot CoCl_2)_2}}]\\&= 4K_T\,[\overline{\mathrm{R}}]^4 + 2\,K_{A,1/2}\,a_H^{\ 2}\,[\overline{\mathrm{R}}]^2 / a_W + \{(K_{A,1/2}\,K_{A,1})^{1/2}\,a_H^{\ 2} / a_W\}\\&\quad \times (1 + K_{A,2}\,a_H^{\ 2} / a_W)\,[\overline{\mathrm{R}}] + [\overline{\mathrm{R}}] + K_{ex,1}\,[\mathrm{Co}^{2+}]\,a_H^{\ 2}\,[\overline{\mathrm{R}}] / a_W^{\ 5}\\&\quad + 2K_{ex,2}\,[\mathrm{Co}^{2+}]\,a_H^{\ 2}\,[\overline{\mathrm{R}}]^2 / a_W^{\ 10} + 4K_2\,K_{ex,2}^{\ \ 2}\,[\mathrm{Co}^{2+}]^2\,a_H^{\ 4}\,[\overline{\mathrm{R}}]^4 / a_W^{\ 20}\end{aligned}\tag{1.15}$$

The material balance for cobalt extracted is expressed as follows.

$$\begin{aligned}[\overline{\mathrm{Co}}] &= [\overline{\mathrm{R\cdot CoCl_2}}] + [\overline{\mathrm{R_2\cdot CoCl_2}}] + 2[\overline{\mathrm{(R_2\cdot CoCl_2)_2}}]\\&= K_{ex,1}\,[\mathrm{Co}^{2+}][\overline{\mathrm{R}}]\,a_H^{\ 2} / a_W^{\ 5} + K_{ex,2}\,[\mathrm{Co}^{2+}][\overline{\mathrm{R}}]^2\ a_H^{\ 2} / a_W^{\ 10}\\&\quad + 2\,K_2\,K_{ex,2}^{\ \ 2}\,[\mathrm{Co}^{2+}][\overline{\mathrm{R}}]^{4\ 2}\,a_H^{\ 4} / a_W^{\ 20}\end{aligned}\tag{1.16}$$

The most likely values of K_{ex} and K_2 were estimated by the nonlinear least square method, assuming that the a_H and a_W values were not affected by the presence of cobalt ion. The values thus obtained are $K_{ex,1} = 4.69 \times 10^{-2}\ (\mathrm{mol}/l)^2$, $K_{ex,2} = 6.19 \times 10^1\ (\mathrm{mol}/l)^6$ and $K_2 = 3.79 \times 10^2\ (\mathrm{mol}/l)^{-1}$. The concentration of the free TOMAC monomer, $[\overline{\mathrm{R}}]$, for each run can now be calculated using an identical procedure employed for the acid extraction. This enables the quantity of cobalt extracted to be calculated using Eq. (1.16). The predicted values thus obtained are shown with solid lines in **Fig. 1.3** and show excellent agreement with the observed data up to maximum loadings.

The variation, with the progress of cobalt loading, of the amounts of water and hydrochloric acid associated in the extractant hydration sphere and cobalt extracts can now be calculated. The predictions are shown with the experimental data in **Fig. 1.4**. The experimental data are seen to fall on respective predictions.

In chloroform diluent a single extract, $\overline{R_2 \cdot CoCl_2}$, has been assumed, since plot of D against $[\overline{R \cdot H_2O}]$ gave a straight line of slope 2, as shown in **Fig. 1.5**. The extraction equilibrium may be formulated as follows.

$$2\overline{R \cdot H_2O} + Co^{2+} + 2Cl^- = \overline{R_2 \cdot CoCl_2} + 2H_2O$$
$$K_{ex} = [\overline{R_2 \cdot CoCl_2}]\, a_W{}^2 / [\overline{R \cdot H_2O}]^2\, a_H{}^2 \qquad (1.17)$$

The most likely value of K_{ex} was estimated to be 4.48 x 10^{-1} $(mol/l)^{-2}$. The prediction of cobalt loading for each run, shown with solid lines in **Fig. 1.6**, is in excellent agreement with the observed data over the whole range of loadings of the extractant. The prediction of the quantities of water and hydrochloric acid in the organic solution is compared with the experimental data in **Fig. 1.7**. Overall agreement between the prediction and observed data is seen. The cobalt extrac–

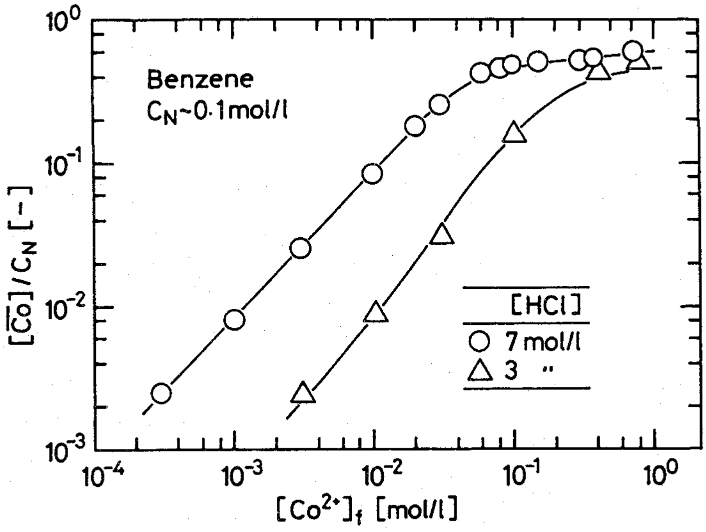

Fig. 1.3. Variation of loading ratio of extractant in benzene with feed concentration of cobalt. Comparison of observed data with prediction shown by solid lines.

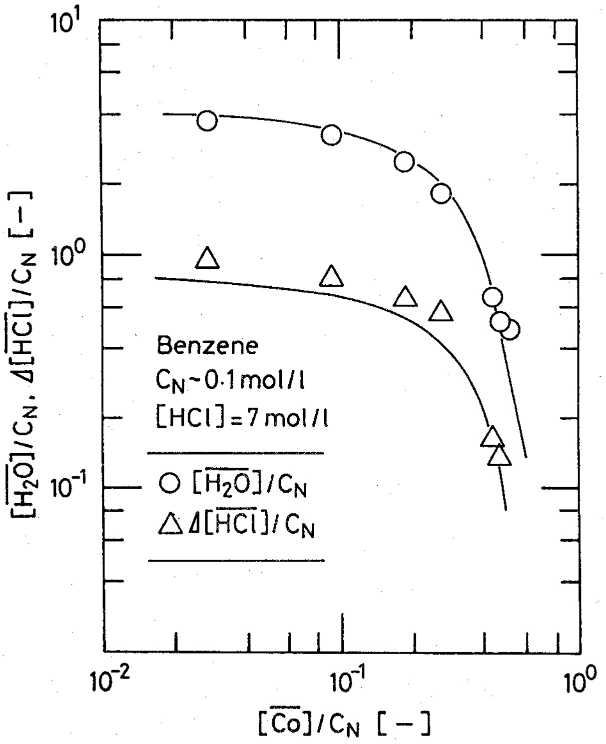

Fig. 1.4. Variation of the amount of water and acid associated with TOMAC in benzene with loading ratio. Comparison of observed data with prediction shown by solid lines.

tion data were actually correlated by the previous scheme,$^{25)}$ in which the role of water and acid liberation was neglected. The present scheme can correlate both cobalt extraction and liberation of water and acid with the progress of cobalt loading for benzene and chloroform diluent systems.

1.3.2 Extraction of Vanadium(V) from Hydrochloric Acid by Tri-*n*-octylmethylammonium Chloride

1.3.2.1 Estimation of amounts of vanadium(V) and vanadium(IV) in hydrochloric acid solutions

In preliminary runs the extraction capability of TOMAC for tetravalent

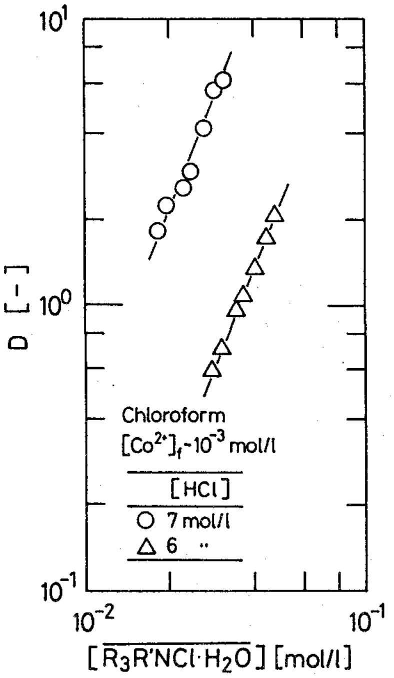

Fig. 1.5. Relationship between distribution ratio of cobalt and concentration of free TOMAC monomer in chloroform diluent system.

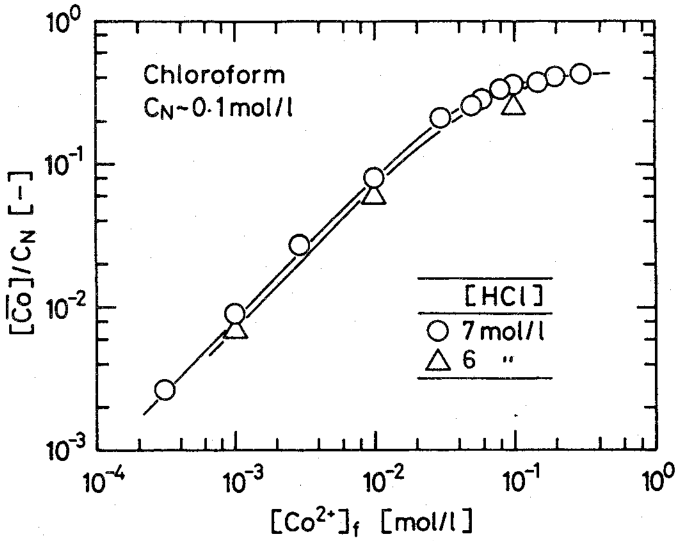

Fig. 1.6. Variation of loading ratio of extractant in chloroform with feed concentration of cobalt. Comparison of observed data with prediction shown by solid lines.

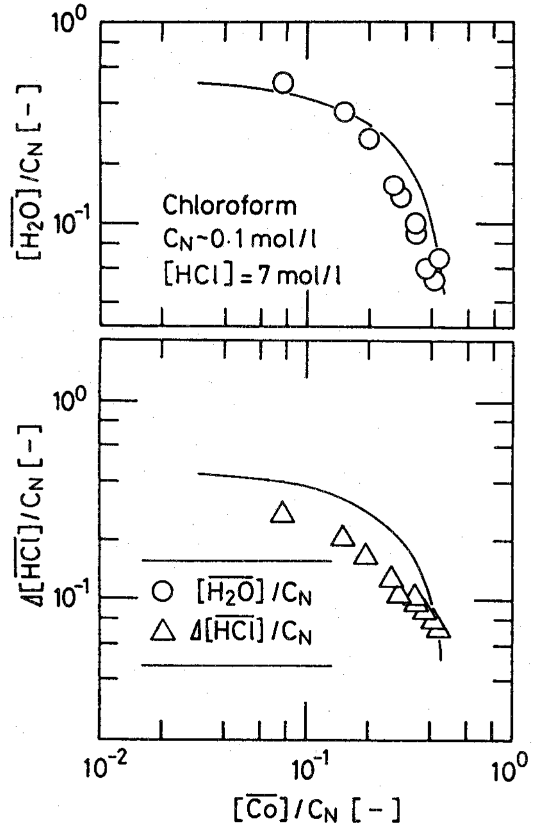

Fig. 1.7. Variation of the amount of water and acid associated with TOMAC in chloroform with loading ratio. Comparison of observed data with prediction shown by solid lines.

vanadium was found to be much lower than that for pentavalent vanadium. Pentavalent vanadium in hydrochloric acid is reported to be partially reduced to tetravalent by Cl^-.[2)] Estimation of the content of pentavalent value in the working solution is therefore needed. Tedesco and de Rumi reported the percentage of reduced vanadium in HCl solutions of various concentrations.[51)] According to their data shown in Table 1 of ref. 51, the extent of vanadium(V) reduction is proportional to the acid concentration, such as 5, 8, 10 and 50% respectively in 2, 3, 6 and 9 mol/*l* HCl solutions. Thus, the concentration of vanadium(V) in the acid solution can be estimated by subtraction of vanadium(IV) concentration from the observed total vanadium concentration of the solution. The structure of pentavalent vanadyl ion changes with solution pH, as reported by Bard *et al.*[2)] In the hydrochloric acid solution used in this study, VO_2^+ is most probable structure, and the concentration of vanadium(V) is expressed as $[VO_2^+]$ in this paper. Extraction of tetravalent vanadium can be ignored, since the distribution ratio of vanadium(IV) is small enough (maximum distribution ratio < 0.11) compared to that of vanadium(V) in the present extractant system. Thus, in the organic phase, vanadium is considered to be pentavalent.

1.3.2.2 Extraction of vanadium(V) by TOMAC in benzene

The monomeric species of TOMAC is considered to take part in the extraction of the acid and vanadium, as in the case of cobalt extraction. The monomer concentration of TOMAC was estimated through a tetramerization model obtained by Miyake *et al.*[34)] and expressed by Eq. (1.1'). For the acid extraction, Eqs. (1.5) ~ (1.7) for benzene and Eqs. (1.9) ~ (1.11) for chloroform are applied.

The variation of distribution ratio, D ($=[\overline{V(V)}]/[VO_2^+]$), with concentration of hydrochloric acid is shown in **Fig. 1.8** for the series of conditions with feed concentration of TOMAC (C_N) = 0.1 and $[VO_2^+]_f = 1.1 \sim 1.3 \times 10^{-3}$ and 1.1×10^{-1} mol/*l*. With increasing acid concentration the ratio D rises, showing a maximum at [HCl] = 4 or 6 mol/*l*. The data obtained with $[VO_2^+]_f \sim 10^{-1}$ mol/*l* might generally be expected to be less than those for $[VO_2^+]_f \sim 10^{-3}$ mol/*l*, since the free (uncomplexed with vanadium) extractant is only slightly reduced by the vanadium extraction in the latter case. The data for $[VO_2^+]_f \sim 10^{-1}$ mol/*l* are, however, seen to be greater than those for $[VO_2^+]_f \sim 10^{-3}$ mol/*l* in the range of acid concentration less than 4 mol/*l*, implying that the formation of vanadium extract containing plural vanadyl ions may be significant in the case of high concentration of feed vanadium.

The slope of $[\overline{V(V)}]$ against $[VO_2^+]$ gives the degree of association of organic vanadium extract. Results are shown in **Fig. 1.9**. Straight lines with slopes of 1.3 and 1.6 are obtained. Thus, the extract is assumed to be monomeric or

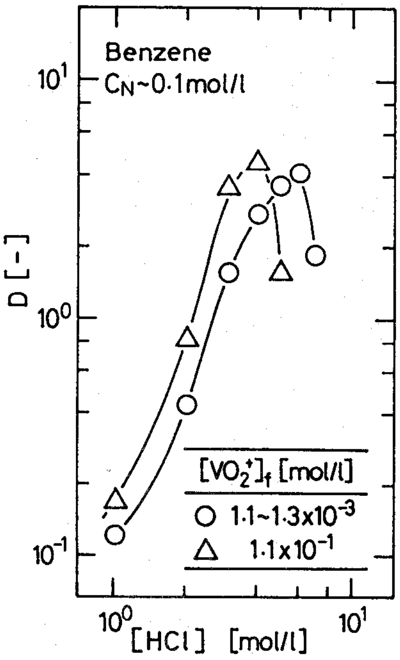

Fig. 1.8. Effect of hydrochloric acid concentration on distribution ratio of vanadium in benzene diluent system.

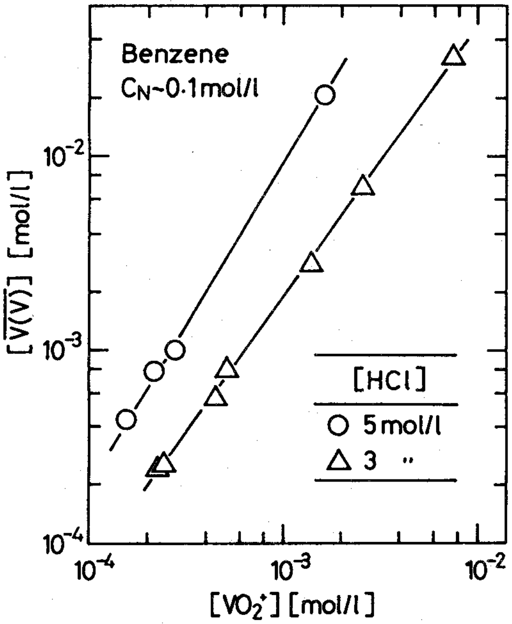

Fig. 1.9. Relationship between organic and aqueous vanadium concentration in benzene diluent system.

dimeric. **Figure 1.10** shows the relationship between D and concentration of free TOMAC monomer (not bound to acid). Slopes of 1 and 1.4 are seen, indicating that one or two molecules of TOMAC monomer are likely to take part in the mechanism of vanadium extraction.

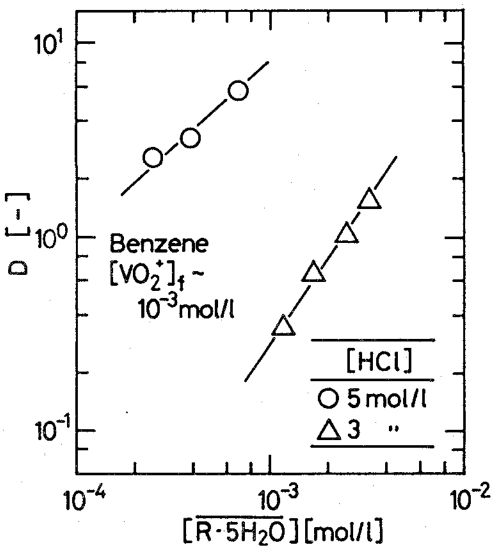

Fig. 1.10. Relationship between distribution ratio of vanadium and concentration of free TOMAC monomer in benzene diluent system.

The loading ratios are plotted against aqueous feed concentration of vanadium in **Fig. 1.11**. The ratio increases with feed vanadium concentration and attains a limiting value of about 1. These results show that the ratio of the extractant to vanadium in the extract entity is 2 : 1 or 1 : 1. Thus, assuming that the water in the salt hydration sphere is replaced by vanadium chloride, the extraction equilibrium formulations are as follows:

$$2\overline{R\cdot 5H_2O} + VO_2^+ + Cl^- = \overline{R_2\cdot VO_2Cl} + 10H_2O$$
$$K_{ex,1} = [\overline{R_2\cdot VO_2Cl}]a_W^{10} / [\overline{R\cdot 5H_2O}]^2[VO_2^+]a_H \qquad (1.18)$$

$$2\overline{R\cdot 5H_2O} + 2VO_2^+ + 2Cl^- = \overline{R_2\cdot (VO_2)_2Cl_2} + 10H_2O$$
$$K_{ex,2} = [\overline{R_2\cdot (VO_2)_2Cl_2}]a_W^{10} / [\overline{R\cdot 5H_2O}]^2[VO_2^+]^2a_H^2 \qquad (1.19)$$

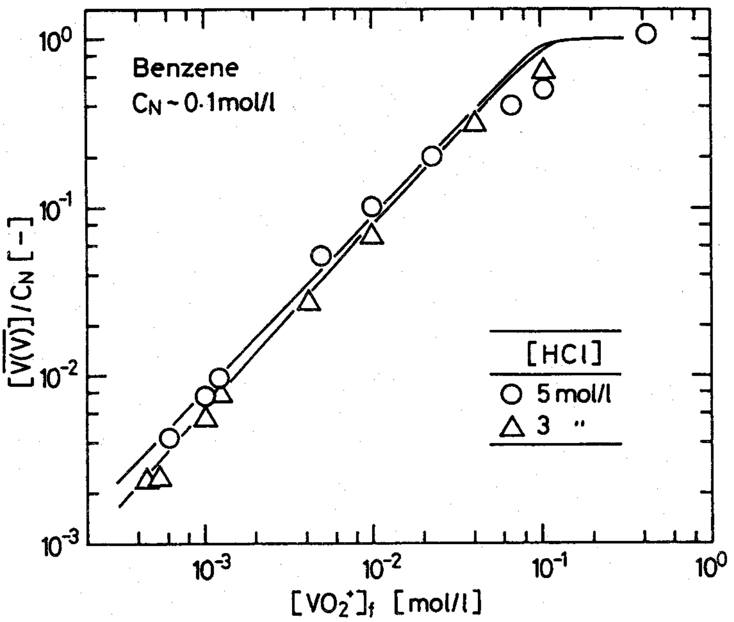

Fig. 1.11. Variation of loading ratio of extractant in benzene with feed concentration of vanadium; comparison of observed data with prediction shown by solid lines.

where R denotes the monomeric species of extractant. The mean ionic activity of hydrochloric acid, a_H, and water activity, a_W, were obtained from acid concentration using literature data.[31)] The material balance for the extractant is expressed by Eq. (1.20), considering the tetramerization of TOMAC and acid complex formation.

$$
\begin{aligned}
C_N &= 4\,[\overline{(\mathrm{R\cdot 5H_2O})_4}] + 2\,[\overline{\mathrm{R_2\cdot HCl\cdot 9H_2O}}] + [\overline{\mathrm{R\cdot HCl\cdot 4H_2O}}] + [\overline{\mathrm{R\cdot (HCl)_2\cdot 3H_2O}}] \\
&\quad + [\overline{\mathrm{R\cdot 5H_2O}}] + 2\,[\overline{\mathrm{R_2\cdot VO_2Cl}}] + 2\,[\overline{\mathrm{R_2\cdot (VO_2)_2Cl_2}}] \\
&= 4\,K_T\,[\overline{\mathrm{R}}]^4 + 2\,K_{A,1/2}\,a_H{}^2\,[\overline{\mathrm{R}}]^2 / a_W + \{(K_{A,1/2}\,K_{A,1})^{1/2}\,a_H{}^2 / a_W\} \\
&\quad \times (1 + K_{A,2}\,a_H{}^2 / a_W)\,[\overline{\mathrm{R}}] + [\overline{\mathrm{R}}] + 2\,K_{ex,1}\,[\mathrm{VO_2}^+][\overline{\mathrm{R}}]^2\,a_H / a_W{}^{10} \\
&\quad + 2\,K_{ex,2}\,[\mathrm{VO_2}^+]^2[\overline{\mathrm{R}}]^2\,a_H{}^2 / a_W{}^{10}
\end{aligned}
\tag{1.20}
$$

C_N and $[\overline{\mathrm{R}}]$ are the feed and free-monomer concentrations of TOMAC, respectively. The material balance for vanadium extracted is expressed as follows.

$$
\begin{aligned}
[\overline{V(V)}] &= [\overline{R_2 \cdot VO_2Cl}] + 2\,[\overline{R_2 \cdot (VO_2)_2Cl_2}] \\
&= K_{ex,1}\,[VO_2^+][\bar{R}]^2\, a_H / a_W^{10} + 2\,K_{ex,2}\,[VO_2^+]^2[\bar{R}]^2\, a_H^2 / a_W^{10} \qquad (1.21)
\end{aligned}
$$

The most likely values, $K_{ex,1}$ and $K_{ex,2}$, were estimated by minimizing the sum of the squares of residuals based on Eqs. (1.20) and (1.21). The values obtained are shown in **Table 1.2**. With these constants and by use of Eq. (1.20) the value of $[\bar{R}]$ can then be calculated for each run, enabling the values of the loading ratio and concentration of water in the organic phase to be calculated. The predicted values are shown by solid lines in Fig. 1.11 and **Fig. 1.12**, and show good agreement with the experimental data.

Table 1.2. Extraction equilibrium constants for vanadium

	$K_{ex,1}$	$K_{ex,2}$
Benzene	4.10×10^3 $[(mol/l)^7]$	1.19×10^6 $[(mol/l)^5]$
Chloroform	4.75×10^{-1} $[(mol/l)^{-1}]$	4.71 $[(mol/l)^{-1}]$

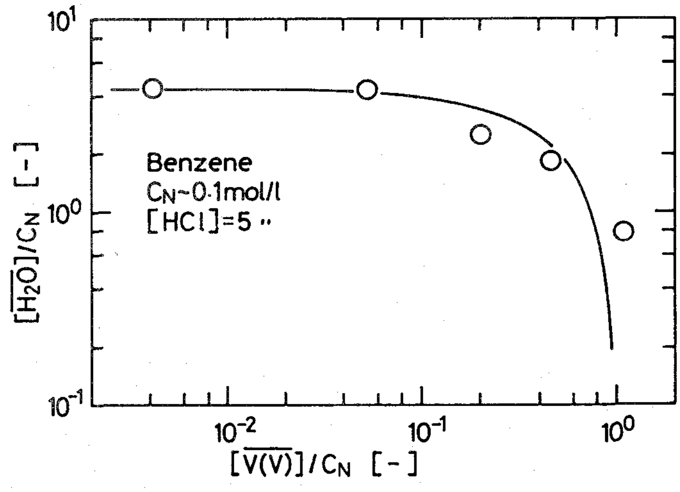

Fig. 1.12. Variation of amount of water associated with TOMAC in benzene with loading ratio; comparison of observed data with prediction shown by solid lines.

1.3.2.3 Extraction of vanadium(V) by TOMAC in chloroform

For the chloroform diluent system a similar approach was applied. The distribution ratio of vanadium increases with acid concentration up to [HCl] = 7 mol/*l*, as shown in **Fig. 1.13**. The data obtained with different feed vanadium(V) concentrations fall on a single line for this diluent. The plot of $[\overline{V(V)}]$ against $[VO_2^+]$ gives a straight line with a slope of 1, indicating that the extract is monomeric.

Figure 1.14 shows the variation of the distribution ratio with the concentration of free TOMAC monomer, $[\overline{R\cdot H_2O}]$, calculated considering the dimerization of TOMAC[10] and acid extraction, expressed by Eqs. (1.3') and (1.9) ~ (1.11). The slope thus obtained is 1.5. The loading ratio increases with the feed vanadium concentration and approaches a value of 1, as shown in **Fig. 1.15**. On the basis of the results described so far, the extraction equilibrium is formulated as follows.

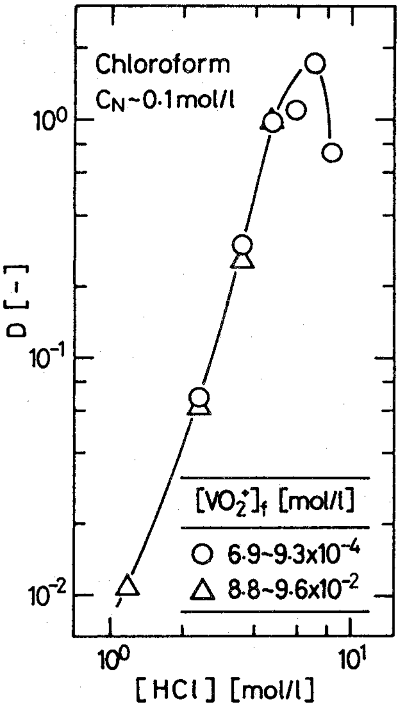

Fig. 1.13. Effect of hydrochloric acid concentration on distribution ratio of vanadium in chloroform diluent system.

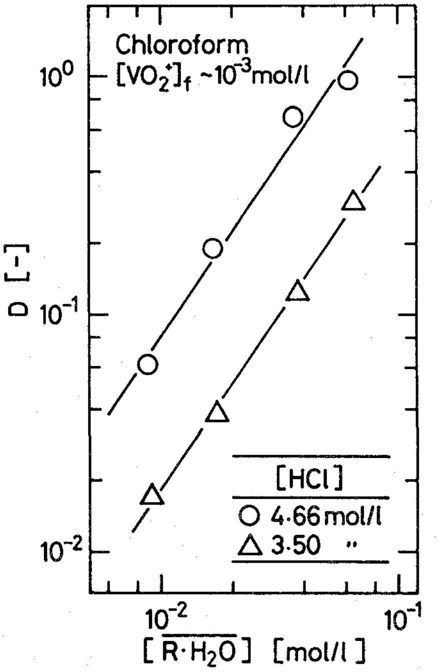

Fig. 1.14. Relationship between distribution ratio of vanadium and concentration of free TOMAC monomer in chloroform diluent system.

$$\overline{\mathrm{R\cdot H_2O}} + \mathrm{VO_2^+} + \mathrm{Cl^-} = \overline{\mathrm{R\cdot VO_2Cl}} + \mathrm{H_2O}$$
$$K_{ex,1} = [\overline{\mathrm{R\cdot VO_2Cl}}]\, a_W / [\overline{\mathrm{R\cdot H_2O}}]\, [\mathrm{VO_2^+}]\, a_H \tag{1.22}$$

$$2\,\overline{\mathrm{R\cdot H_2O}} + \mathrm{VO_2^+} + \mathrm{Cl^-} = \overline{\mathrm{R_2\cdot VO_2Cl}} + 2\mathrm{H_2O}$$
$$K_{ex,2} = [\overline{\mathrm{R_2\cdot VO_2Cl}}]\, a_W^{\,2} / [\overline{\mathrm{R\cdot H_2O}}]^2\, [\mathrm{VO_2^+}]\, a_H \tag{1.23}$$

The material balance for the extractant and vanadium extracted are expressed by Eqs. (1.24) and (1.25), respectively.

$$C_N = 2\,[\overline{\mathrm{(R\cdot H_2O)_2}}] + 2\,[\overline{\mathrm{R_2\cdot HCl\cdot H_2O}}] + [\overline{\mathrm{R\cdot HCl}}] + [\overline{\mathrm{R\cdot (HCl)_2}}] + [\overline{\mathrm{R\cdot H_2O}}]$$
$$+ [\overline{\mathrm{R\cdot VO_2Cl}}] + 2\,[\overline{\mathrm{R_2\cdot VO_2Cl}}] \tag{1.24}$$

$$[\overline{\mathrm{V(V)}}] = [\overline{\mathrm{R\cdot VO_2Cl}}] + [\overline{\mathrm{R_2\cdot VO_2Cl}}] \tag{1.25}$$

The most likely K_{ex} values obtained are shown in Table 1.2. A prediction of vanadium loading is made and is shown in Fig. 1.15 by solid lines. The vanadium extraction behavior is actually correlated in a solvating diluent.

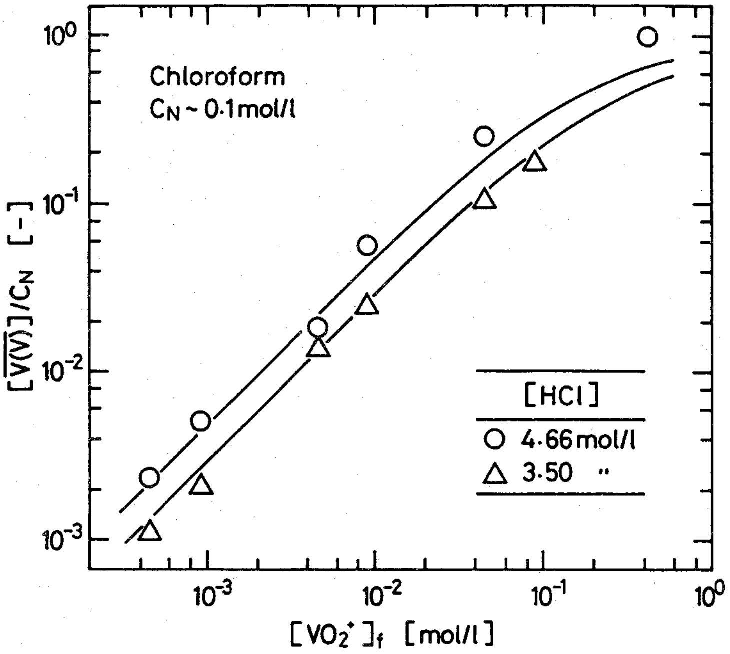

Fig. 1.15. Variation of loading ratio of extractant in chloroform with feed concentration of vanadium; comparison of observed data with prediction shown by solid lines.

1.3.3 Extraction of Rare-Earth Elements by Tri-*n*-octylmethylammonium Nitrate

The extraction of rare-earth elements in the system containing TOMAN as an extractant diluted with xylene and ammonium nitrate as a salting-out agent was already reported.[27)] In this section, the extraction mechanism of the elements is summarized.

The association of the extractants in xylene is expressed by the following simple model, where S denotes the monomeric species of TOMAN.

$$4\overline{S} = \overline{S_4},\ K_T = [\overline{S_4}] / [\overline{S}]^4 \qquad (1.26)$$

The tetramerization constant was determined as $K_T = 10^7\ (\mathrm{mol}/l)^{-3}$. Eight water molecules are assumed to be associated with each tetramer molecule. The tetramer is, therefore, likely to form a hydration sphere, and the monomer is not stabilized by water molecules. The extraction of ammonium nitrate by TOMAN is expressed as follows, where $a_{NO_3^-}$ is mean ionic activity of ammonium nitrate, which is 2.04 in 6 mol/l NH_4NO_3.[31)]

$$NH_4^+ + NO_3^- + 4\overline{S} = \overline{NH_4NO_3 \cdot 4S},\ K_S = [\overline{NH_4NO_3 \cdot 4S}] / [\overline{S}]^4 a_{NO_3^-} \qquad (1.27)$$

K_S is determined as $6.6 \times 10^5\ (\mathrm{mol}/l)^5$.

The extraction of the rare–earth elements is assumed to occur via reaction with monomer of the extractant, in competition with the extraction of ammonium nitrate. The extraction equilibrium is formulated as follows, where Ln denotes rare–earth element.

$$\begin{aligned} &Ln^{3+} + 3NO_3^- + 5\overline{S} = \overline{Ln(NO_3)_3 \cdot 5S} \\ &\quad K_{105} = [\overline{Ln(NO_3)_3 \cdot 5S}] / [Ln^{3+}][\overline{S}]^5 a_{NO_3}{}^{-3} \end{aligned} \qquad (1.28)$$

$$\begin{aligned} &Ln^{3+} + 3NO_3^- + \overline{Ln(NO_3)_3 \cdot 5S} = \overline{\{Ln(NO_3)_3\}_2 \cdot 5S} \\ &\quad K_{205} = [\overline{\{Ln(NO_3)_3\}_2 \cdot 5S}] / [Ln^{3+}][\overline{Ln(NO_3)_3 \cdot 5S}] a_{NO_3}{}^{-3} \end{aligned} \qquad (1.29)$$

The extraction equilibrium constants obtained, K_{105} and K_{205}, are shown in **Table 1.3**. This scheme analyses the extraction data for the whole range of the loadings of the extractant.

The extractability decreases with position in the atomic number series of the elements, apart from a slight increase from Gd to Tb. The behavior of extraction is divided into the four tetrads such as La–Nd, Sm–Gd, Gd–Ho and Er–Lu with the behavior of Y lying between Tm and Yb. The separation factor of Pr and

Table 1.3. Extraction equilibrium constants for rare-earth elements in TOMAN system. $[NH_4NO_3] = 6$ mol/*l*.

$[\overline{\text{TOMAN}}]$ [mol/*l*]		La	Ce	Pr	Nd	Sm
1.0	K_{105}	$7.82\text{x}10^{10}$	$5.00\text{x}10^{10}$	$2.85\text{x}10^{10}$	$1.41\text{x}10^{10}$	$5.32\text{x}10^{9}$
	K_{205}	$1.63\text{x}10^{-1}$	$4.10\text{x}10^{-1}$	$5.40\text{x}10^{-1}$	$8.36\text{x}10^{-1}$	1.40
0.4	K_{105}	$8.60\text{x}10^{10}$	$5.31\text{x}10^{10}$	$2.92\text{x}10^{10}$	$1.56\text{x}10^{10}$	$5.10\text{x}10^{9}$
	K_{205}	$2.89\text{x}10^{-1}$	$2.15\text{x}10^{-1}$	$4.33\text{x}10^{-1}$	$7.63\text{x}10^{-1}$	1.22

$[\overline{\text{TOMAN}}]$ [mol/*l*]		Gd	Dy	Yb	Y
1.0	K_{105}	$2.28\text{x}10^{9}$	$2.38\text{x}10^{9}$	$6.27\text{x}10^{8}$	$7.88\text{x}10^{8}$
	K_{205}	$9.95\text{x}10^{-1}$	1.43	$3.35\text{x}10^{-1}$	$5.42\text{x}10^{-1}$
0.4	K_{105}	$2.15\text{x}10^{9}$	$2.28\text{x}10^{9}$	$6.81\text{x}10^{8}$	$7.76\text{x}10^{8}$
	K_{205}	$8.29\text{x}10^{-1}$	1.06	$2.28\text{x}10^{-1}$	$4.40\text{x}10^{-1}$

Nd, $\beta_{\text{Pr/Nd}}$, is 1.8 for low loadings. It is greater than that obtained with D2EHPA or tri-*n*-butylphosphate (TBP) ($\beta_{\text{Pr/Nd}} = 1.3 \sim 1.5$). The extraction performance of TOMAN for lighter elements has a tendency to decrease with loading more sharply than for the heavier elements. This adversely affects the separation of adjacent elements. The loading of the organic phase must therefore be carefully controlled to achieve an effective separation.

1.4 Summary

The extraction mechanism of hydrochloric acid, cobalt and vanadium(V) from the acid solution by tri-*n*-octylmethylammonium chloride (TOMAC) has been studied, employing benzene as a diluent to weakly solvate the extractant and metal extract and chloroform as a solvating effect diluent, with the following results.

(1) The behavior of the association of the extractant was expressed by a simple tetramerization model as shown in Eq. (1.1') in benzene and a dimerization model in Eq. (1.3') in chloroform. Five water molecules are associated to

each extractant in benzene and 1.2 in chloroform. One water molecule is replaced by one hydrochloric acid molecule when equilibrated with acid, and the mechanism of extraction is expressed by the stepwise relationships given by Eqs. (1.5) ~ (1.7) in the benzene diluent system and by Eqs. (1.9) ~ (1.11) in chloroform.

(2) For the extraction of cobalt, a simple scheme occurring in both diluents is presented which assumes that the extraction occurs via reaction with the monomeric species of the extractant and via the replacement of water in the salt hydration sphere by cobalt chloride. This extraction occurs in competition with the extraction of acid. The mechanism of extraction is expressed by the relationships given by Eqs. (1.12) ~ (1.14) in benzene, and by a simple relationship given by Eq. (1.17) in chloroform. The liberation of water and acid with the progress of cobalt loading of the extractant from the organic solution is expressed satisfactorily by the present extraction schemes for acid and cobalt in both diluent systems.

(3) In the case of extraction of vanadium(V), the extraction equilibrium formulations given by Eqs. (1.18) and (1.19) for benzene diluent and Eqs. (1.22) and (1.23) for chloroform diluent were presented. These formulations expressed satisfactorily the extraction of vanadium(V) over a wide range of vanadium loading in both diluent systems, in line with the cases of the cobalt extraction.

In section 1.3.3, the extraction of rare-earth elements by tri-*n*-octylmethylammonium nitrate (TOMAN) in the presence of ammonium nitrate as a salting-out agent was summarized. The extraction schemes of ammonium nitrate and the elements were described.

Chapter 2 Separation and Purification of Rare Metals by Solvent Extraction and Redox Reactions

2.1 Introduction

The solvent extraction process used for rare metals normally consists of three stages: extraction, scrubbing, and stripping. Usually, separation is effected at the extraction stage on the basis of difference in distribution ratio between the metals in the feed solution. When selective stripping of the target metal can be included, a much higher separation efficiency is expected to obtain. Reduction of the extracted metal is very effective in the stripping operation, since the extracted metal is very effective in the stripping operation, since the distribution ratio is considerably reduced in magnitude. There may be three effective method to reduce the metals in the solvent extraction process; by adding reducing agent (chemical reduction), by electrochemical reduction and by photochemical reduction. Electroreduction and photoreduction methods require no reduction agent and are, therefore, free from contamination.

In the Purex process for the recovery of plutonium and uranium from waste nuclear fuels, it is known that plutonium is stripped selectively by chemical reduction from the tetravalent to the trivalent state.44,53) Peppard *et al.* reported that the distribution ratio of Eu^{2+} was much smaller than that of Eu^{3+} in bis(2-ethylhexyl)phosphoric acid (D2EHPA) system.38) The extracted Eu was reduced by Cr^{2+} and Zn amalgam in the aqueous phase and was stripped effectively from the organic phase. In the commercial plant, Eu^{3+} is reduced to Eu^{2+} by Zn powder prior to extraction, remaining Eu^{2+} in the aqueous phase selectively. The chemical-reductive stripping of cerium,55) uranium20) and iron45,50) were also investigated using the reducing agent such as hydrogen peroxide, Fe^{2+}, L-ascorbic acid and SO_2 gas. Electro-reductive stripping of cerium19) and plutonium3,4) were reported. The photochemical reduction of lanthanide and actinide has been studied by several investigators. The trivalent Eu was reduced to the divalent state by using a low-pressure mercury lamp or an ArF excimer laser in aqueous solutions. The reduced Eu was precipitated as $EuSO_4$ and was separated from the other lanthanide.$^{12)}$ In alcoholic media, γ-ray$^{21)}$ or high-pressure mercury lamp$^{21)}$ were also usable for the photoreduction of Eu^{3+}. The purification of the rare-earth elements using lasers as light source was summarized by Donohue.$^{13)}$ The photoreduction of uranyl nitrate,$^{11,42)}$ plutonium$^{6)}$ and neptunium$^{14,15,52)}$ was also investigated aiming to apply the techniques in the nuclear fuel reprocessing.$^{5,17)}$ In the case of the pentavalent vanadium, photochemical reduction to the tetravalent state was possible by using an argon laser in aqueous perchloric acid solutions.$^{22)}$

In this chapter, the separation and purification of rare metals by solvent extraction followed by reductive stripping has been investigated. As the case studies, separation of vanadium and molybdenum by solvent extraction using tri-*n*-octylmethylammonium chloride (TOMAC, $R_3R'NCl$) as extractant and subsequent selective stripping of vanadium by chemical and electrochemical reduction, and the separation of europium from samarium and gadolinium by combination of electroreduction or photoreduction and the solvent extraction techniques have been investigated. It has been reported that V and Mo were separated from aqueous acidic media by solvent extraction processes using tri-*n*-butylphosphate (TBP),$^{26)}$ D2EHPA, and tri-*n*-octylamine (TOA).$^{8)}$ The present separation process differs from these in that extraction is carried out from neutral solutions. The present results may be applied to the previously reported processes to enhance the separation efficiency. L-ascorbic acid was used as the reducing agent, and a platinum electrode was used for the electroreduction of V. For the electrochemical and photochemical reduction of Eu, a titanium plate electrode and a low-pressure mercury lamp were used.

2.2 Experimental

1) Vanadium and molybdenum Aqueous stock solutions of vanadium and

molybdenum were prepared by dissolving sodium metavanadate ($NaVO_3$) and sodium molybdate ($Na_2MoO_4 \cdot 2H_2O$) respectively in distilled water. The ionic strength of these solutions was adjusted to the required values with sodium chloride. The pH of the feed solutions was adjusted with either hydrochloric acid or sodium hydroxide solutions using a pH meter (Orion Research model 611). L–ascorbic acid was used for the vanadium reduction at the stripping stage. TOMAC (KEX–L–84, Koei Kagaku Kogyo Co., Ltd.) was purified by the procedure developed for the purification of Aliquat 336[46)] and was diluted with benzene.

The extraction of V and Mo was carried out by shaking equal volumes of the organic and aqueous feed solutions containing ca. 0.01 mol/*l* $NaVO_3$ and Na_2MoO_4 for about 2 hours for equilibration at 25°C. The two phases were separated and the metal concentration in the aqueous raffinate solution was determined to obtain the extraction percentage, *E*. This was done because a quantitative stripping of the metals by single contact with stripping solution was not feasible. It was confirmed in preliminary runs that the organic metal concentrations obtained from the raffinate solution measurement and mass balance were in good agreement with those obtained from repeated contacts with fresh stripping solutions. Distribution ratios of penta– and tetravalent vanadium were determined by batch extraction of $NaVO_3$ and $VOCl_2$, respectively.

Stripping was carried out by shaking equal volumes of the metal–loaded organic solution and aqueous solution together for about 2 hours at 25°C. The organic solution was prepared by shaking a pH 7 aqueous solution containing ca. 0.01 mol/*l* $NaVO_3$ and 0.01 mol/*l* Na_2MoO_4 and benzene solution containing 0.015 mol/*l* TOMAC. The extraction percentages of vanadium and molybdenum were greater than 98% and less than 8%, respectively, and the resulting organic solution contained ca. 9.3×10^{-3} mol/*l* vanadium and ca. 7.6×10^{-4} mol/*l* molybdenum.

2) Rare–earth elements Rare–earth chlorides were prepared by dissolving Eu_2O_3 (supplied by Shin–Etsu Chemical Co., Ltd., Tokyo, 99.9%), Sm_2O_3 and

Gd_2O_3 (supplied by Nippon Yttrium Co., Ltd., Tokyo, 99.9%) in hydrochloric acid and then removing the excess acid by evaporation. Alkyl phosphoric acid extractants, D2EHPA and di-5-methyl-2-(1-methylneohexyl)neodecanoyl phosphoric acid (DP-18) were supplied by Daihachi Chemicals Ind. Co. Ltd., Osaka, and were diluted with xylene. Extraction of the elements was carried out by shaking equal volumes of the organic solution (0.4 mol/*l* DP-18 or 0.2 mol/*l* D2EHPA) and pH 6 aqueous solution (containing ca. 0.02 mol/*l* or 5×10^{-3} mol/*l* $SmCl_3$, $EuCl_3$ and $GdCl_3$ for DP-18 or D2EHPA systems, respectively) at 25°C. The concentrations of these elements in the resulting organic phases were ca. 2.1×10^{-3} mol/*l* and ca. 4.3×10^{-3} mol/*l* in the DP-18 and D2EHPA solutions, respectively. To determine the elements remaining in the organic phase, the organic solution was stripped with 1 mol/*l* HCl (for DP-18) or 6 mol/*l* HCl (for D2EHPA) solution. The photochemical reduction of Eu was carried out by using a 20 W low-pressure mercury lamp (Eikohsha), which had emission peaks of 184.9 nm and 253.7 nm. When only the 253.7 nm line was required, the 184.9 nm line was cut off with a filter.

3) Measurements The concentration of the metals in aqueous solution the was determined by use of an inductively coupled argon plasma emission spectrophotometer (Nippon Jarrell-Ash ICAP-575MarkII). The voltammetry and electrolysis were performed with a potentiostat (Hokuto Denko HA-303), a function generator (Hokuto Denko HB-104) and an X-Y recorder (Yokogawa type 3022). The chloride concentration in the organic phases was measured using a Volhardt titration method. The absorption spectra of the aqueous and organic solutions were measured with an UV-vis spectrophotometer (Shimadzu UV-265FW).

2.3 Results and Discussion

2.3.1 Chemical–Reductive Stripping of Vanadium in Solvent Extraction Process for Separation of Vanadium and Molybdenum

2.3.1.1 Extraction of vanadium and molybdenum by TOMAC

1) Extraction of vanadium   Performance of vanadium extraction by TOMAC at various equilibrium pH values are shown in **Fig. 2.1**, where $[V]_f$ and $[\overline{\mathrm{TOMAC}}]_f = 0.01$ mol/*l*. Almost all vanadyl ions are extracted at a pH of 6 ~ 7, whereas the extraction percentage is reduced to less than 30% at pH > 10. The quantity of chloride ion released from the organic phase and into the aqueous phase during the course of extraction ($\Delta[\mathrm{Cl}^-]$) was determined and was compared with the concentration of vanadyl ion extracted into the organic phase ($[\overline{V}]$). The pH dependence of the ratio $\Delta[\mathrm{Cl}^-]/[\overline{V}]$ so obtained is also given in Fig. 2.1. An exchange of chloride anions for vanadyl ions apparently occurs

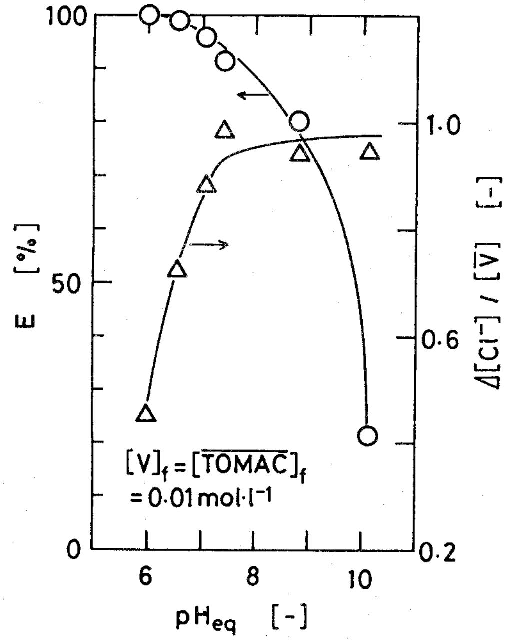

Fig. 2.1. Effect of equilibrium pH on extraction performance of vanadium and on ratio of chloride released to vanadium extracted.

during the extraction, but the ratio of chloride to vanadyl varies with pH. This result may be attributed to the formation of polyvanadate anions in the aqueous solution. Bard *et al.*[2)] and Rossotti *et al.*[43)] have reported that the structure of pentavalent vanadyl ion changes with solution pH as shown in **Table 2.1**. If one $R_3R'N^+$ molecule is assumed to be consumed for each negative electric charge of the vanadyl species during extraction, the resulting ratio values, $\Delta[Cl^-]/[\overline{V}]$, are predicted to vary in magnitude from 0.4 to 2 depending on the aqueous–phase pH value. As shown in Table 2.1, the observed ratio values appear to be in good agreement with the predicted values, with the exception of the case of pH > 8.5. The vanadyl anions are, therefore, extracted with their structure retained. Thus, an anion exchange extraction mechanism appears to be applicable to the extraction and the following schemes (2.1) and (2.2) may be postulated.

Table 2.1. Structures of the pentavalent vanadyl and hexavalent molybdate ions and comparison of the predicted and observed ratio values of chloride ions released and metal ions (M) extracted at various pH.

Solution pH [-]	Structure	Predicted $\Delta[Cl^-]/[\overline{M}]$ [-]	Observed $\Delta[Cl^-]/[\overline{M}]$ [-]
2 ~ 6.5	$H_2V_{10}O_{28}^{4-}$ $HV_{10}O_{28}^{5-}$ $V_{10}O_{28}^{6-}$	0.4 0.5 0.6	0.4 ~ 0.7
6.5 ~ 8.2	$(VO_3^-)_n$ (n=1~4)	1	0.8 ~ 1
8.5 ~ 13	$V_2O_7^{4-}$	2	1
1 ~ 6	$Mo_7O_{24}^{6-}$ $Mo_8O_{26}^{4-}$	0.86 0.5	0.5
pH > 6	MoO_4^{2-}	2	1.7 ~ 2.7

$$\text{pH} < 6.5: \quad n\overline{\text{R}_3\text{R'NCl}} + \text{H}_{6-n}\text{V}_{10}\text{O}_{28}{}^{n-} = \overline{(\text{R}_3\text{R'N})_n\text{H}_{6-n}\text{V}_{10}\text{O}_{28}} + n\text{Cl}^- \quad (n=4 \sim 6) \quad (2.1)$$

$$\text{pH} > 6.5: \quad n\overline{\text{R}_3\text{R'NCl}} + (\text{VO}_3{}^-)_n = \overline{(\text{R}_3\text{R'N})_n(\text{VO}_3)_n} + n\text{Cl}^- \quad (n=1 \sim 4) \quad (2.2)$$

Sato *et al.* have reported that the pentavalent vanadyl ion is extracted as $V_2O_7{}^{4-}$ from sodium hydroxide solution by TOMAC.[46)] But in the present work the observed ratio fails to agree with the predicted value (=2) at pH greater than 8.5. This may be due to the low concentration of vanadium (less than 10^{-2} mol/*l*) used in the present experimental conditions. The formation of pyrovanadate ion, $V_2O_7{}^{4-}$, actually is reported by Bard *et al.*[2)] to occur at a vanadium concentration level greater than 10^{-2} mol/*l*.

2) Extraction of molybdenum The dependence of extraction performance and of the ratio $\Delta[\text{Cl}^-]/[\overline{\text{Mo}}]$ on pH are shown in **Fig. 2.2**. The *E* value decreases as the equilibrium pH increases, and reaches a value of less than 10% at

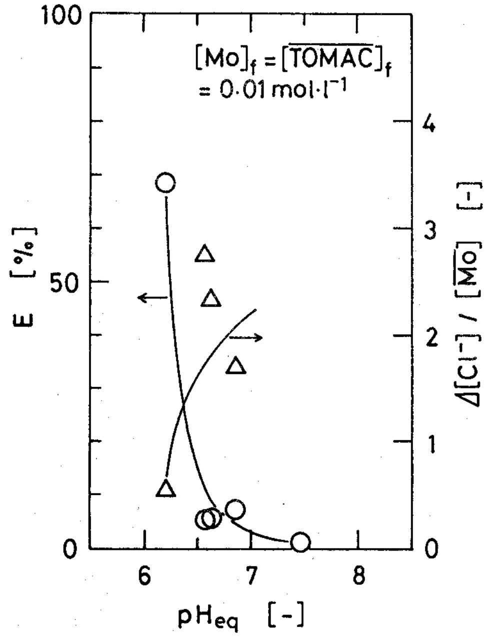

Fig. 2.2. Effect of equilibrium pH on extraction performance of molybdenum and on ratio of chloride released to molybdenum extracted.

pH > 6.5. The structure of the hexavalent molybdate anion is MoO_4^{2-} in this pH region, as reported by Bard *et al.*,2) and the observed ratio values (1.7 – 2.7) are in agreement with the predicted value (=2). On the other hand, the *E* value at pH < 6.5 is about ten times greater, and the ratio value is reduced to 0.5. If the formation of polymeric species such as $Mo_7O_{24}^{6-}$ and $Mo_8O_{26}^{4-}$ as reported by Aveston *et al.*1) is assumed, the present results seem reasonable, since the observed ratio value is very near the predicted value as shown in Table 2.1. Thus, these polymeric species are the main species extracted at pH < 6.5. The extraction equilibria for molybdenum can be described by the following relations.

$$\text{pH} < 6.5: \quad 6\overline{R_3R'NCl} + Mo_7O_{24}^{6-} = \overline{(R_3R'N)_6Mo_7O_{24}} + 6Cl^- \qquad (2.3)$$

$$4\overline{R_3R'NCl} + Mo_8O_{26}^{4-} = \overline{(R_3R'N)_4Mo_8O_{26}} + 4Cl^- \qquad (2.4)$$

$$\text{pH} > 6.5: \quad 2\overline{R_3R'NCl} + MoO_4^{2-} = \overline{(R_3R'N)_2MoO_4} + 2Cl^- \qquad (2.5)$$

3) Extraction of vanadium and molybdenum from mixed solutions **Figure 2.3** shows the performance of vanadium and molybdenum extraction from mixed solutions containing equal quantities of each metal (0.01 mol/*l*) as a function of the equilibrium pH. The extraction behavior of both metals in solution is found to be very similar to that found for single–metal extraction, as shown in Figs. 2.1 and 2.2. An equilibrium pH of 7 to 8 should be employed for effective separation of the two metals.

The concentration of TOMAC also influences the separation efficiency. As shown in **Fig. 2.4**, the extraction of vanadium increases appreciably with TOMAC concentration, whereas the extraction of molybdenum is less affected.

With a TOMAC concentration of 0.015 mol/*l* and an input aqueous pH value of 7.0, the resulting equilibrium pH value obtained was ca. 7.4. Under these conditions, the extraction percentages for vanadium and molybdenum were greater than 98% and less than 8%, respectively. Using a feed solution containing 9.43×10^{-3} mol/*l* vanadium and 1.01×10^{-2} mol/*l* molybdenum, the

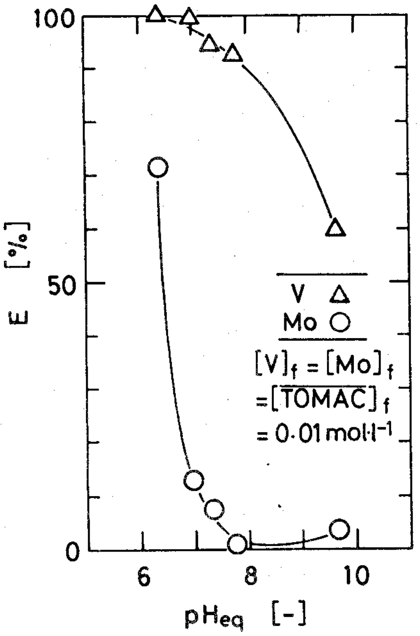

Fig. 2.3. Relationship between equilibrium pH and extraction performance of vanadium and molybdenum.

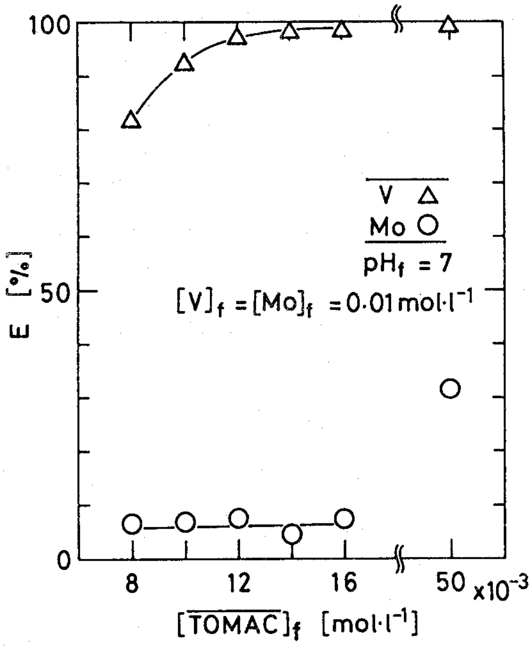

Fig. 2.4. Effect of TOMAC concentration on extraction performance of vanadium and molybdenum at pH 7.

concentration of vanadium in the organic phase was 9.26×10^{-3} mol/*l*, which was more than 12 times greater than that of molybdenum (7.59×10^{-4} mol/*l*). More than 92% molybdenum (9.37×10^{-3} mol/*l*) remained in the raffinate aqueous solution; in molar terms, its quantity was more than 50 times greater than that of vanadium (1.75×10^{-4} mol/*l*).

2.3.1.2 Further purification of vanadium by reductive stripping

To improve the separation of the two metals, the scrubbing of molybdenum and / or the selective stripping of vanadium is needed. In this study, the method of selective stripping of vanadium by chemical reduction was investigated.

A series of runs using a stripping solution containing 1 mol/*l* chloride anion at various pH values were carried out. The effect of input pH on stripping performance is shown in **Fig. 2.5.** It is seen that the stripping performance shows a minimum value at $pH_f = 2$ (pH_{eq} = ca. 2.3) and less than 1% of both metals is transferred into the stripping solution. This minimum stripping is likely caused

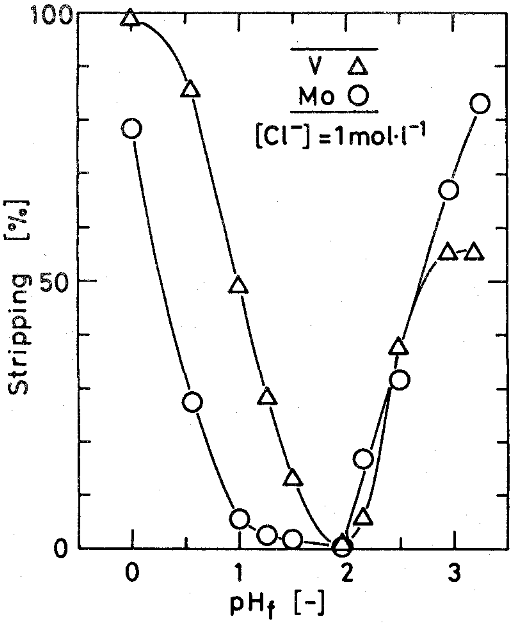

Fig. 2.5. Effect of stripping solution pH on stripping performance of vanadium and molybdenum.

by the very stable structure of the pentavalent vanadyl ion and the hexavalent molybdate ion at this pH in the organic phase. At this pH the effect on the stripping performance of the addition of L–ascorbic acid as a reduction agent was investigated. The results are shown in **Fig. 2.6**. The stripping of vanadium was remarkably enhanced, whereas that of molybdenum was insensitive to the addition of the reduction agent. The valency of the vanadium stripped into the aqueous phase was investigated spectroscopically. The visible absorption spectrum of this bluish–green phase is shown in **Fig. 2.7**, together with the spectra of tetravalent vanadium (vanadyl sulfate, $VOSO_4$) and trivalent vanadium (vanadium chloride, VCl_3) at pH 2. The aqueous phase after stripping showed a spectroscopic feature similar to that of a mixture of tetra– and trivalent vanadium. Thus, pentavalent vanadium is likely to be reduced to a mixed state of tetra– and trivalent vanadium by L–ascorbic acid, where the reduced vanadium species exists as cations such as VO^{2+} (tetravalent) and V^{3+} (trivalent). TOMAC is basically an anion exchanger and acts as an extractant for anionic species.

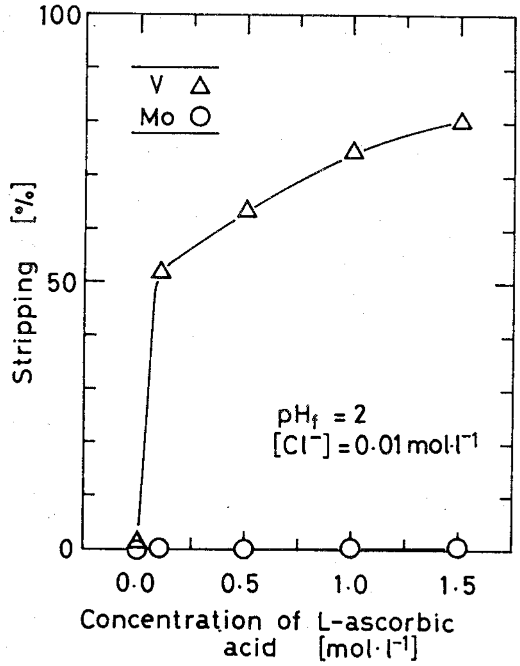

Fig. 2.6. Effect of addition of L–ascorbic acid on stripping performance of vanadium and molybdenum at pH 2.

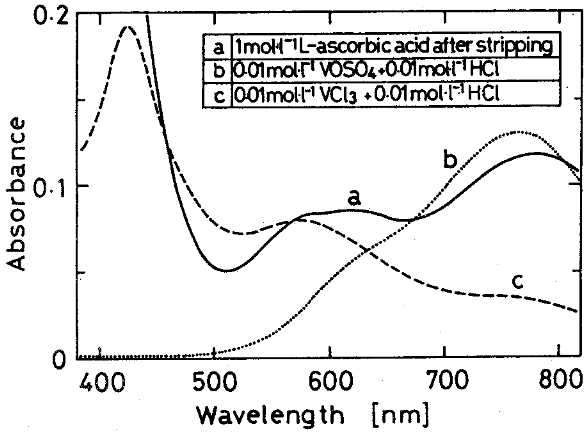

Fig. 2.7. Visible absorption spectra of aqueous solutions containing vanadyl ions.

Consequently, these cationic species are hardly extracted. For molybdenum, the colorless hexavalent molybdate anion in the organic phase was converted to the form of yellowish species by the addition of L–ascorbic acid and still remained in the organic phase. These yellowish species are not characterized exactly, but are likely to be anionic species. The stripping performance remains at an extremely low level, as in the case without a reduction agent. No precipitation was observed in either the aqueous or the organic phases during the stripping operation.

Figure 2.8 shows the relationship between the stripping solution pH and the stripping performance for both metals for the case of an aqueous solution containing 1 mol/*l* L–ascorbic acid and ca. 0.01 mol/*l* chloride anions (hydrochloric acid and/or sodium chloride being used). The separation efficiency, which is defined as the molar ratio of vanadium to molybdenum, in the resulting stripping solution after stripping is also shown in Fig. 2.8. The percentage stripping of vanadium increases with decreasing pH, while that for molybdenum shows a minimum value at pH values of 1.8 ~ 2. This leads to the appearance of a maximum in the separation efficiency at pHs of 1.8 ~ 2. The condition at which vanadium is stripped most efficiently is however not always suitable for separation and purification of vanadium and molybdenum. The effect of the composi–

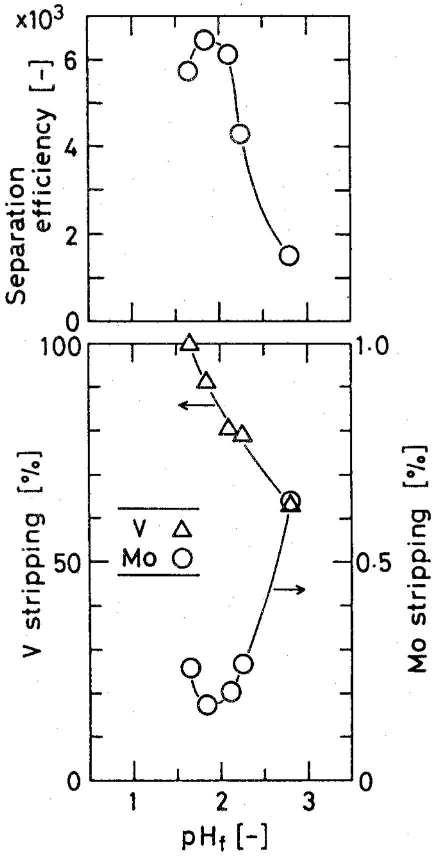

Fig. 2.8. Effect of stripping solution pH on stripping performance of vanadium and molybdenum and on separation efficiency. Concentrations of L–ascorbic acid and chloride anion are 1 mol/*l* and ca. 0.01 mol/*l*, respectively.

tion of the stripping solution on the stripping performance is shown in **Table 2.2**. With 1 mol/*l* L–ascorbic acid solution, the percentage stripping for vanadium reaches 91.3% and a separation efficiency of 6.47 x 10^3 is obtained. On decreasing the concentration of the reduction agent, the stripping performance for both metals decreases. However, the separation efficiency increases up to a value of 1.64 x 10^4 with further decrease in concentration of the reduction agent to 0.1 mol/*l*. Thus, the solution pH and concentration of the reduction agent must be carefully selected to achieve high separation efficiency and/or high percentage recovery.

Table 2.2. Stripping performance of vanadium and molybdenum, and separation efficiency at various conditions. The organic solution used contains 9.26 x 10^{-3} mol/*l* vanadium and 7.59 x 10^{-4} mol/*l* molybdenum. Each stripping solution contains 0.01 mol/*l* hydrochloric acid.

Concentration of L-ascorbic acid [mol/*l*]	pH_f [-]	Stripping [%] V	Stripping [%] Mo	Separation efficiency [-]
0.1	2.03	64.7	0.048	1.64 x 10^4
0.5	1.91	85.0	0.074	1.40 x 10^4
1.0	1.83	91.3	0.172	6.47 x 10^3

2.3.2 Electro-Reductive Stripping of Vanadium in Solvent Extraction Process for Separation of Vanadium and Molybdenum

2.3.2.1 Mechanism of electrolysis and structure of electrochemical cell

Electrical conductivity of the organic phase is principal factor of the two-phase electrolysis[16,19]. The conductivity should be greater than 0.1 S/cm to reduce the metal ion in the organic phase at the organic phase/electrode interface[16]. Otherwise, mass transfer of metal ion from the organic into aqueous phase must occur and this is followed by the charge transfer at the aqueous phase/electrode interface. The latter mechanism is likely to be applied for this TOMAC/benzene system, since the electrical conductivity of benzene is extremely small. Furthermore, contact of the organic solution with the electrode must be avoided, because the electrolytic current is much decreased when the electrode surface is covered by benzene.

Figure 2.9 shows a two-compartment electrochemical cell used for electro-reductive stripping. The cathodic and anodic compartment were separated by a cation exchange membrane (Aldrich Nafion417). The working electrode is 12 x 2 cm platinum mesh (40 mesh). Platinum black electrode (7.5 cm^2 area) and titanium plate electrode (7.5 cm^2 area) were also used. Equal volumes (15 m*l*) of the organic and aqueous solutions were agitated and electrolyzed in the

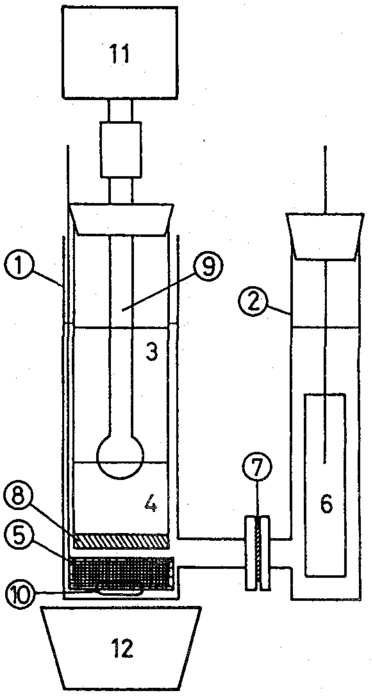

1 : Cathodic compartment
2 : Anodic compartment
3 : Organic phase (15 m*l*)
4 : Aqueous phase (15 m*l*)
5 : Cathode (platinum mesh)
6 : Anode (platinum plate)
7 : Cation exchange membrane (Nafion417)
8 : Sintered glass filter
9 : Agitator
10 : Stirring bar
11 : Stirring motor
12 : Magnetic stirrer

Fig. 2.9. Two–compartment electrochemical cell for electro–reductive stripping.

cathodic compartment at room temperature. The sintered glass filter equipped in the cell could separate the organic solution from cathode, even when the agitation speed was as high as 2000 min^{-1}. The aqueous solution in the anodic compartment was same as that in the cathodic compartment.

The stripping performance of vanadium and molybdenum showed the minimum value at aqueous phase feed pH = 2 as shown in Fig. 2.5, and this pH condition was suitable for the selective stripping of vanadium by chemical reduction using L–ascorbic acid. For the electro–reductive stripping, however, this pH condition is not suitable, because the mass transfer of vanadyl anion into the aqueous phase hardly occurs. Actually, a stripping yield of vanadium was less than 1% by 24 hours electrolysis when 0.01 mol/*l* HCl solution was used. Thus, 0.1 mol/*l* hydrochloric acid solution was used as the aqueous phase. In addition, 0.2 mol/*l* HCl solution was also used for comparison. The stripping yields by contact with 0.1 and 0.2 mol/*l* HCl (without electrolysis) respectively were ca. 22% and 50% for vanadium and 1.4% and 6.0% for molybdenum.

2.3.2.2 Electro-reductive stripping of vanadium

The current–voltage curve obtained by use of Pt electrode in 0.1 mol/*l* HCl solution containing 0.01 mol/*l* $NaVO_3$ is shown in **Fig. 2.10**. The reduction current of pentavalent vanadium is seen at $E < -0.5$ V, where E is defined as the potential of cathode vs. anode. It is also found that the onset potential of hydrogen generation is ca. −1.5 V. The relationship between the electrolysis voltage and the stripping yields of vanadium and molybdenum is shown in **Fig. 2.11**. No difference in the stripping yield is seen in the voltage range of −1.5 ~ −2.5 V, although the observed electric current increased with the electrolysis voltage. Thus, −1.5 V is adopted as the suitable electrolysis voltage to reduce efficiently the pentavalent vanadyl ion with minimum hydrogen generation. With the progress of electrolysis, the aqueous phase turned light blue. **Figure 2.12** shows the visible absorption spectrum of 0.1 mol/*l* HCl aqueous solution after electro-reductive stripping, together with the spectra of tetravalent vanadyl ion (VO^{2+})

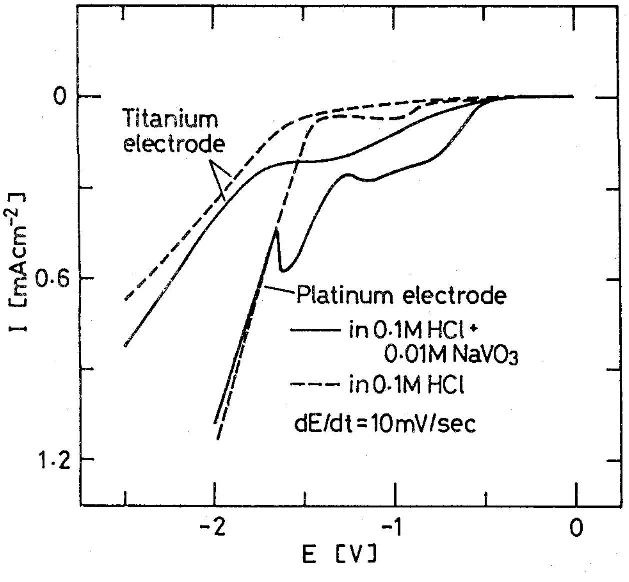

Fig. 2.10. Current–voltage curves obtained by use of platinum and titanium plate electrode in 0.1 mol/*l* hydrochloric acid solution containing 0.01 mol/*l* $NaVO_3$.

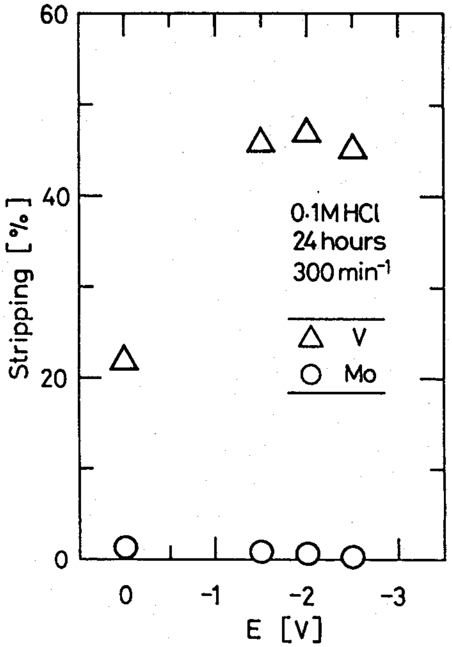

Fig. 2.11. Effect of electrolysis voltage on stripping yield of vanadium and molybdenum.

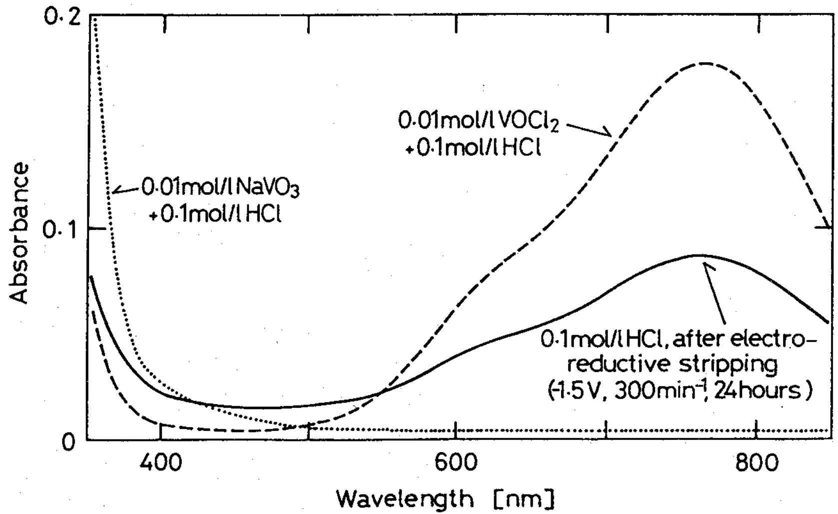

Fig. 2.12. Visible absorption spectra of 0.1 mol/*l* HCl aqueous solutions after electro-reductive stripping and containing tetra- or pentavalent vanadyl ions.

and pentavalent vanadyl ion (VO_3^-) at pH 1. The spectroscopic feature of the stripping solution is similar to that of the $VOCl_2$ solution, and this indicates that the pentavalent VO_3^- anion is reduced to the tetravalent VO^{2+} cation. Since TOMAC acts as an anion exchanger in the pH range observed, VO^{2+} is hardly extracted, and stripped efficiently. The anode reaction was Cl_2 generation.

The relationship between the electrolysis time and stripping yields at the various agitation speeds in the aqueous and organic phases is shown in **Fig. 2.13**. The data at time = 0 show the stripping yields at equilibrium without electrolysis. The increase of the agitation speed from 300 to 1000 min^{-1} brought a considerable increase in the stripping rate, but further increase from 1000 to 2000 min^{-1} had little effect on the rate. The stirring speed of magnetic stirrer in the cathodic compartment is found not to affect the stripping rate, thus the speed is fixed at 800 min^{-1}. The stripping percentage of vanadium attains to 80% by 15 hours electrolysis at 1000 ~ 2000 min^{-1}, while that of molybdenum was

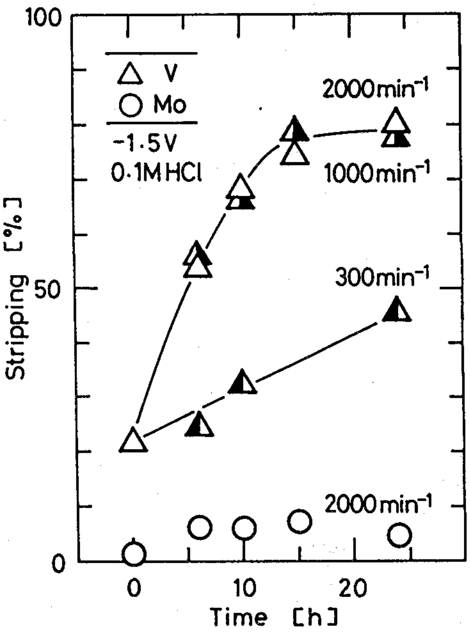

Fig. 2.13. Effect of electrolysis time on stripping yield of vanadium and molybdenum at various agitation speed for the case using 0.1 mol/*l* HCl solution as aqueous phase.

smaller than 7%. The concentration of vanadium in the stripping solution (6.95 x 10^{-3} mol/*l*) was about 400 times greater than that of molybdenum (1.82 x 10^{-5} mol/*l*).

Figure 2.14 shows the stripping yield of both metals in the case using 0.2 mol/*l* HCl as the aqueous solution. The stripping rate of vanadium slightly increases, while that of molybdenum also increases up to 12.6%, thus the separation is less effective than in the case using 0.1 mol/*l* HCl.

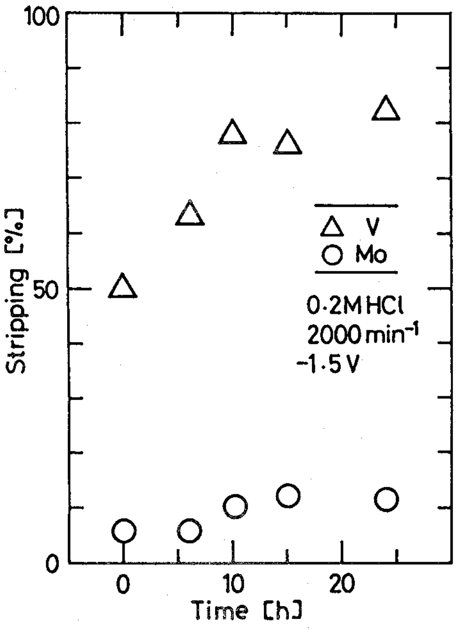

Fig. 2.14. Effect of electrolysis time on stripping yield of vanadium and molybdenum for the case using 0.2 mol/*l* HCl solution as aqueous phase.

From a kinetic point of view, the chemical–reductive stripping is very fast (the reduction is accomplished within several minutes). The chemical method also shows higher selectivity of vanadium stripping, as shown in Table 2.2.

The concentrations of the pentavalent and tetravalent vanadyl ions in the aqueous phase during the electro–reductive stripping are estimated as follows. The distribution ratios of those ions have been obtained; $D_{V(V)}$ = 3.57 and $D_{V(IV)}$ = 4.29 x 10^{-2} in 0.1 mol/*l* HCl, $D_{V(V)}$ = 0.99 and $D_{V(IV)}$ = 6.10 x 10^{-2} in 0.2 mol/*l*

HCl from the distribution data obtained with $NaVO_3$ or $VOCl_2$ solutions. During the course of the reductive stripping, the concentration of vanadium in the organic phase, $[\overline{V}]$, is

$$[\overline{V}] = D_{V(V)}[V(V)] + D_{V(IV)}[V(IV)] \tag{2.6}$$

where [V(V)] and [V(IV)] are the concentration of the penta– and tetravalent vanadium in the aqueous phase, respectively. The total vanadium concentration in the aqueous phase, [V], is expressed by Eq. (2.7).

$$[V] = [V(V)] + [V(IV)] \tag{2.7}$$

The concentration changes of V(V) and V(IV) calculated by use of Eqs. (2.6) and (2.7) are shown in **Fig. 2.15**. The concentration of pentavalent vanadium in 0.2 mol/*l* HCl solution is greater than that in 0.1 mol/*l* HCl during the stripping process, while almost no difference is seen in that of tetravalent vanadium in both systems. This indicates that the apparent difference in the stripping yield

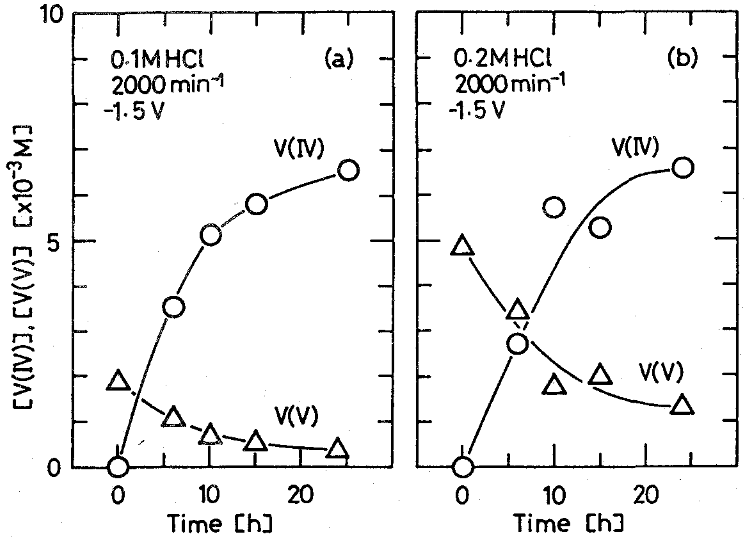

Fig. 2.15. Effect of electrolysis time on concentration of pentavalent and tetravalent vanadyl ons in aqueous phase. (a) 0.1 mol/*l* HCl, (b) 0.2 mol/*l* HCl.

between the two systems shown in Figs. 2.13 and 2.14 is caused by the difference in the concentration of pentavalent ion [V(V)], and that the reduction rates of vanadium are almost identical in both systems. That is, in the condition of the agitation speed of 2000 min^{-1}, there seem to be two considerable factors governing the stripping rate. One is the diffusion of pentavalent vanadium through the sintered glass filter into the compartment containing the cathode. The other is the electrochemical reduction of pentavalent vanadium at the cathode.

2.3.2.3 Effect of type of the working electrode on the stripping yields

In order to enhance the electrochemical reduction rate and thus the stripping yield, two other types of working electrodes were tested; Pt–black electrode and titanium plate electrode. Platinum–black electrode has actually a greater working area than Pt mesh electrode, and the greater electrolytic current was seen in the electro–reductive stripping. The stripping performance is, however, similar to that obtained using Pt mesh electrode. This result suggests that the diffusion of vanadyl anion through the glass filter is likely to be rate controlling, not the electrochemical reduction of the anion at the cathode. The greater current seems to be caused by a high ability for the hydrogen generation of Pt–black, not the high activity for the reduction of vanadium.

Current–voltage curve obtained by use of the titanium plate electrode in 0.1 mol/*l* HCl solution containing 0.01 mol/*l* $NaVO_3$ is shown in Fig. 2.10. Although the current density of hydrogen generation decreases in comparison with the case using the platinum electrode, the reduction current of VO_3^- also decreases. Electro–reductive stripping was carried out and the results are shown in **Fig. 2.16**. The low electrochemical activity of titanium electrode is likely to bring the small stripping rate of vanadium compared with Pt mesh electrode.

2.3.2.4 Repeated use of the organic solution for extraction of vanadium and molybdenum

An organic solution after 24 hours electro–reductive stripping using 0.2

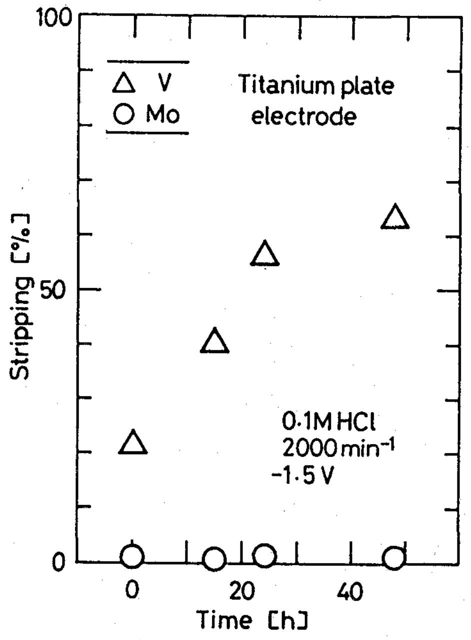

Fig. 2.16. Effect of electrolysis time on stripping yield of vanadium and molybdenum for the case using 0.1 mol/*l* HCl solution as aqueous phase and titanium plate as working electrode.

mol/*l* HCl solution contained vanadium and molybdenum in amounts of 1.54×10^{-3} mol/*l* and 5.16×10^{-4} mol/*l*, respectively. This organic solution was used for an extraction from pH 7 aqueous solution containing ca. 0.01 mol/*l* vanadium and molybdenum, which was the same as used in the first extraction. Extraction percentages of 98.1% for vanadium and 14.2% molybdenum were obtained, and the resulting organic solution contained 1.07×10^{-2} mol/*l* vanadium and 1.99×10^{-3} mol/*l* molybdenum, which were nearly equal to those in the first extraction. In this point, the electrochemical method is superior to the chemical method, since the organic phase after chemical–reductive stripping is required to be washed with HCl solution before the repeated use for metal extraction.

2.3.3 Electrochemical Reduction and Solvent Extraction for Separation of Europium from Samarium and Gadolinium

2.3.3.1 Electrochemical reduction of Eu in aqueous solution

The electro–reduction of Eu in aqueous solution was carried out using a two–compartment electrochemical cell separated by a cation exchange membrane (Aldrich Nafion417) shown in **Fig. 2.17**. The aqueous solution in the anodic compartment was 1 mol/*l* $(NH_4)_2SO_4$ adjusted to pH 3, and that in the cathodic compartment was the same solution containing ca. 0.01 mol/*l* $SmCl_3$, $EuCl_3$ and $GdCl_3$. When an anion exchange membrane was used, pH of the solution in the cathodic compartment was increased in the course of electrolysis, resulting in precipitation of rare–earth hydroxides. The cation exchange membrane enabled protons in the anodic compartment to move into the cathodic compartment and the pH could be maintained during the course of electrolysis. The transport of Eu^{3+} from the cathodic into anodic compartment was negligible. The working electrode was a titanium plate (7.5 cm^2 area), which had a higher hydrogen overvoltage than that of platinum electrode. Prior to the electrochemi–

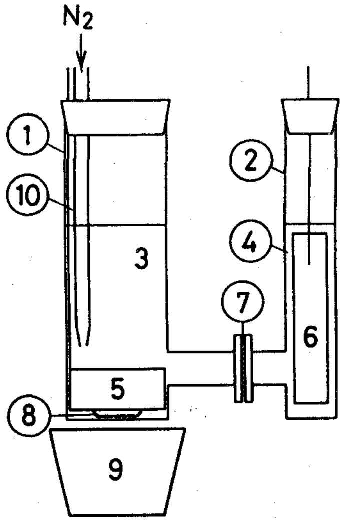

1 : Cathodic compartment
2 : Anodic compartment
3 : Aqueous solution (30 m*l*)
4 : 0.1 mol/*l* H_2SO_4
5 : Cathode (titanium plate, 7.5 cm^2 area)
6 : Anode (platinum plate)
7 : Cation exchange membrane (Nafion417)
8 : Stirring bar
9 : Magnetic stirrer
10 : N_2 bubbling tube

Fig. 2.17. Two–compartment electrochemical cell for electro–reduction of Eu in aqueous solution.

cal measurement or electrolysis, N_2 gas was bubbled into the aqueous solution to purge the dissolved oxygen. The current–voltage curve obtained by use of the cell is shown in **Fig. 2.18.** The voltage E was defined as the potential of cathode vs. anode. The reduction current of Eu^{3+} was seen, together with that of the hydrogen generation. The electrolysis voltage of –2.5 ~ –3 V was found to be suitable to reduce the trivalent Eu. The relationship between electrolysis time and metal concentration in the aqueous solution is shown in **Fig. 2.19.** The aqueous feed solution of pH 3 in the cathodic compartment was stirred at 800 min^{-1} by using a magnetic stirrer. The concentration of Eu decreased with the electrolysis, while those of Sm and Gd were almost constant, indicating that Eu precipitated selectively as $EuSO_4$. The surface of the titanium electrode slightly became white, therefore $EuSO_4$ precipitated mainly on the electrode surface. The white precipitate obtained was dissolved in 2 mol/*l* HCl solution and the metal concentrations were measured. The contents were found to be 97.1% of Eu, 2.5% of Sm and 0.4% of Gd. Samarium showed a little tendency for copre–

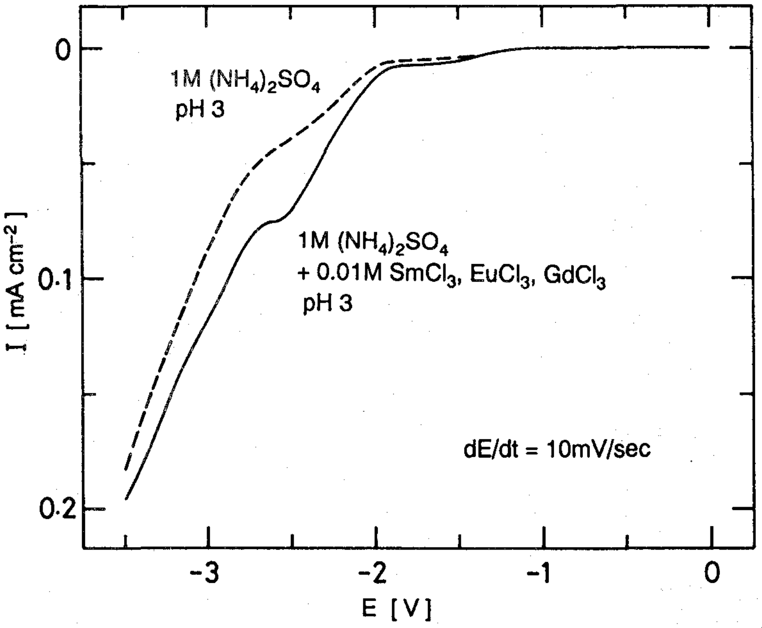

Fig. 2.18. Current–voltage curves obtained by use of titanium electrode in 1 mol/*l* $(NH_4)_2SO_4$ (pH 3) solution containing 0.01 mol/*l* rare–earth elements.

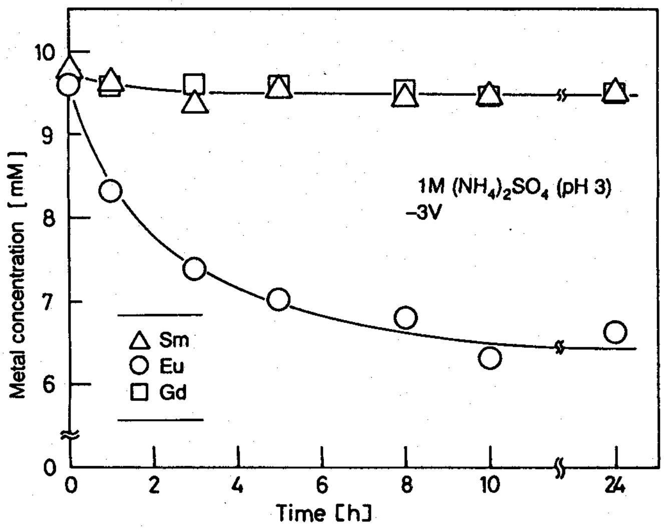

Fig. 2.19. Relationship between electrolysis time and metal concentrations in 1 mol/*l* $(NH_4)_2SO_4$ aqueous solution.

cipitation. The separation factors (= $([Eu]_p/[Ln]_p)/([Eu]_f/[Ln]_f)$ where Ln is Sm or Gd), $\beta_{Eu/Sm}$ and $\beta_{Eu/Gd}$, were 38.8 and 243, respectively.

2.3.3.2 Electro–reductive stripping of Eu

Since the electrical conductivity of the metal–loaded DP–18/xylene and D2EHPA/xylene solutions is extremely small, it is unlikely to reduce the extracted Eu at the organic phase/electrode interface. Thus, Eu^{3+} must be reduced at the aqueous phase/electrode interface after the mass transfer of Eu from the organic phase into aqueous phase, as in the case of electro–reductive stripping of vanadium described in the previous section. Furthermore, contact of the organic solution with the electrode must be avoided, since the electrolytic current of Eu^{3+} reduction is much decreased when the electrode surface is covered by the organic solution.

Figure 2.20 shows the two–compartment electrochemical cell used for the electro–reductive stripping. The aqueous solutions in the cathodic and anodic compartments were 1 mol/*l* $(NH_4)_2SO_4$ of appropriate pH. The dissolved

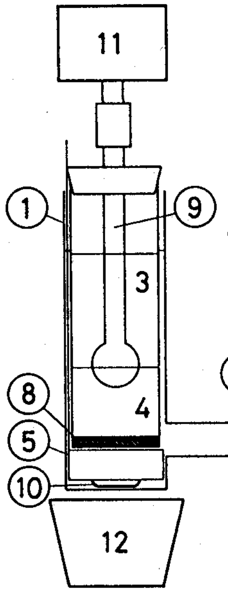

1 : Cathodic compartment
2 : Anodic compartment
3 : Organic phase (15 m*l*)
4 : Aqueous phase (15 m*l*)
5 : Cathode (titanium plate, 7.5 cm^2 area)
6 : Anode (platinum plate)
7 : Cation exchange membrane (Nafion417)
8 : Sintered glass filter
9 : Agitator
10 : Stirring bar
11 : Stirring motor
12 : Magnetic stirrer

Fig. 2.20. Two–compartment electrochemical cell for electro–reductive stripping of Eu.

oxygen in the aqueous solutions had been purged by N_2 gas bubbling prior to electrolysis. Equal volumes (15 m*l*) of the metal–loaded organic and aqueous solutions were agitated and electrolyzed in the cathodic compartment at room temperature. The agitation speeds of the agitator and the magnetic stirrer were 1500 min^{-1} and 800 min^{-1}, respectively. The sintered glass filter equipped in the cell could prevent the cathode from meeting with the organic solution.

The transport of Eu is an important factor of the electro–reductive stripping, since Eu^{3+} must transfer from the organic phase into aqueous phase prior to the electroreduction. The stripping performance of alkyl phosphoric acid extractants such as DP–18 or D2EHPA showed strong dependence on the stripping solution pH, as shown in **Fig. 2.21**. The three metals showed almost identical stripping performances in each system, and were stripped in the higher pH region in the DP–18 system than in the D2EHPA system. The region of pH < 3.5 in the DP–18 system and pH < 2.5 in the D2EHPA system are needed to transfer the elements into the aqueous phase. To avoid the hydrogen generation during the course of electrolysis which obstructs the Eu^{3+} reduction, the DP–18 system is recommended, since the operation at high pH is plausible.

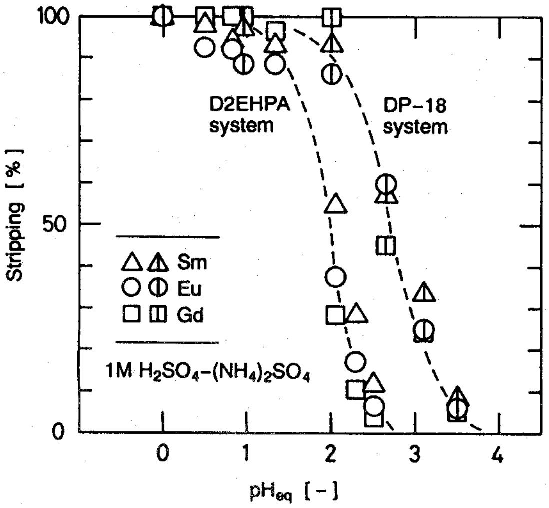

Fig. 2.21. Effect of stripping solution pH on stripping performances of Sm, Eu and Gd in DP–18 and D2EHPA systems.

Figure 2.22 shows the relationship between the aqueous phase final pH and the relative mole fraction of Eu in the precipitate, the aqueous and organic phase after 48 hours electrolysis at –3V in the DP–18 and D2EHPA systems, where the feed amount of Eu in the organic phase is made as 100%. The fraction of Eu in the precipitate was calculated by the mass–balance. In the range of pH greater than 3 in the DP–18 system and pH greater than 2.4 in the D2EHPA system, no precipitation of $EuSO_4$ occurred, since the mass transfer of Eu^{3+} from the organic into aqueous phase hardly occurred. At pH < 2.9, 40 ~ 60% of the feed Eu was precipitated in the DP–18 system. In this case, the amount of Eu remaining in the organic phase was smaller than that obtained without electrolysis shown by the closed triangular keys. This indicates that the electrolysis can enhance the stripping of Eu. In the D2EHPA system, the similar results were obtained, except for the pH condition. The precipitation of $EuSO_4$ occurred at pH < 2.3.

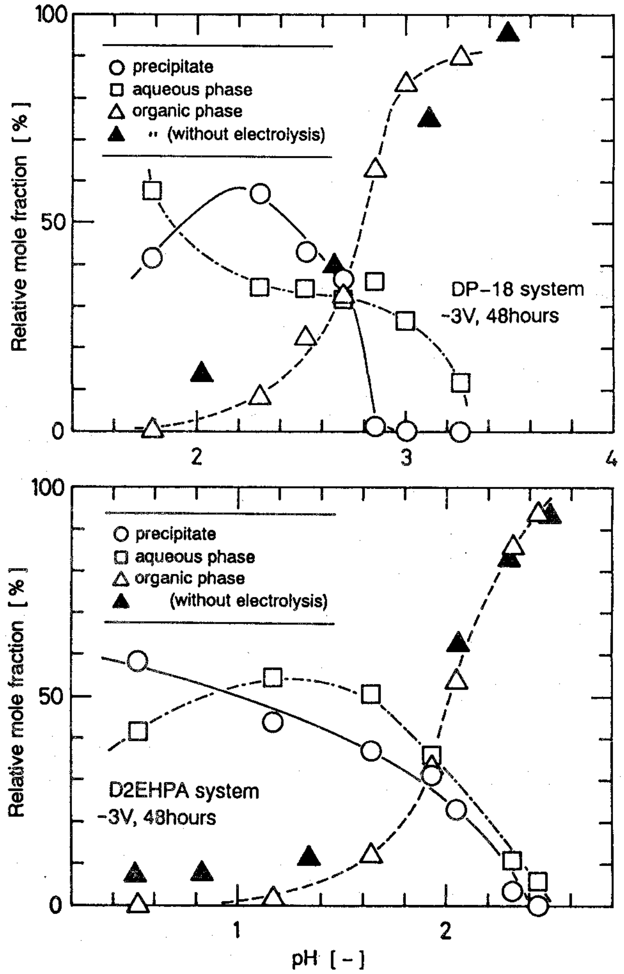

Fig. 2.22. Relationship between aqueous phase final pH and relative mole fraction of Eu in precipitate, aqueous and organic phase after 48 hours electrolysis at -3V in DP-18 and D2EHPA systems.

The effect of electrolysis time on stripping yields of Sm and Gd and the precipitation of $EuSO_4$ at various final pH conditions in the DP-18 system is shown in **Fig. 2.23**. The purity of Eu in the precipitate was more than 95% in all cases. The recovery of Eu as $EuSO_4$ attained up to 83.2% at pH 1.8. The stripping of Sm and Gd decreases with increasing pH. The selective recovery of Eu as the $EuSO_4$ precipitate is, therefore, plausible, remaining Sm and Gd in the organic phase. In the case of 72 hours electrolysis at pH 2.9, the fractions of

$EuSO_4$ and Eu^{3+} in the aqueous phase were 38.7% and 17.6%, respectively, and the stripping percentage was the sum of them, 56.3%, while the stripping percentages of Sm and Gd was 40.3% and 25.6%, respectively. However, it seems to be difficult to remain all of the Sm and Gd in the organic phase because of the very similar stripping performances of the three elements as shown in Fig. 2.21.

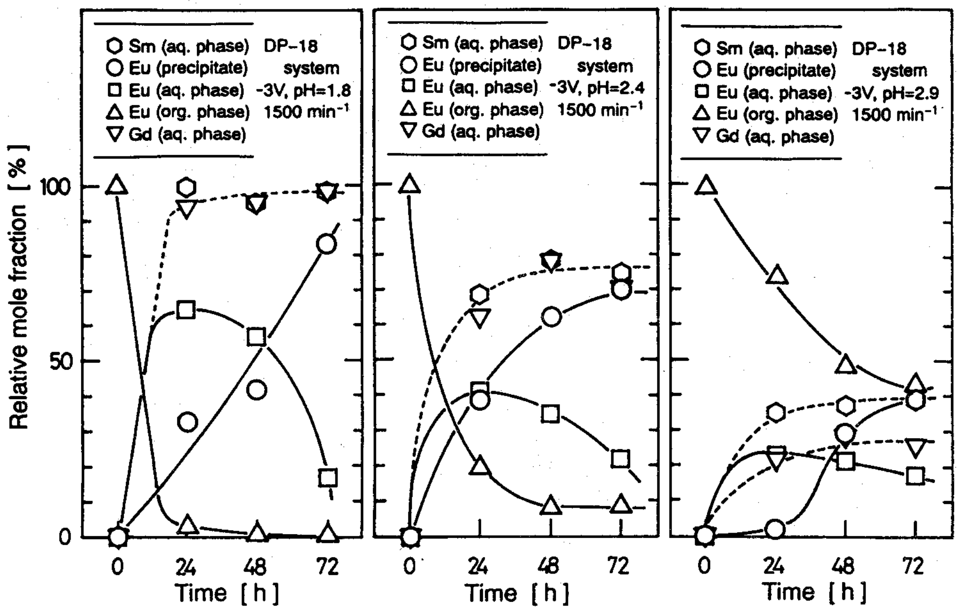

Fig. 2.23. Effect of electrolysis time on stripping yield of Sm and Gd and precipitation of $EuSO_4$ at various final pH conditions in DP-18 system.

2.3.4 Photochemical Reduction and Solvent Extraction for Separation of Europium from Samarium and Gadolinium

2.3.4.1 Photochemical reduction of Eu in aqueous solution

The photochemical reduction of Eu^{3+} in aqueous solution is shown as Eq. (2.8), where (H_2O) is a coordinated water.[13)]

$$Eu^{3+}(H_2O)_n \xrightarrow{h\nu} Eu^{2+}(H_2O)_{n-1} + H^+ + \cdot OH \qquad (2.8)$$

The radical (·OH) must be scavenged to avoid the back reaction, *i.e.*, the oxidation of Eu^{2+}. An alcohol such as 2–propanol or an ester such as isopropyl formate scavenges the radical effectively.[12)]

$$(CH_3)_2CHOH + \cdot OH \longrightarrow H_2O + (CH_3)_2\dot{C}OH \tag{2.9}$$

The organic radical formed can reduce Eu^{3+}.

$$(CH_3)_2\dot{C}OH + Eu^{3+} \longrightarrow Eu^{2+} + H^+ + (CH_3)_2C{=}O \tag{2.10}$$

In this study, isopropyl formate or 2–propanol was used as the scavenger. Since Eu^{2+} is not stable in aqueous solution, it must be removed as precipitate immediately. Ammonium sulfate was used as a precipitation agent to make $EuSO_4$.

Figure 2.24 shows the absorption spectra of aqueous solutions containing $EuCl_3$. The absorption at 195 nm corresponds to a charge–transfer band.[13)] In the solution containing Eu^{3+} and SO_4^{2-}, an absorption band around the wavelength of 235 nm also appeared, which was attributed to a shift of the charge–transfer band.[12)] This suggests that a longer wavelength light as well as a shorter wavelength light is employed for the photoreduction.

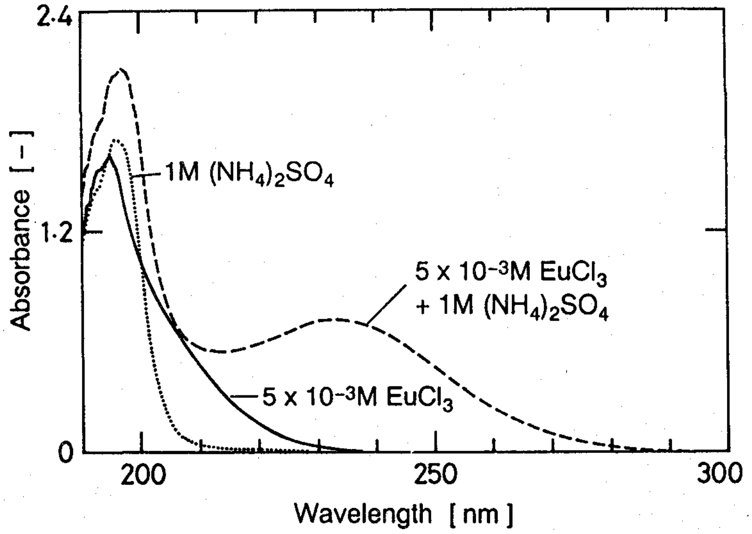

Fig. 2.24. Absorption spectra of aqueous solutions containing $EuCl_3$.

The photochemical reduction of Eu in aqueous solution was carried out in a beaker type glass bottle with agitation at 800 min^{-1} by using a magnetic stirrer. The relationships between irradiation time and concentration of Sm, Eu and Gd in 0.85 mol/*l* $(NH_4)_2SO_4$ aqueous solution using 2–propanol and isopropyl formate as the scavenger are shown in **Figs. 2.25 and 2.26**, respectively. The concentration of Eu decreased with photolysis, while that of Sm and Gd slightly decreased, indicating that Eu precipitated selectively as $EuSO_4$. The white precipitate obtained was separated by centrifuge and was dissolved in concentrated HNO_3 to measure the metal concentrations. The purity of Eu in the precipitate was more than 97% in all cases. In the case of 2–propanol employed, the precipitation occurred in a shorter time (80% of the feed Eu precipitated in 4

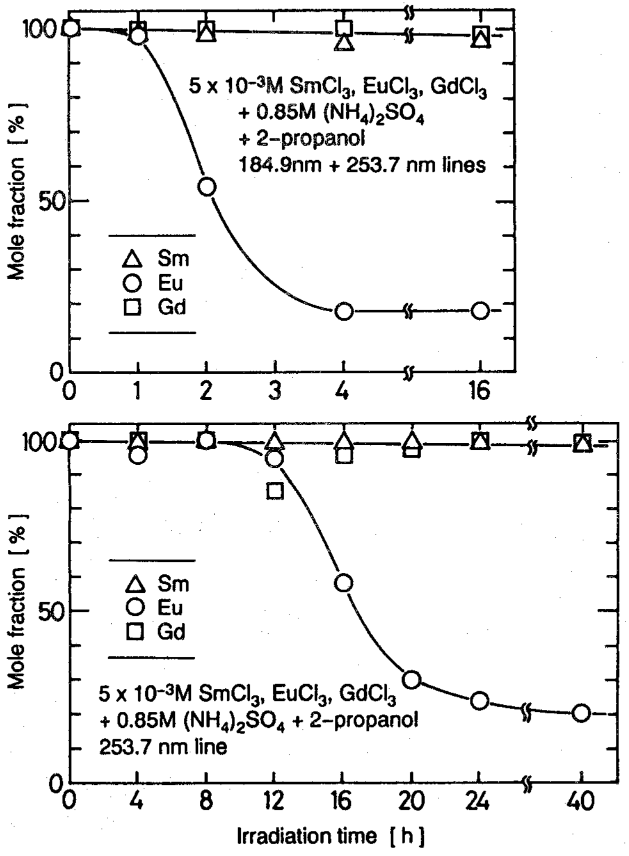

Fig. 2.25. Relationship between irradiation time and mole fractions of rare–earth elements in $(NH_4)_2SO_4$ aqueous solution using 2–propanol as scavenger.

hours) than in the case of isopropyl formate, since 2–propanol was water–soluble and scavenged the ·OH radical effectively. The 184.9 nm line was seemed to be effective for the photoreduction of Eu^{3+}. On the other hand, when isopropyl formate was used as the scavenger, the precipitation of $EuSO_4$ hardly occurred in first 12 hours, since the solubility of isopropyl formate was small to dissolve in the aqueous phase in several hours. No deference was seen between the cases of both 184.9 nm and 253.7 nm lines used and 253.7 nm line alone used, when isopropyl formate was employed. In the case of concentration of the rare–earth chloride being 1 x 10^{-2} mol/*l*, the precipitation of $EuSO_4$ occurred more slowly. Seventy percent of the feed Eu precipitated in 28 hours.

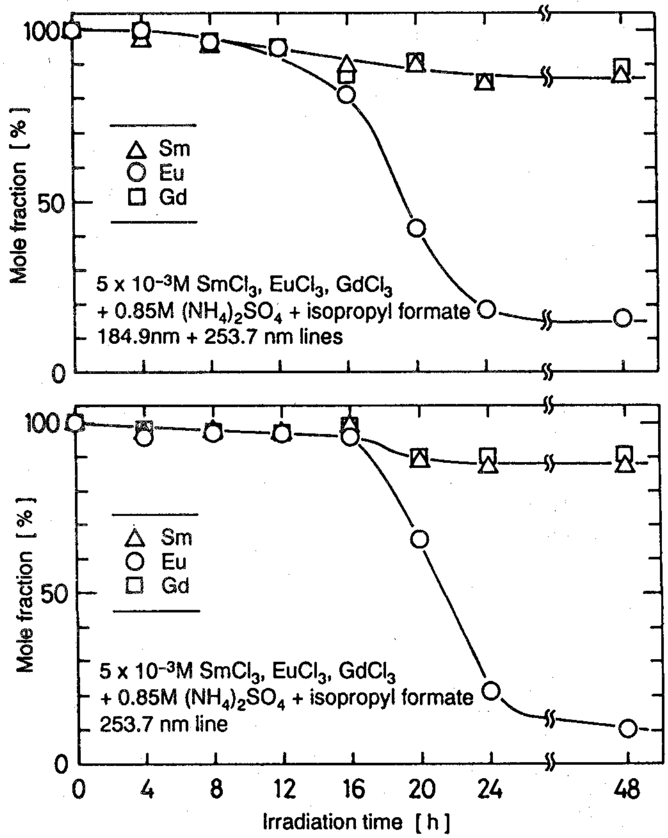

Fig. 2.26. Relationship between irradiation time and mole fractions of rare–earth elements in $(NH_4)_2SO_4$ aqueous solution using isopropyl formate as scavenger.

2.3.4.2 Photo-reductive stripping of Eu

Figure 2.27 shows the absorption spectra of the metal-loaded and non-loaded D2EHPA/xylene solutions. No absorption band which correspond to the charge-transfer band is seen. The photoreduction of Eu seems to be occurring only when the coordinated water and scavenger are located near the Eu^{3+} ion, *i.e.*, it does not occur in the organic phase. Therefore, Eu^{3+} must be reduced in the aqueous phase after the mass transfer of Eu has occurred from the organic phase into the aqueous phase. The aqueous solution of $pH < 2.5$ must be used as in the case of electro-reductive stripping in the D2EHPA system. When water-soluble scavengers such as ethanol, 1-butanol, 2-propanol, 3-pentanol, ammonium sulfite and formic acid were used, white undesirable precipitate containing Sm, Eu and Gd was obtained by mixing the organic and aqueous solutions. In the case of isopropyl formate employed, such undesirable precipitates were not observed. However, it hardly worked as scavenger, since it was soluble in the organic phase and not in the aqueous phase when the two phases were mixed in a beaker type glass bottle. Thus, isopropyl formate must be separated from the organic phase.

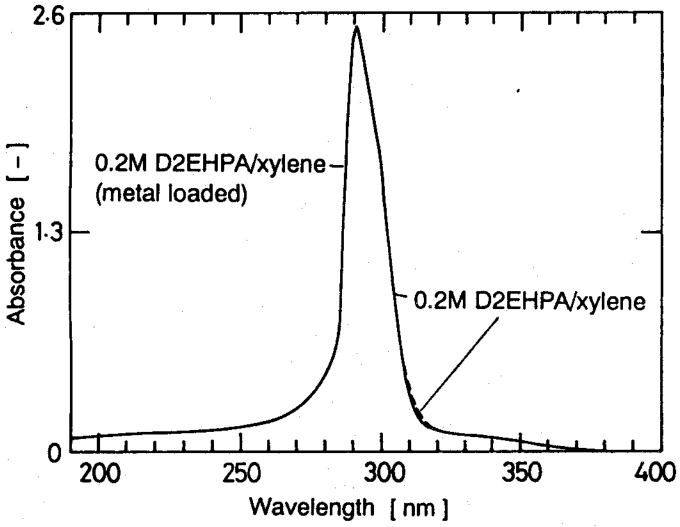

Fig. 2.27. Absorption spectra of metal-loaded and non-loaded D2EHPA/ xylene solutions.

Figure 2.28 shows a two–compartment photochemical cell separated by a sintered glass filter used for the photo–reductive stripping. The metal–loaded organic solution (25 m*l*), aqueous solution (1 mol/*l* H_2SO_4–$(NH_4)_2SO_4$, 22 m*l*) and scavenger (isopropyl formate, 3 m*l*) were agitated and photolyzed at room temperature. Both agitation speeds of the agitator and the magnetic stirrer were $800\ \text{min}^{-1}$.

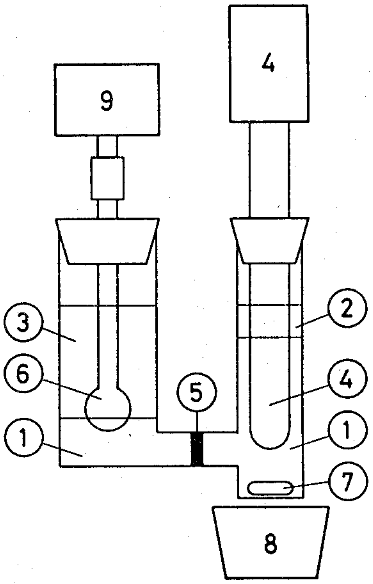

1 : Aqueous solution (22 m*l*)
2 : Isopropyl formate (3 m*l*)
3 : Organic phase (25 m*l*)
4 : Low–pressure mercury lamp
5 : Sintered glass filter
6 : Agitator
7 : Stirring bar
8 : Magnetic stirrer
9 : Stirring motor

Fig. 2.28. Two–compartment photochemical cell for reductive stripping of Eu.

The effect of the irradiation time on the stripping yields of Sm and Gd and the precipitation of $EuSO_4$ is shown in **Fig. 2.29**, where the feed amounts of elements in the organic phase are made as 100%. The pH values in the figure shows the aqueous phase final pH. The fraction of Eu in the precipitate was calculated by the mass–balance. The purity of Eu in the precipitate was more than 95% in all cases. The recovery of Eu as $EuSO_4$ attained to 68% at pH 0.4. The stripping of Sm and Gd decreases with increasing pH. The selective recovery of Eu as the $EuSO_4$ precipitate is, therefore, plausible, remaining Sm and Gd in the organic phase. However, it seems to be difficult to remain all of the Sm and Gd in the organic phase because of the very similar stripping performances of the three elements, as encountered previously in the electro-reductive stripping.

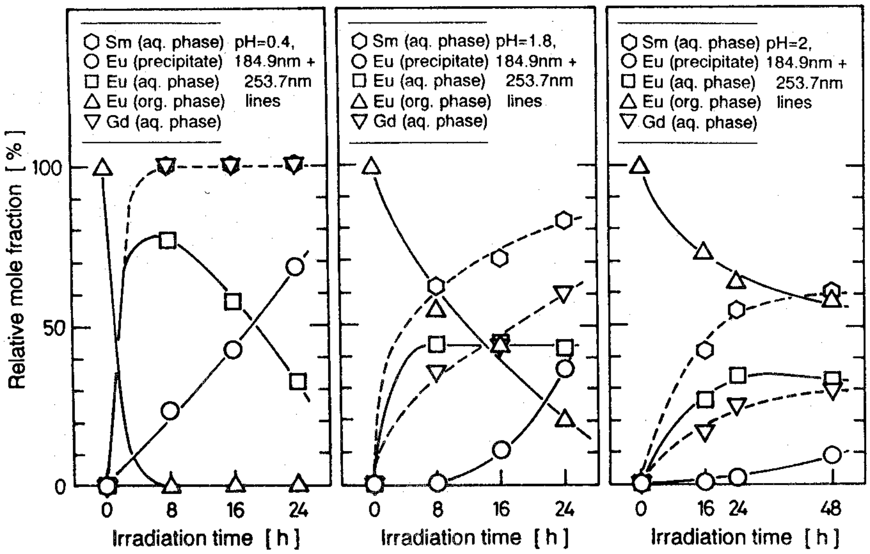

Fig. 2.29. Effect of irradiation time on stripping yield of Sm and Gd and precipitation of $EuSO_4$ at various final pH conditions

2.4 Summary

The separation and purification of rare metals by solvent extraction followed by reductive stripping has been studied with the following results.

(1) Vanadium was extracted from neutral solutions preferentially by tri-*n*-octylmethylammonium chloride (TOMAC) as compared to molybdenum. The resulting vanadium concentration in the organic phase was more than 12 times that of molybdenum. The extracted vanadium was selectively stripped by the chemical reduction method, in which the vanadium is reduced from a pentavalent anion to tetra- and trivalent cations. The appropriate selection of reduction agent concentration and of solution pH gave high separation efficiency and percentage recovery. The highest separation efficiency obtained by this process was 1.64×10^4.

(2) The pentavalent vanadyl anion was reduced to the tetravalent vanadyl

cation at the aqueous electrolyte/electrode interface in the two-phase system. The reduced vanadium was stripped efficiently, whereas the molybdenum remained in the organic phase. At the low agitation speed such as 300 min^{-1}, the stripping rate was influenced by the mass transfer of vanadyl ion from the organic into aqueous phase. At the higher agitation speed such as 1000 ~ 2000 min^{-1}, the diffusion in the glass filter and the electrochemical reduction of vanadyl ion at the aqueous phase/electrode interface affected the stripping rate. The organic solution after electro-reductive stripping was reusable for the extraction of vanadium and molybdenum without any further treatments.

(3) The trivalent Eu was reduced to the divalent state by electroreduction method using a two-compartment cell separated by a cation exchange membrane and equipped with a titanium plate electrode. In $(NH_4)_2SO_4$ aqueous solution containing equal amounts of $SmCl_3$, $EuCl_3$ and $GdCl_3$, $EuSO_4$ precipitated selectively by electroreduction. The purity of Eu in the precipitate was more than 97%. In the two-phase system consisted of metal-loaded di-5-methyl-2-(1-methylneohexyl)neodecanoyl phosphoric acid (DP-18) or bis(2-ethylhexyl)phosphoric acid (D2EHPA) diluted with xylene and $(NH_4)_2SO_4$ aqueous solutions, Eu^{3+} was reduced at the aqueous phase/electrode interface and $EuSO_4$ precipitated selectively in the aqueous phase. The recovery of Eu as $EuSO_4$ from the organic solution containing equal amounts of three elements was dependent on the aqueous phase pH and attained up to 83.2% at pH 1.8 in the DP-18 system. The purity of Eu in the precipitate was more than 95%.

(4) The trivalent Eu was reduced to the divalent state by UV light irradiation with a low-pressure mercury lamp. In $(NH_4)_2SO_4$ aqueous solution containing equal amounts of $SmCl_3$, $EuCl_3$, $GdCl_3$ and scavenger (2-propanol or isopropyl formate), $EuSO_4$ precipitated selectively by photoreduction. The purity of Eu in the precipitate was more than 97%. In the two-phase system consisted of D2EHPA/xylene containing the three elements and $(NH_4)_2SO_4$ aqueous solution, Eu^{3+} was reduced in the aqueous phase using isopropyl formate as scavenger and $EuSO_4$ precipitated selectively. The recovery of Eu as

$EuSO_4$ from the organic solution containing equal amounts of the three elements was dependent on the aqueous phase pH and attained up to 68% at pH 0.4. The purity of Eu in the precipitate was more than 95%.

Chapter 3 Separation and Purification of Rare–Earth Elements by Synergistic Extraction

3.1 Introduction

The modification of the extracted species by adding the other extractant may be one of the effective method to improve the extraction and separation of rare metals. In this chapter, the separation and purification of rare–earth elements by synergistic extraction has been studied. The synergistic extraction of the elements using a mixture of tri–*n*–octylmethylammonium nitrate (TOMAN) and β–diketone extractant (α–acetyl–*m*–dodecylacetophenone : LIX54) has already been reported[28)] and will be summarized in section 3.3.1. The other combination of alkyl phosphoric acid and TOMAN has been studied. As acid extractant, di–5–methyl–2–(1–methylneohexyl)neodecanoyl phosphoric acid (DP–18) was used. Extraction equilibrium formulations have been established for synergistic extraction as well as for extraction by DP–18 alone.

3.2 Experimental

Tri–*n*–octylmethylammonium chloride (TOMAC) was dissolved in xylene to around 1 mol/*l*, and converted to the nitrate form (TOMAN) by contacting with 2 mol/*l* nitric acid. The resulting solution was rinsed with distilled water. Alkyl phosphoric acid extractant, di–5–methyl–2–(1–methylneohexyl)neodecanoyl phosphoric acid was used as delivered as DP–18 from Daihachi Chemicals Ind. Co., Ltd., Japan. The active ingredient in DP–18 was determined as 72wt% by alkaline titration. The influence of impurities (monoesters (3%), olefins and alcohols) on the extraction was neglected, and only the diester was assumed to be effective for the extraction. The organic solution for the extraction was prepared by diluting the extractants with xylene. Rare–earth nitrates were prepared by dissolving oxides (supplied by Shin–Etsu Chem. Ind. Co. Ltd., Tokyo, 99.9% or by Nippon Yttrium Co. Ltd., Tokyo, 99.9%) in nitric acid and removing the excess acid by evaporation. Stock solution of the individual rare-earth elements were prepared by dissolving each nitrate in distilled water and were standardized by EDTA titration using xylenol orange as indicator. Ammonium nitrate of 6 mol/*l* was used a as salting-out agent.

Equal volumes of an organic and an aqueous solution were equilibrated at 25°C. A weighed organic sample was stripped with 1 mol/*l* nitric acid. The rare-earth concentration in aqueous solutions was determined with an inductively coupled argon plasma atomic emission spectrophotometer (Nippon Jarrell-Ash ICAP-575MarkII).

3.3 Results and Discussion

3.3.1 Synergistic Extraction of Rare-Earth Elements by Tri-*n*-octylmethyl-ammonium Nitrate and β-Diketone

In this section, the extraction of rare-earth elements in the LIX54 and LIX54-TOMAN systems containing ammonium nitrate as a salting-out agent is summarized. The detail study was already reported.[28)]

The extraction performance of LIX54 for the elements increases with position in the atomic number series. The behavior of extraction is divided into four tetrads, with the behavior of Y lying between Dy and Ho. Water and ammonium nitrate are not extracted. The extraction scheme is formulated as follows, where RH and R denote LIX54 and anion of LIX54, respectively.

$$\mathrm{Ln^{3+}} + 4\overline{\mathrm{RH}} = \overline{\mathrm{LnR_3RH}} + 3\mathrm{H^+} \tag{3.1}$$

The extraction equilibrium constants obtained are 1.0×10^{-10} for Nd, 3.98×10^{-9} for Dy and 3.89×10^{-8} *l*/mol for Yb.

In the LIX54-TOMAN system, the extraction performance of the mixed extractant is essentially identical to that of TOMAN alone in the range of pH 2 ~ 3, since LIX54 is a weak extractant by itself. With increase of pH a strong synergism appears, and the relative increase in the performance increases with the atomic number of the element. The synergistic extraction scheme is made as follows. At low loading of the organic phase,

$$\mathrm{Ln^{3+} + 2NO_3^- + \overline{RH} + 5\overline{S} = \overline{Ln(NO_3)_2R\cdot 5S} + H^+}$$

$$K_{115} = [\overline{\mathrm{Ln(NO_3)_2R\cdot 5S}}][\mathrm{H^+}] \,/\, [\mathrm{Ln^{3+}}][\overline{\mathrm{RH}}][\overline{\mathrm{S}}]^5 a_{\mathrm{NO_3}}{}^{-2} \qquad (3.2)$$

$$\mathrm{Ln^{3+} + NO_3^- + 2\overline{RH} + 4\overline{S} = \overline{Ln(NO_3)R_2\cdot 4S} + 2H^+}$$

$$K_{124} = [\overline{\mathrm{Ln(NO_3)R_2\cdot 4S}}][\mathrm{H^+}] \,/\, [\mathrm{Ln^{3+}}][\overline{\mathrm{RH}}]^2[\overline{\mathrm{S}}]^4 a_{\mathrm{NO_3}}{}^{-} \qquad (3.3)$$

At high loading of the organic phase,

$$\mathrm{Ln^{3+} + 3NO_3^- + \overline{Ln(NO_3)_2R\cdot 5S} = \overline{Ln(NO_3)_3Ln(NO_3)_2R\cdot 5S}}$$

$$K_{215} = [\overline{\mathrm{Ln(NO_3)_3Ln(NO_3)_2R\cdot 5S}}] \,/\, [\mathrm{Ln^{3+}}][\overline{\mathrm{Ln(NO_3)_2R\cdot 5S}}] a_{\mathrm{NO_3}}{}^{-3} \qquad (3.4)$$

$$\mathrm{Ln^{3+} + 3NO_3^- + \overline{Ln(NO_3)R_2\cdot 4S} = \overline{Ln(NO_3)_3Ln(NO_3)R_2\cdot 4S}}$$

$$K_{224} = [\overline{\mathrm{Ln(NO_3)_3Ln(NO_3)R_2\cdot 4S}}] \,/\, [\mathrm{Ln^{3+}}][\overline{\mathrm{Ln(NO_3)R_2\cdot 4S}}] a_{\mathrm{NO_3}}{}^{-3} \qquad (3.5)$$

The extraction equilibrium constants for Nd, Dy and Yb are shown in **Table 3.1**. This scheme expresses the extraction behavior of the elements for the whole range of the loadings of the extractant.

The separation factors with the mixed extractants laid between those attained by TOMAN alone and those by LIX54 alone. The separation of Nd, Yb and Y may be possible with the following procedure. Yttrium is extracted like as middle rare–earth element at pH 6, but like as heavy element at pH 2 ~ 3. It is thus possible to extract the light and middle elements at pH 2 ~ 4 and subsequently to extract the heavy elements at pH 6, leaving Y in the aqueous phase. The separation of Nd, Dy and Yb is not effective in the high loading region.

Table 3.1. Extraction equilibrium constants for Nd, Dy and Yb in system of TOMAN alone for $[\overline{\mathrm{TOMAN}}] = 0.1$ mol/*l*, and those for synergistic adducts in LIX54–TOMAN system.

		Nd	Dy	Yb
K_{105}	$[(\mathrm{mol}/l)^{-8}]$	1.87×10^{10}	2.39×10^{9}	7.22×10^{8}
K_{205}	$[(\mathrm{mol}/l)^{-4}]$	7.73×10^{-2}	8.75×10^{-1}	2.30×10^{-1}
K_{115}	$[(\mathrm{mol}/l)^{-7}]$	7.7×10^{4}	5.3×10^{4}	7.9×10^{4}
K_{124}	$[(\mathrm{mol}/l)^{-5}]$	8.1×10^{-2}	2.0×10^{-1}	2.1
K_{215}	$[(\mathrm{mol}/l)^{-6}]$	1.3×10^{-1}	4.4×10^{-2}	0
K_{224}	$[(\mathrm{mol}/l)^{-1}]$	1.3×10^{-1}	1.3×10^{-1}	5.1×10^{-2}

Thus the loading of the organic phase as well as aqueous–phase proton concentration must be carefully controlled to achieve an effective separation.

3.3.2 Synergistic Extraction of Rare–Earth Elements by Tri–*n*–octylmethylammonium Nitrate and Alkyl Phosphoric Acid

3.3.2.1 Extraction of rare–earth elements by DP–18 or TOMAN alone

1) DP–18 The effect of proton concentration on the distribution ratios of Nd, Tb and Er is shown in **Fig. 3.1.** A slope of −1.5 was obtained. Since the rare–earth cations are trivalent, one or two nitrate anions are likely to be contained in the extracted species in order to compensate the positive charge of the metal cations. The extractant is assumed to exist as dimer in an apolar solvent, as in the case of bis(2–ethylhexyl)phosphoric acid (D2EHPA)37) and didodecylphosphoric acid.29) The variation of the distribution ratios at pH 2 and pH 2.3 with the concentration of dimeric DP–18, $[\overline{(\mathrm{RH})_2}]$, is shown in **Fig. 3.2.** Straight lines of slope = 3 are obtained in the range of $[\overline{(\mathrm{RH})_2}] = 0.018 \sim 0.22$ mol/*l*. Thus, the following extraction equilibrium formulations are made.

$$\mathrm{Ln}^{3+} + 3\overline{(\mathrm{RH})_2} + \mathrm{NO_3}^- = \overline{\mathrm{LnR_2(NO_3)\cdot 4(RH)}} + 2\mathrm{H}^+$$

$$K_{ex,1} = [\overline{\mathrm{LnR_2(NO_3)\cdot 4(RH)}}][\mathrm{H}^+]^2 / [\mathrm{Ln}^{3+}][\overline{(\mathrm{RH})_2}]^3 a_{\mathrm{NO_3}^-} \qquad (3.6)$$

$$Ln^{3+} + 3\overline{(RH)_2} + 2NO_3^- = \overline{LnR(NO_3)_2{\cdot}5(RH)} + H^+$$

$$K_{ex,2} = [\overline{LnR(NO_3)_2{\cdot}5(RH)}][H^+] \,/\, [Ln^{3+}][\overline{(RH)_2}]^3 a_{NO_3}{}^{-2} \qquad (3.7)$$

where $a_{NO_3^-}$ is mean ionic activity of ammonium nitrate, which is 2.04 in 6 mol/*l* NH_4NO_3.[31] RH and R denote the DP–18 extractant and anion of DP–18, respectively. The material balances for the extractant and rare–earth element extracted are expressed by Eqs. (3.8) and (3.9).

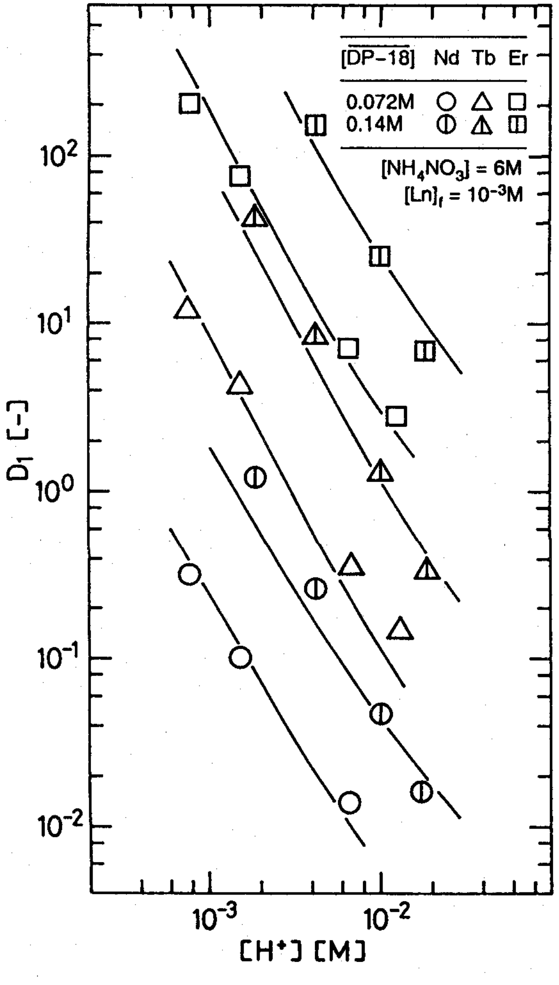

Fig. 3.1. Effect of proton concentration on distribution ratio of rare–earth elements in DP–18 system; comparison of observed data with prediction.

$$[\overline{\mathrm{RH}}]_f = 6[\overline{\mathrm{LnR_2(NO_3)\cdot 4(RH)}}] + 6[\overline{\mathrm{LnR(NO_3)_2\cdot 5(RH)}}] + 2[\overline{\mathrm{(RH)_2}}]$$
$$= 6K_{ex,1}[Ln^{3+}][\overline{\mathrm{(RH)_2}}]^3 a_{\mathrm{NO_3}}{}^{-} / [\mathrm{H^+}]^2 + 6K_{ex,2}[\mathrm{Ln^{3+}}][\overline{\mathrm{(RH)_2}}]^3 a_{\mathrm{NO_3}}{}^{-2} / [\mathrm{H^+}]$$
$$+ 2[\overline{\mathrm{(RH)_2}}] \qquad (3.8)$$

$$[\overline{\mathrm{Ln}}] = [\overline{\mathrm{LnR_2(NO_3)\cdot 4(RH)}}] + [\overline{\mathrm{LnR(NO_3)_2\cdot 5(RH)}}]$$
$$= K_{ex,1}[\mathrm{Ln^{3+}}][\overline{\mathrm{(RH)_2}}]^3 a_{\mathrm{NO_3}}{}^{-} / [\mathrm{H^+}]^2 + K_{ex,2}[\mathrm{Ln^{3+}}][\overline{\mathrm{(RH)_2}}]^3 a_{\mathrm{NO_3}}{}^{-2} / [\mathrm{H^+}]$$
$$(3.9)$$

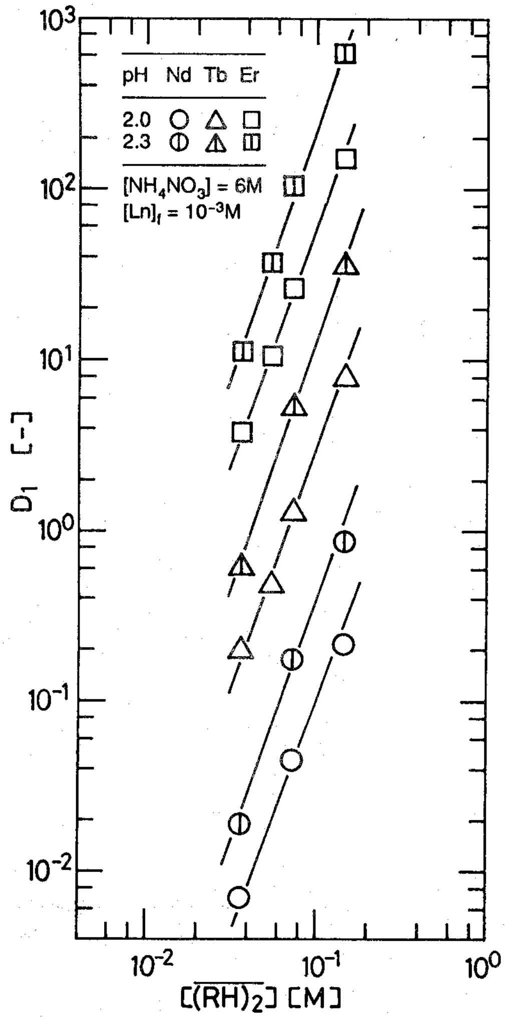

Fig. 3.2. Effect of concentration of DP−18 extractant on distribution ratio of rare-earth elements in DP−18 system.

The most likely values, $K_{ex,1}$ and $K_{ex,2}$, were estimated by minimizing the sum of the residuals based on Eqs. (3.8) and (3.9). The constants obtained for Nd, Tb and Er are shown in **Table 3.2**. With these constants, distribution ratios can be predicted and are shown in Fig. 3.1 by solid lines, which show good agreement with the experimental data. The variation of the distribution ratio with the atomic number is shown in **Fig. 3.3**. The extractability of the elements by DP-18 increases continuously with increasing atomic number, as in the case of D2EHPA.[36)]

2) TOMAN The extraction of rare-earth elements by TOMAN alone was already described in section 1.3.3. The extraction equilibrium constants, K_{105} and K_{205}, for Nd, Tb and Er are shown in Table 3.2, and $K_S = 6.6 \times 10^5$ (mol/*l*)$^{-5}$. The distribution ratios, D_0, for Nd, Tb and Er in the 0.1 mol/*l* TOMAN system are 1.31, 0.25 and 0.15, respectively. In the 0.2 mol/*l* TOMAN system, these are 3.33, 0.61 and 0.38, respectively.

3.3.2.2 Extraction of rare-earth elements with mixed extractant, DP-18 and TOMAN

Figure 3.4 shows the variation of the observed distribution ratio, *D*, with proton concentration in the DP-18-TOMAN system. As compared with D_1

Table 3.2. Extraction equilibrium constants for Nd, Tb and Er in DP-18 alone system, in TOMAN alone system and those for synergistic adducts in DP-18-TOMAN system.

		Nd	Tb	Er
$K_{ex,1}$	[(mol/*l*)$^{-2}$]	2.27×10^{-3}	1.25×10^{-1}	2.52
$K_{ex,2}$	[(mol/*l*)$^{-4}$]	1.82×10^{-2}	1.89	6.87×10^{1}
K_{105}	[(mol/*l*)$^{-8}$]	1.87×10^{10}	2.59×10^{9}	1.56×10^{9}
K_{205}	[(mol/*l*)$^{-4}$]	7.73×10^{-1}	1.40	1.03
K_{112}	[(mol/*l*)$^{-4}$]	6.20×10^{2}	3.76×10^{3}	3.05×10^{3}
K_{122}	[(mol/*l*)$^{-3}$]	6.78×10^{1}	4.05×10^{2}	1.36×10^{2}

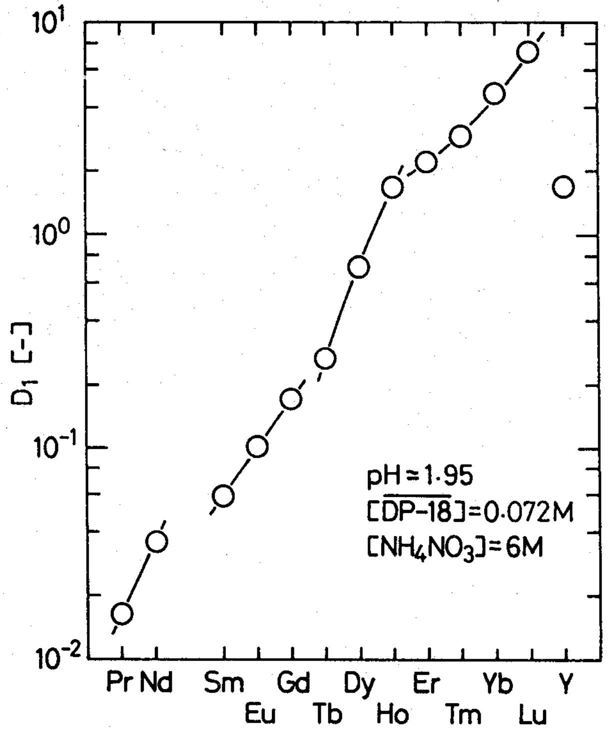

Fig. 3.3. Variation of distribution ratio of rare-earth elements with atomic number in DP–18 system.

values shown in Fig. 3.1 and with D_0 values, enhancement of the extractability by synergistic effect is seen. For Nd, the effect is pronounced in the range of $[H^+] < 10^{-2}$ mol/*l*, while for Tb the effect is seen throughout the pH range. For Er, the enhancement of extraction is less favored; the distribution ratio in the DP–18–TOMAN system is almost identical to that in the DP–18 alone system.

The mechanism of synergistic extraction is investigated as follows. The observed distribution ratio, D, is assumed to consist of the contributions from TOMAN alone (D_0), DP–18 alone (D_1) and synergistic adducts (D_S). Thus,

$$D_S = D - D_0 - D_1 \tag{3.10}$$

The method of slope analysis is applicable here. The effect of proton concentra–

tion on D_S is shown in **Fig. 3.5**. The straight lines of slope −1.5 are obtained in the several extractant conditions, indicating that one or two nitrate anions are involved in the extraction to compensate the positive charge of the trivalent rare–earth cations. The effect of extractant concentration on D_S is shown in **Fig. 3.6**. The plot of D_S vs. $[\overline{(RH)_2}]$ gives the straight lines of slope 1.4. Thus, one or two $(RH)_2$ are involved in the extraction. As for the effect of TOMAN concentration, the slopes 0.4 and 0.6 are obtained. Since most TOMAN is associated as tetramer in the present range of concentration as shown in section 1.3.3, the values of D_S are considered to be proportional to the 2nd power of the monomeric concentration of TOMAN. On the basis of these findings, extraction equilibrium formulations for the synergistic extraction can be made as Eqs. (3.11) and (3.12) where S denotes the monomeric species of TOMAN.

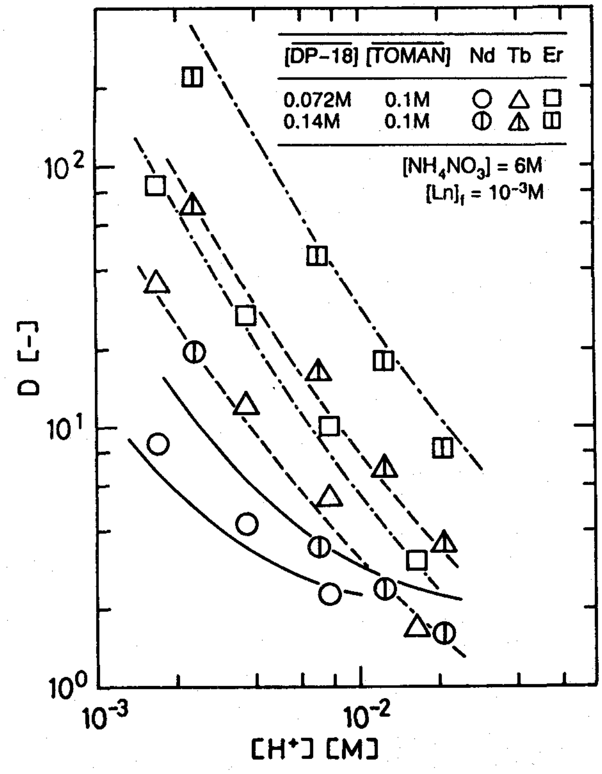

Fig. 3.4. Effect of proton concentration on distribution ratio of rare–earth elements in DP–18–TOMAN system; comparison of observed data with prediction.

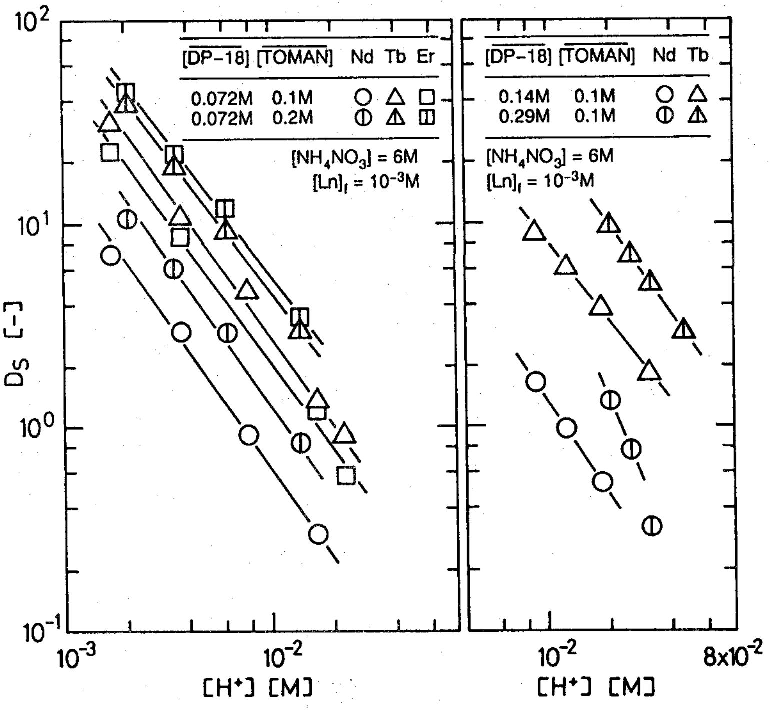

Fig. 3.5. Effect of proton concentration on distribution ratio of synergistic adducts.

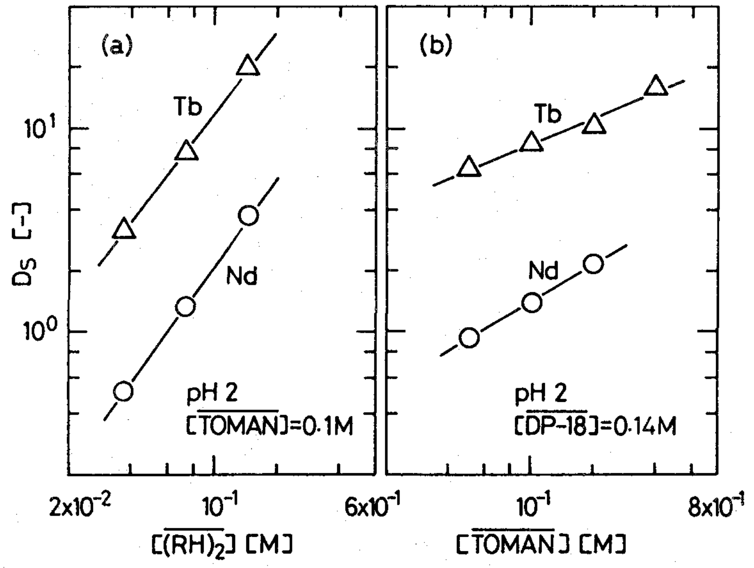

Fig. 3.6. Effect of (a) DP-18 and (b) TOMAN concentration on distribution ratio of synergistic adducts.

$$\mathrm{Ln^{3+} + 2NO_3^- + \overline{(RH)_2} + 2\overline{S} = \overline{LnR(NO_3)_2(RH)\cdot 2S} + H^+}$$

$$K_{112} = [\overline{\mathrm{LnR(NO_3)_2(RH)\cdot 2S}}][\mathrm{H^+}] \,/\, [\mathrm{Ln^{3+}}][\overline{\mathrm{(RH)_2}}][\overline{\mathrm{S}}]^2 a_{\mathrm{NO_3}}{}^{-2} \qquad (3.11)$$

$$\mathrm{Ln^{3+} + NO_3^- + 2\overline{(RH)_2} + 2\overline{S} = \overline{LnR_2(NO_3)\cdot 2(RH)\cdot 2S} + 2H^+}$$

$$K_{122} = [\overline{\mathrm{LnR_2(NO_3)\cdot 2(RH)\cdot 2S}}][\mathrm{H^+}]^2 \,/\, [\mathrm{Ln^{3+}}][\overline{\mathrm{(RH)_2}}]^2[\overline{\mathrm{S}}]^2 a_{\mathrm{NO_3}}{}^{-} \qquad (3.12)$$

The material balances of DP–18 and TOMAN are expressed by Eqs. (3.13) and (3.14), respectively.

$$\begin{aligned}
[\overline{\mathrm{RH}}]_{\mathrm{f}} &= 6[\overline{\mathrm{LnR_2(NO_3)\cdot 4(RH)}}] + 6[\overline{\mathrm{LnR(NO_3)_2\cdot 5(RH)}}] + 2[\overline{\mathrm{LnR(NO_3)_2(RH)\cdot 2S}}] \\
&\quad + 4[\overline{\mathrm{LnR_2(NO_3)\cdot 2(RH)\cdot 2S}}] + 2[\overline{\mathrm{(RH)_2}}] \\
&= 6K_{ex,1}[\mathrm{Ln^{3+}}][\overline{\mathrm{(RH)_2}}]^3 a_{\mathrm{NO_3}}{}^{-} / [\mathrm{H^+}]^2 + 6K_{ex,2}[\mathrm{Ln^{3+}}][\overline{\mathrm{(RH)_2}}]^3 a_{\mathrm{NO_3}}{}^{-2} / [\mathrm{H^+}] \\
&\quad + 2K_{112}[\mathrm{Ln^{3+}}][\overline{\mathrm{(RH)_2}}][\overline{\mathrm{S}}]^2 a_{\mathrm{NO_3}}{}^{-2} / [\mathrm{H^+}] \\
&\quad + 4K_{122}[\mathrm{Ln^{3+}}][\overline{\mathrm{(RH)_2}}]^2[\overline{\mathrm{S}}]^2 a_{\mathrm{NO_3}}{}^{-} / [\mathrm{H^+}]^2 + 2[\overline{\mathrm{(RH)_2}}] \qquad (3.13)
\end{aligned}$$

$$\begin{aligned}
[\overline{\mathrm{TOMAN}}]_{\mathrm{f}} &= 4[\overline{\mathrm{S_4}}] + [\overline{\mathrm{S}}] + 4[\overline{\mathrm{NH_4NO_3\cdot 4S}}] + 5[\overline{\mathrm{Ln(NO_3)_3\cdot 5S}}] \\
&\quad + 5[\overline{\mathrm{\{Ln(NO_3)_3\}_2\cdot 5S}}] + 2[\overline{\mathrm{LnR(NO_3)_2(RH)\cdot 2S}}] \\
&\quad + 2[\overline{\mathrm{LnR_2(NO_3)\cdot 2(RH)\cdot 2S}}] \\
&= 4K_T[\overline{\mathrm{S}}]^4 + [\overline{\mathrm{S}}] + 4K_S[\overline{\mathrm{S}}]^4 a_{\mathrm{NO_3}}{}^{-2} + 5K_{105}[\mathrm{Ln^{3+}}][\overline{\mathrm{S}}]^5 a_{\mathrm{NO_3}}{}^{-3} \\
&\quad \times (1 + K_{205}[\mathrm{Ln^{3+}}] a_{\mathrm{NO_3}}{}^{-3}) + 2K_{112}[\mathrm{Ln^{3+}}][\overline{\mathrm{(RH)_2}}][\overline{\mathrm{S}}]^2 a_{\mathrm{NO_3}}{}^{-2} / [\mathrm{H^+}] \\
&\quad + 2K_{122}[\mathrm{Ln^{3+}}][\overline{\mathrm{(RH)_2}}]^2[\overline{\mathrm{S}}]^2 a_{\mathrm{NO_3}}{}^{-} / [\mathrm{H^+}]^2 \qquad (3.14)
\end{aligned}$$

The concentrations of $\overline{\mathrm{(RH)_2}}$ and $\overline{\mathrm{TOMAN}}$ monomer in each run can be calculated using the Newton–Raphson method, when temporary values of K_{112} and K_{122} are given. These extraction equilibrium constants are calculated by the Marquadt method to minimize the sum of the squares of residuals, which calculated on the basis of the material balance of the rare–earth element shown by Eq. (3.15).

$$
\begin{aligned}
[\overline{\mathrm{Ln}}] &= [\overline{\mathrm{LnR_2(NO_3)\cdot 4(RH)}}] + [\overline{\mathrm{LnR(NO_3)_2\cdot 5(RH)}}] + [\overline{\mathrm{Ln(NO_3)_3\cdot 5S}}] \\
&\quad + [\overline{\{\mathrm{Ln(NO_3)_3}\}_2\cdot 5\mathrm{S}}] + [\overline{\mathrm{LnR(NO_3)_2(RH)\cdot 2S}}] + [\overline{\mathrm{LnR_2(NO_3)\cdot 2(RH)\cdot 2S}}] \\
&= K_{ex,1}[\mathrm{Ln}^{3+}][\overline{(\mathrm{RH})_2}]^3 a_{\mathrm{NO_3}^-} / [\mathrm{H}^+]^2 + K_{ex,2}[\mathrm{Ln}^{3+}][\overline{(\mathrm{RH})_2}]^3 a_{\mathrm{NO_3}^-}{}^{2} / [\mathrm{H}^+] \\
&\quad + K_{105}[\mathrm{Ln}^{3+}][\overline{\mathrm{S}}]^5 a_{\mathrm{NO_3}^-}{}^{3} \times (1 + 2K_{205}[\mathrm{Ln}^{3+}] a_{\mathrm{NO_3}^-}{}^{3}) \\
&\quad + K_{112}[\mathrm{Ln}^{3+}][\overline{(\mathrm{RH})_2}][\overline{\mathrm{S}}]^2 a_{\mathrm{NO_3}^-}{}^{2} / [\mathrm{H}^+] \\
&\quad + K_{122}[\mathrm{Ln}^{3+}][\overline{(\mathrm{RH})_2}]^2[\overline{\mathrm{S}}]^2 a_{\mathrm{NO_3}^-} / [\mathrm{H}^+]^2 \qquad (3.15)
\end{aligned}
$$

The most appropriate values of K_{112} and K_{122} estimated by trial–and–error are shown in Table 3.2. Using these constants, the net distribution ratios of Nd, Tb and Er in the DP–18–TOMAN system are predicted and shown in Fig. 3.4 by solid lines. The synergistic extraction of the rare–earth elements are correlated well by the present extraction equilibrium formulations.

3.4 Summary

The extraction of rare–earth elements (Nd, Tb and Er) by di–5–methyl–2–(1–methylneohexyl)neodecanoyl phosphoric acid (DP–18) extractant and by DP–18–tri–*n*–octylmethylammonium nitrate (TOMAN) mixed extractant has been studied. In the DP–18 system, the extraction is expressed by Eqs. (3.6) and (3.7), and the extractability increases with the atomic number series. In the DP–18–TOMAN system, enhancement of the extractability by synergistic effect is observed. For Nd, the effect is favored at $[\mathrm{H}^+] < 10^{-2}$ mol/*l*, while the effect is observed in the all pH range of the present condition for Tb. For Er, the enhancement of extraction is less favored. A synergistic extraction scheme for the elements is presented as Eqs. (3.11) and (3.12), which accurately expresses the extraction behaviors. The mechanism of synergistic extraction of the rare–earth elements by TOMAN–β–diketone (α–acetyl–*m*–dodecylacetophenone : LIX54) was summarized in section 3.3.1. The extraction scheme was established.

Chapter 4 Separation and Purification of Rare–Earth Elements by Solvent Extraction and Aqueous–Phase Complexing Reaction

4.1 Introduction

In the rare–earth series, the chemical properties of adjacent members are very similar, making it very difficult to separate and purify the individual elements. Modification of the aqueous phase species by adding a water–soluble complexing agent may be an effective approach to coping with the limitation. As for the effect of the complexing agent on extraction and separation, Minagawa *et al.* reported on the selective extraction of yttrium over other heavy elements, based on the difference in the stability constants of the complexing agent with Y and the other elements.33) Matsuyama *et al.* found that the separation of Y and Er was achieved effectively by a non–equilibrium separation method using the difference in the extraction rates in the presence of the complexing agent.32) As the complexing agent, diethylenetriaminepentaacetic acid, DTPA, was employed in their studies. Organophosphoric acid extractants, 2–ethylhexylphosphonic acid mono–2–ethylhexyl ester (EHPNA), were employed of which the extractability of the elements increased with atomic number series.

In this chapter, the effect of addition of a complexing agent to tri–*n*–octylmethylammonium nitrate (TOMAN) and TOMAN–β–diketone (α–acetyl–*m*–dodecylacetophenone : LIX54) systems containing ammonium nitrate as a salting–out agent has been studied. The extraction of rare–earth elements by TOMAN and LIX54–TOMAN has already been studied27,28) and the extraction mechanism of the elements in the systems was summarized in section 1.3.3 and section 3.3.1, respectively. The extractability of the elements decreases with atomic number apart from a slight increase from Gd to Tb in the TOMAN system. The stability constants of the complexing agent and the rare–earth elements increase with the atomic number for light and middle series.56) A prospective process may therefore be established. Based on the results of the equilibrium studies, simulation of the extraction and separation of Pr and Nd by continuous countercurrent mixer–settler batteries was carried out to examine the effect of the complexing agent under conditions which might be employed in commercial operation. The complexing agent is generally added to the feed scrubbing solution and, therefore, separation of the elements from the complexing agent at the final stage of the extraction is needed. Extraction behavior of tri–*n*–butylphosphate (TBP) in aqueous solution was also studied.

4.2 Experimental

Tri–*n*–octylmethylammonium nitrate (TOMAN) and rare–earth nitrates were prepared as described in the section 3.2. β–Diketone extractant, α–acetyl–*m*–dodecylacetophenone was used as delivered as LIX54 from Henkel Co., Minneapolis, USA. Tri–*n*–butylphosphate (TBP) was supplied by Wako Pure Chem. Ind. Ltd. as analytically pure reagent grade. These extractants were diluted with xylene. Ammonium nitrate (6 mol/*l*) was used as a salting–out agent. Water–soluble complexing agents, ethylenediaminetetraacetic acid (EDTA, available as disodium salt type), diethylenetriaminepentaacetic acid (DTPA) and trans–1,2–cyclohexanediaminetetraacetic acid (CyDTA) were supplied by Dojindo Laboratories. Concentration of the complexing agent in the solution was determined by titration using Zn standard solution and xylenol orange as indicator.

The procedure for measurement of extraction equilibrium of rare–earth elements was identical to that described in the section 3.2. The stripping solution was 1 mol/*l* nitric acid.

4.3 Results and Discussion

4.3.1 Extraction equilibrium of single rare-earth elements in TOMAN-EDTA and LIX54-TOMAN-EDTA systems

The effect of proton concentration on the distribution ratio of a single rare-earth element in both systems is shown in **Fig. 4.1.** The EDTA concentration was about half the feed concentration of lanthanide. In the TOMAN-EDTA system, the distribution ratio was insensitive to pH in the range observed, whereas it increased with pH value in the LIX54-TOMAN-EDTA system. When the concentration of EDTA was further increased above that of the rare-earth element, almost no metal was found to be extracted. Thus, it is assumed here that (i) all EDTA in the aqueous phase makes 1 : 1 complex with the rare earth; (ii) this complex is inactive for extraction, and only free rare-earth ions (not complexed with EDTA) can take part in the extraction.

The feed concentration of rare-earth element a, $[a]_f$, is shown as Eq. (4.1), where L and aL denote EDTA and rare earth-EDTA complex, respectively.

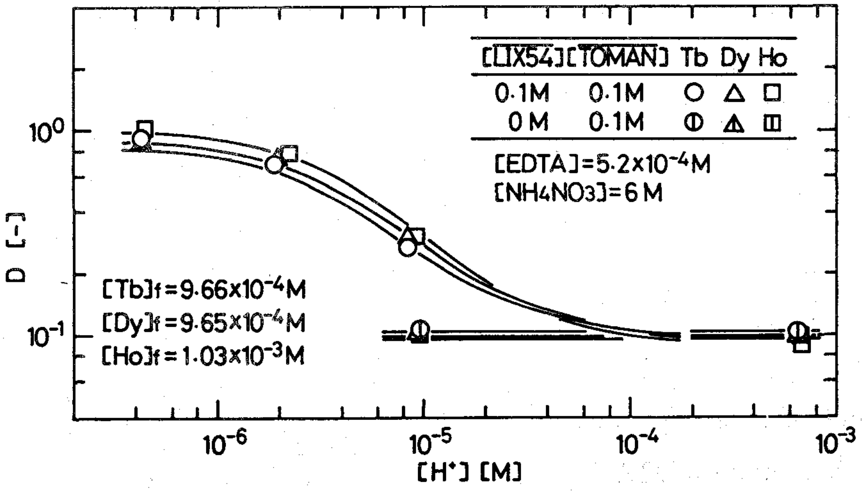

Fig. 4.1. Effect of proton concentration on distribution ratio of single rare-earth elements in TOMAN-EDTA and LIX54-TOMAN-EDTA systems; comparison of observed data with prediction shown by solid lines.

$$[\mathrm{a}]_\mathrm{f} = [\mathrm{a}] + [\mathrm{aL}] + [\bar{\mathrm{a}}] \tag{4.1}$$

The distribution ratio in the absence of complexing agent, D_0, is

$$D_0 = [\bar{\mathrm{a}}] / [\mathrm{a}] \tag{4.2}$$

Thus, the concentration of the element in the organic phase is shown by Eq. (4.3).

$$[\bar{\mathrm{a}}] = D_0([\mathrm{a}]_\mathrm{f} - [\mathrm{aL}]) / (1 + D_0) \tag{4.3}$$

Total metal concentration in the aqueous phase, $[\mathrm{a}]_\mathrm{aq}$, is

$$\begin{aligned}[\mathrm{a}]_\mathrm{aq} &= [\mathrm{a}] + [\mathrm{aL}] = [\mathrm{a}]_\mathrm{f} - [\bar{\mathrm{a}}] = [\mathrm{a}]_\mathrm{f} - D_0([\mathrm{a}]_\mathrm{f} - [\mathrm{aL}]) / (1 + D_0) \\ &= ([\mathrm{a}]_\mathrm{f} + D_0[\mathrm{aL}]) / (1 + D_0)\end{aligned} \tag{4.4}$$

Combining these equations, the net distribution ratio, D, is expressed as follows.

$$D = [\bar{\mathrm{a}}] / [\mathrm{a}]_\mathrm{aq} = D_0([\mathrm{a}]_\mathrm{f} - [\mathrm{aL}]) / ([\mathrm{a}]_\mathrm{f} + D_0[\mathrm{aL}]) \tag{4.5}$$

Since all the complexing agent is assumed to complex the rare–earth element, [aL] equals the feed concentration of the complexing agent, $[\mathrm{L}]_\mathrm{f}$. Thus, Eq. (4.5) is expressed as

$$D = D_0([\mathrm{a}]_\mathrm{f} / [\mathrm{L}]_\mathrm{f} - 1) / ([\mathrm{a}]_\mathrm{f} / [\mathrm{L}]_\mathrm{f} + D_0) \tag{4.6}$$

The values of D are calculated by using Eq. (4.6) and D_0 values determined in the systems without EDTA,[27,28] and are shown in Fig. 4.1 by solid lines, which show excellent agreement with the experimental data in both extraction systems. In the TOMAN–EDTA system, D is constant since D_0 is constant at pH 3 ~ 6.

In the LIX54–TOMAN–EDTA system, D increases with pH value since D_0 increases, and approaches respective limiting values.

4.3.2 Extraction equilibrium of plural rare–earth elements in TOMAN–EDTA and LIX54–TOMAN–EDTA systems

Extraction of Tb, Dy and Ho, and Y, Er, Tm, Yb and Lu were carried out using a mixed solution containing EDTA at a concentration about half the total metal concentration, and the results are shown in **Fig. 4.2** and **Fig. 4.3**. **Figures 4.4 and 4.5 (a) and (b)** show the effect of EDTA concentration on the distribution ratio and separation factor for the case of Tb–Dy–Ho and Y–Er–Tm–Yb–Lu in the TOMAN system. Although the extraction is decreased by addition of EDTA, separation factors are found to increase. This is because the order of extractability by TOMAN is Tb > Dy > Ho and Er > Tm > Y > Yb > Lu, and the order of magnitude of stability constants of EDTA complex are Tb < Dy < Ho and Y < Er < Tm < Yb < Lu.$^{56)}$ In the LIX54–TOMAN system without EDTA, heavier lanthanide is more extractable than lighter lanthanide in the high pH region.$^{28)}$ In the system containing EDTA, however, lighter lanthanide is extracted preferentially even at pH = 6, indicating that the extractability is governed by the difference in the stability constant of the rare earth–EDTA complex.

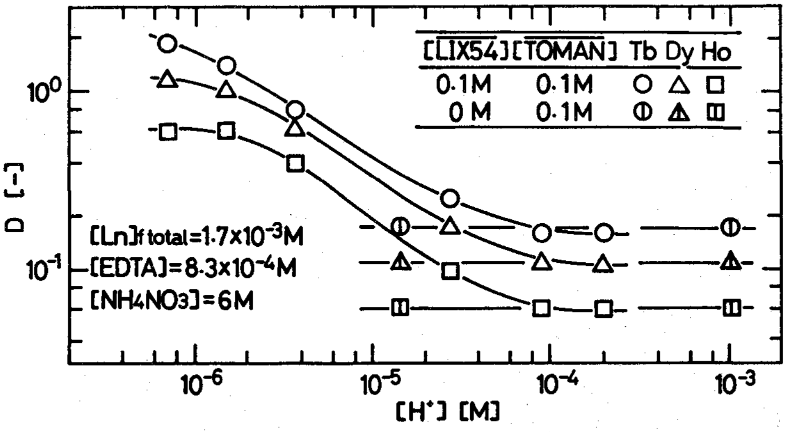

Fig. 4.2. Effect of proton concentration on distribution ratio of ternary rare–earth elements in TOMAN–EDTA and LIX54–TOMAN–EDTA systems; comparison of observed data with prediction shown by solid lines.

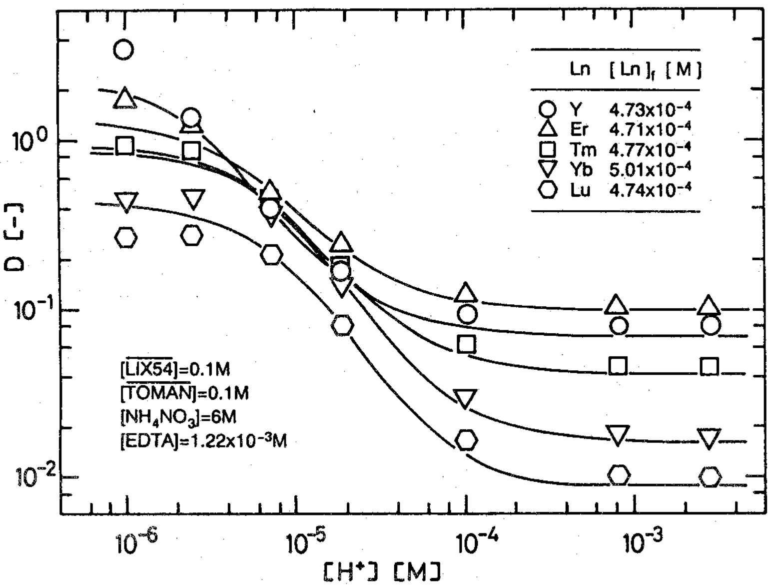

Fig. 4.3. Effect of proton concentration on distribution ratio of Y, Er, Tm, Yb and Lu in LIX54–TOMAN–EDTA system; comparison of observed data with prediction shown by solid lines.

The ratio of the stability constants between two rare–earth elements is calculated from the distribution data of rare–earth elements as follows. The constants K_a and K_b for the elements a and b, respectively, are defined by Eq. (4.7).

$$K_a = [aL] / [a][L], \quad K_b = [bL] / [b][L] \tag{4.7}$$

The ratio of the constants is

$$K_a / K_b = [aL][b] / [a][bL] \tag{4.8}$$

[a] and [b] are calculated by experimental values of $[\bar{a}]$ and $[\bar{b}]$, and the distribution ratios in the absence of EDTA, $D_{0,a}$ and $D_{0,b}$, by Eq. (4.9).

$$[a] = [\bar{a}] / D_{0,a}, \quad [b] = [\bar{b}] / D_{0,b} \tag{4.9}$$

As for [aL] and [bL],

$$[aL] = [a]_{aq} - [a], \quad [bL] = [b]_{aq} - [b] \tag{4.10}$$

Thus,

$$K_a / K_b = (D_{0,a}[a]_{aq} / [\bar{a}] - 1) / (D_{0,b}[b]_{aq} / [\bar{b}] - 1) \tag{4.11}$$

The ratios of stability constants thus calculated from the distribution data are shown in **Table 4.1.** These values almost agree with the literature data obtained by Wheelwright *et al.*[56)] in KNO_3 solution of ionic strength = 0.1 by the polarographic method.

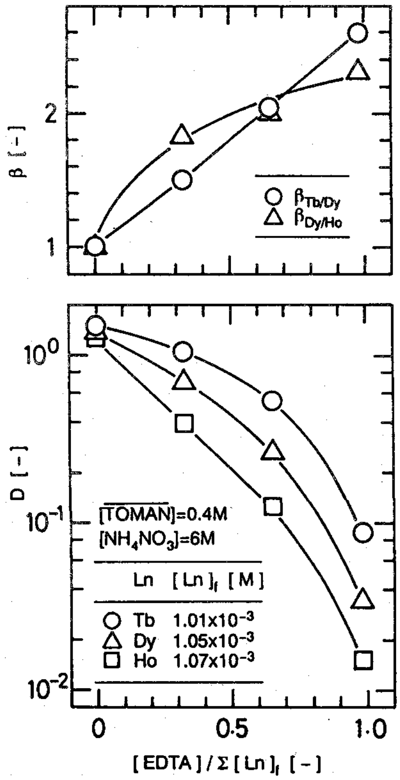

Fig. 4.4. Effect of EDTA concentration on distribution ratio and separation factor of Tb, Dy and Ho in TOMAN-EDTA system.

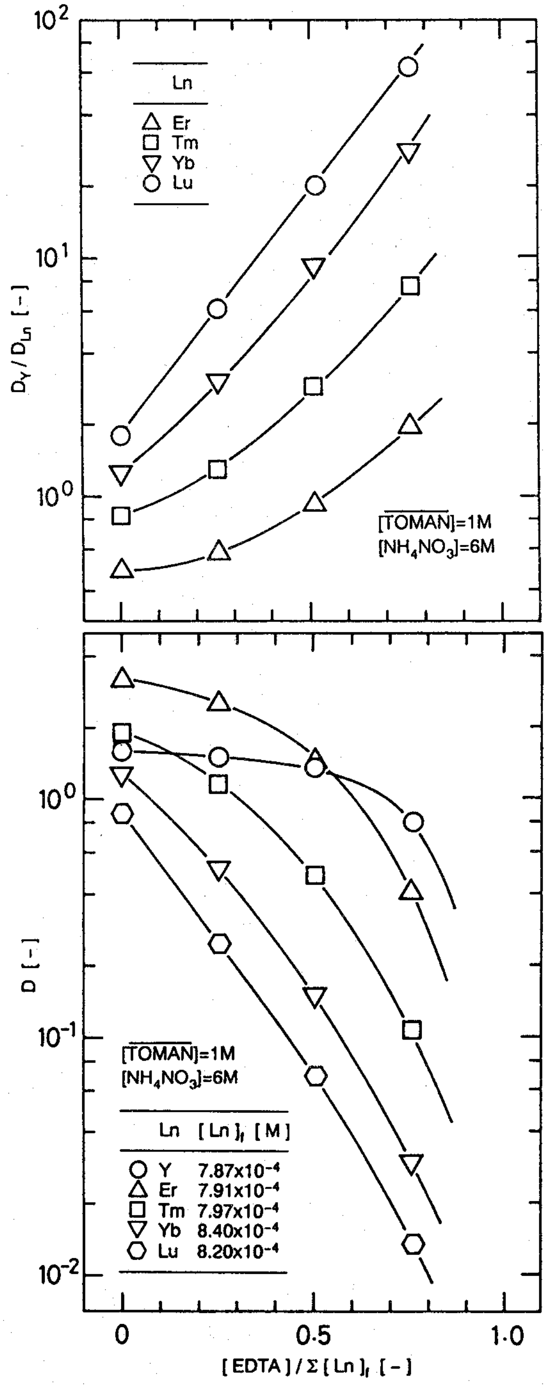

Fig. 4.5. Effect of EDTA concentration on (a) distribution ratio and (b) separation factor of Y, Er, Tm, Yb and Lu in TOMAN–EDTA system.

Table 4.1. Ratio of stability constant of rare–earth–EDTA complexes in 6 mol/*l* NH_4NO_3 system and determined by Wheelwright *et al.*[56] in KNO_3 system with polarographic method.

Ln1	Ln2	K_{Ln1} / K_{Ln2}	Wheelright *et al.*
Nd	Pr	1.62	1.58
Tb	Dy	0.40	0.43
Tb	Ho	0.18	0.12
Er	Lu	0.10	0.08
Tm	Lu	0.26	0.26
Yb	Lu	0.63	0.55
Y	Lu	0.017	0.008

In the ternary rare–earth elements (a, b and c) system, distribution ratios, D_a, D_b and D_c are predicted using the data of the ratio of stability constants as follows. The feed concentrations of the respective metals are expressed by Eqs. (4.12) ~ (4.14).

$$[a]_f = [a] + [aL] + [\bar{a}] = [a] + [aL] + D_{0,a}[a] \tag{4.12}$$

$$[b]_f = [b] + [bL] + D_{0,b}[b] \tag{4.13}$$

$$[c]_f = [c] + [cL] + D_{0,c}[c] \tag{4.14}$$

The ratios of stability constants are

$$K_a / K_c = [aL][c] / [a][cL] \tag{4.15}$$

$$K_b / K_c = [bL][c] / [b][cL] \tag{4.16}$$

Combining Eqs. (4.12) to (4.16) gives Eqs. (4.17) and (4.18).

$$[a]_f = (1 + D_{0,a} + K_a[cL] / K_c[c])[a] \tag{4.17}$$

$$[b]_f = (1 + D_{0,b} + K_b[cL] / K_c[c])[b] \tag{4.18}$$

When a temporary value of [cL] is given, [c] is calculated using Eq. (4.14); thus [a] and [b] are obtained by Eqs. (4.17) and (4.18) in order to calculate [aL] and [bL] using Eqs. (4.12) and (4.13). An appropriate [cL] is determined by trial–and–error to satisfy the material balance for EDTA shown by Eq. (4.19).

$$[\mathrm{L}]_{\mathrm{f}} = [\mathrm{aL}] + [\mathrm{bL}] + [\mathrm{cL}] \tag{4.19}$$

Thus, net distribution ratios for each elements are obtained using Eq. (4.20).

$$D_{\mathrm{i}} = D_{0,\mathrm{i}}[\mathrm{i}] \,/\, ([\mathrm{i}] + [\mathrm{iL}]) \quad (\mathrm{i} = \mathrm{a, b, c}) \tag{4.20}$$

The predicted values of D thus obtained are shown in Figs. 4.2 and 4.3 by solid lines, which show good agreement with the experimental values.

Table 4.2 and **Fig. 4.6** show the effect of addition of several chelating agents, DTPA, CyDTA and EDTA, on separation of rare–earths in TOMAN system. The separation is apparently enhanced in every tetrads.

4.3.3 Appropriate composition of extractant and pH condition for effective separation of rare–earth elements

The effect of extractant component on the distribution ratio is shown in **Fig. 4.7**. In the system of $[\overline{\text{TOMAN}}] = 0.6$ mol/l and $[\overline{\text{LIX54}}] = 0.05$ mol/l, separation is achieved efficiently at pH < 4. Since the order of extractability is Tb < Dy < Ho in the LIX54–TOMAN system in the high pH region, the effect of addition of EDTA is canceled to some extent. Thus, the TOMAN–EDTA system is more suitable for separation of these middle rare–earth elements. For a separation of heavier elements such as Y/Er separation, however, the extractability of TOMAN in the presence of EDTA is too small for effective separation, as shown in Fig. 4.5. A combination of TOMAN and LIX54 may be efficient for Y/Er separation, since the addition of LIX54 enhances the extractability of these elements.

Table 4.2. Separation factor in TOMAN / xylene for neighboring rare–earth elements. Effect of complexing agents on the separation factors. [$\overline{\text{TOMAN}}$] = 0.4 mol/*l*, [NH_4NO_3] = 6 mol/*l*.

Agent	[Agent]/Σ[Ln]$_f$		β^0	β
DTPA	0.52	Pr / Nd	1.95	5.01
CyDTA	0.49	Sm / Eu	1.46	1.57
		Eu / Gd	1.65	1.74
EDTA	0.55	Tb / Dy	1.05	1.84
		Dy / Ho	1.15	2.09
EDTA	0.51	Er / Tm	1.62	2.62
		Tm / Yb	1.42	2.77
		Yb / Lu	1.38	2.14
		Tm / Y	1.23	0.487

β^0 : separation factor in the absence of complexing agent
β : separation factor in the presence of complexing agent
DTPA : diethylenetriaminepentaacetic acid
CyDTA : trans–1,2–cyclohexanediaminetetraacetic acid
EDTA : ethylenediaminetetraacetic acid

The rate of extraction is assumed to be influenced by the metal exchange reaction of rare earth–EDTA complex in the aqueous phase as well as transfer of metal ion between the aqueous and organic phases. Exchange between Pr in aqueous phase and Nd in organic phase in the TOMAN–EDTA system was studied experimentally and the results are shown in **Table 4.3**. In TOMAN only system, an equilibrium is achieved immediately; 99% of Pr was extracted and 90% of Nd moved into the aqueous phase by only two strokes. In TOMAN–EDTA system, however, the reaction rate was found to be influenced by aqueous solution pH. At pH 2.8 the exchange reaction is fairly fast, while it is slow at pH 5.9. These results are likely to be caused by slow exchange reaction between Pr–EDTA complex and Nd in the high pH region, as in the case using DTPA.[9,32,33] Non–equilibrium operation was found not to be effective for

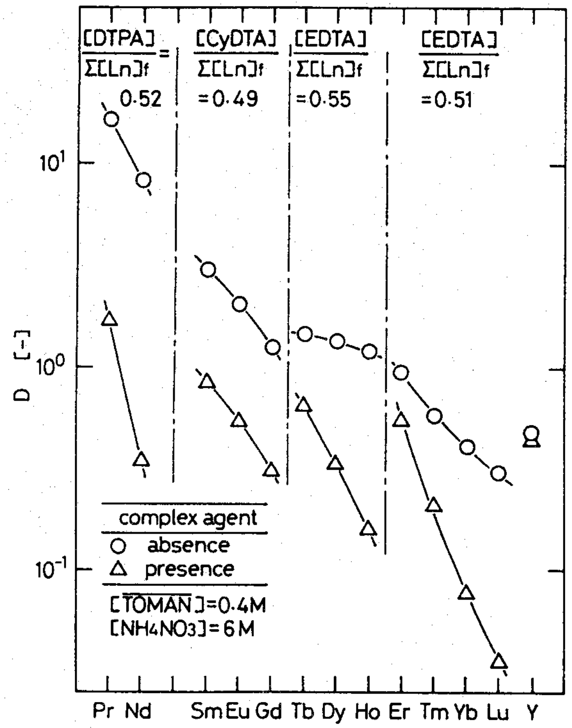

Fig. 4.6. Variation of the distribution ratio with atomic number of rare-earth elements. Effect of complexing agents on the distribution ratios.

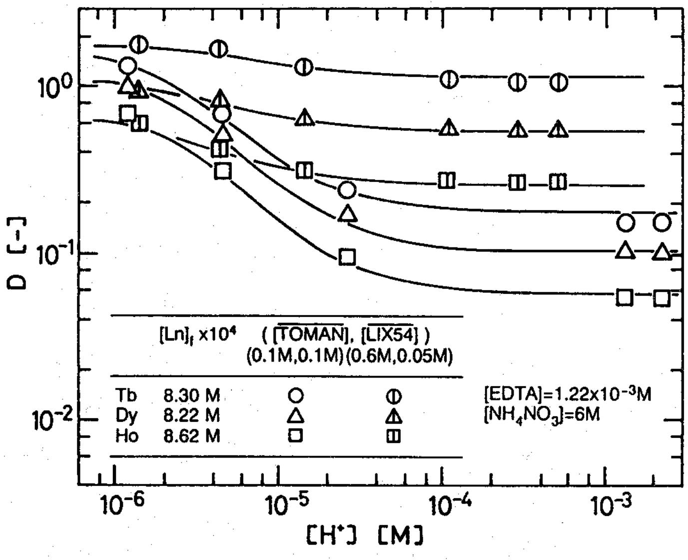

Fig. 4.7. Effect of proton concentration on distribution ratio in LIX54–TOMAN–EDTA system with different extractant concentrations.

Table 4.3. Exchange reaction between Pr in aqueous phase and Nd in organic phase in (a) TOMAN and (b) TOMAN–EDTA systems. $[\overline{\mathrm{TOMAN}}] = 0.4$ mol/l, $[\mathrm{NH_4NO_3}] = 6$ mol/l, $[\overline{\mathrm{Nd}}]_f = [\mathrm{Pr}]_f = 2.3 \times 10^{-3}$ mol/l and $[\mathrm{EDTA}] = 2.3 \times 10^{-3}$ mol/l.

(a) absence of EDTA

	2 strokes		5 strokes		equilibrium	
	Pr	Nd	Pr	Nd	Pr	Nd
$[\mathrm{Ln}]_{aq} \times 10^4$[mol/$l$]	1.71	2.35	1.33	2.44	1.45	2.61
$[\overline{\mathrm{Ln}}] \times 10^4$ [mol/l]	20.9	20.7	21.4	20.7	21.2	20.5
$[\overline{\mathrm{Pr}}] / [\overline{\mathrm{Pr}}]_{eq}$ [–]	0.99	–	1.01	–	1	–
$[\mathrm{Nd}] / [\overline{\mathrm{Nd}}]_{eq}$ [–]	–	0.90	–	0.94	–	1
pH	4.47		4.44		4.46	

(b) presence of EDTA

$[\mathrm{Ln}]_{aq} \times 10^4$[mol/$l$]	12.2	10.9	8.79	13.8	8.36	14.6
$[\overline{\mathrm{Ln}}] \times 10^4$ [mol/l]	11.8	12.3	14.2	9.49	14.6	8.82
$[\overline{\mathrm{Pr}}] / [\overline{\mathrm{Pr}}]_{eq}$ [–]	0.81	–	0.97	–	1	–
$[\mathrm{Nd}] / [\overline{\mathrm{Nd}}]_{eq}$ [–]	–	0.77	–	0.95	–	1
pH	2.76		2.78		2.80	

$[\mathrm{Ln}]_{aq} \times 10^4$[mol/$l$]	21.4	3.22	21.7	3.34	9.18	15.2
$[\overline{\mathrm{Ln}}] \times 10^4$ [mol/l]	1.37	19.9	1.44	19.8	14.0	8.19
$[\overline{\mathrm{Pr}}] / [\overline{\mathrm{Pr}}]_{eq}$ [–]	0.10	–	0.11	–	1	–
$[\mathrm{Nd}] / [\overline{\mathrm{Nd}}]_{eq}$ [–]	–	0.21	–	0.22	–	1
pH	5.90		5.89		5.88	

separation in the range pH 2 ~ 6.[35] On the other hand, the complexing ability of EDTA was found to decrease with decreasing pH. Consequently, the suitable pH for equilibrium separation process using TOMAN and EDTA is about 3.

4.3.4 Recovery of rare–earth element from aqueous phase containing EDTA

Rare earth–EDTA complex formed is inactive for extraction by TOMAN or LIX54–TOMAN. Thus, a method of recovering the elements from the raffinate must be devised. Since the stability constant of rare–earth element–EDTA complex decreases with decrease of pH of the solution, it is feasible to dissociate the complex into rare–earth ion and EDTA in the acidic region. Thus, TBP was used as a feasible extractant that is active in the acidic region. As shown in **Fig. 4.8**, the distribution ratio of Dy from the solution containing EDTA increases with decreasing pH, and approaches the value obtained in the absence of EDTA at pH < 1. This indicates that rare earth can be extracted into the organic phase by TBP at pH < 1, leaving EDTA in the aqueous phase. In this pH region, EDTA tends to precipitate as the protonated form, but it was found that the extraction could be achieved before precipitation occurred.

4.4 Simulation

Based on the results of the equilibrium studies, simulation of separation by the countercurrent cascade shown in **Fig. 4.9** was carried out to examine the effect of complexing agent in mixer–settler batteries for extraction and scrubbing. The separation of Pr and Nd was employed as a model system, since this

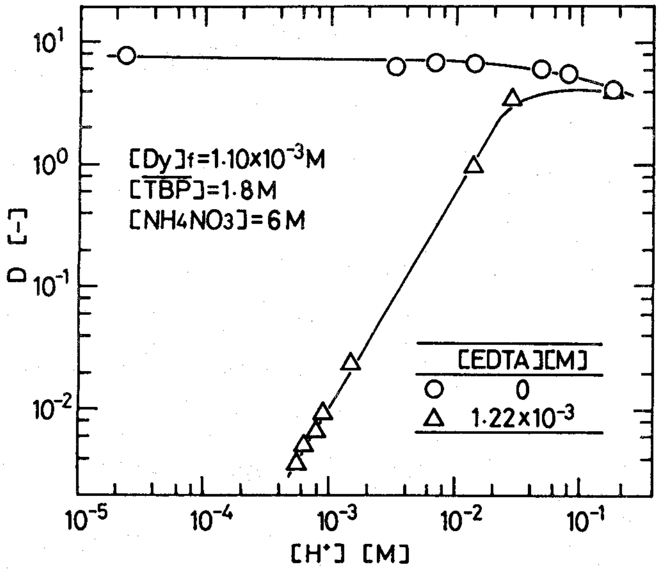

Fig. 4.8. Extraction of Dy by TBP from aqueous solution in the presence and absence of complexing agent.

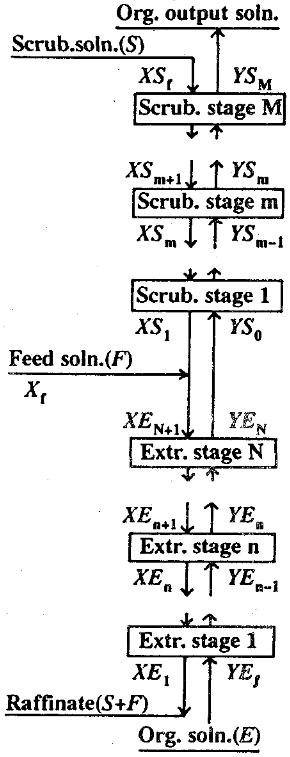

Fig. 4.9. Flow chart of cunter–current cascade.

combination was known to be rather difficult by the conventional process. The TOMAN and TOMAN–EDTA systems are applicable, since the addition of LIX54 is less effective in enhancing the extractability of these lighter rare–earth elements.[28)] The ratio value of the stability constants, $K_{\mathrm{Nd}} / K_{\mathrm{Pr}}$, of 1.62 was used in the present simulation.

1) TOMAN system In the scrubbing stage, metal concentrations in the aqueous and organic phases leaving a stage m are related by the equilibrium relation:

$$XS_{\mathrm{m}} = YS_{\mathrm{m}} / D_{0,\mathrm{m}} \tag{4.21}$$

where $D_{0,\mathrm{m}}$ is the distribution ratio of the element in stage m, which can be calculated using extraction equilibrium formulations in the TOMAN system shown in section 1.3.3. The material balance on the element in the portion of the scrubbing cascade from stage M to stage m is

$$E \cdot YS_{m-1} + S \cdot XS_f = E \cdot YS_M + S \cdot XS_m \tag{4.22}$$

where E and S are flow rates of the organic and scrubbing solutions, respectively. When the metal concentration in the feed scrubbing solution $XS_f = 0$, Eq. (4.22) is simplified to Eq. (4.23).

$$YS_{m-1} = (S / E)XS_m + YS_M \tag{4.23}$$

Thus, when a temporary value of YS_M is given, XS_m (m = M ~ 1) is calculated using Eq. (4.21), and then YS_{m-1} is obtained using Eq. (4.23) to give YS_0. The input aqueous metal concentration in the extraction cascade, XE_{N+1}, is then shown as

$$XE_{N+1} = (F \cdot X_f + S \cdot XS_1) / (F + S) \tag{4.24}$$

where F and X_f are the flow rate and metal concentration of the aqueous feed solution, respectively.

In the extracting cascade, the extraction equilibrium and material balance from stage 1 to stage n are expressed by Eqs. (4.25) and (4.26), respectively.

$$YE_n = D_{0,n} \cdot XE_n \quad (n = 1 \sim N) \tag{4.25}$$

$$E \cdot YE_f + (S + F)XE_{n+1} = E \cdot YE_n + (S + F)XE_1 \tag{4.26}$$

When a temporary value of XE_1 is given and $YE_f = 0$, YE_n (n = 1 ~ N) is calculated using Eqs. (4.25) and (4.26). These calculations are carried out iteratively until YE_N becomes identical with YS_0. The results obtained for the case $F : E : S$

$= 1 : 1 : 1$, $N = 10$ and $M = 5$ are shown in **Fig. 4.10**. The overall fractional recovery for Nd and Pr, ρ_{Nd} and ρ_{Pr}, are 15.7% and 49.8% respectively and the overall decontamination factor f ($= \rho_{Pr} / \rho_{Nd}$), is 3.17.

2) TOMAN–EDTA system The extraction equilibrium is expressed as follows when EDTA is added to the feed scrubbing solution. In the scrubbing cascade, concentrations of free (uncomplexed) Nd and Pr in the aqueous phase, [Nd] and [Pr], are

$$[\mathrm{Nd}] = [\overline{\mathrm{Nd}}] / D_{0,\mathrm{Nd}}, \quad [\mathrm{Pr}] = [\overline{\mathrm{Pr}}] / D_{0,\mathrm{Pr}} \tag{4.27}$$

When a temporary value of the concentration of Pr–EDTA complex, [PrL], is given, [NdL] is calculated as follows.

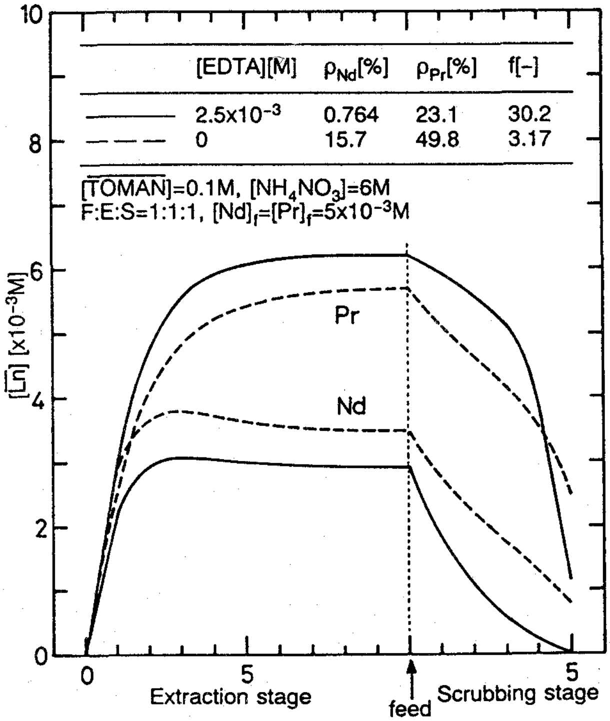

Fig. 4.10. Simulation of Nd / Pr separation in TOMAN and TOMAN–EDTA systems by countercurrent batteries of 10 extraction stages and 5 scrubbing stages in the case of $F : E : S = 1 : 1 : 1$.

$$[\mathrm{NdL}] = (K_{\mathrm{Nd}} / K_{\mathrm{Pr}})[\mathrm{Nd}][\mathrm{PrL}] / [\mathrm{Pr}] \tag{4.28}$$

The appropriate [PrL] value is determined by trial–and–error to satisfy the material balance of EDTA expressed by Eq. (4.29).

$$[\mathrm{L}]_{\mathrm{f}} = [\mathrm{NdL}] + [\mathrm{PrL}] \tag{4.29}$$

where $[\mathrm{L}]_{\mathrm{f}}$ is the concentration of EDTA in the feed scrubbing solution. The material balance of rare–earth element expressed by Eq. (4.22) is also applicable to this system, as $XS_{\mathrm{Nd}} = [\mathrm{Nd}] + [\mathrm{NdL}]$, $XS_{\mathrm{Pr}} = [\mathrm{Pr}] + [\mathrm{PrL}]$.

In the extraction cascade, XE_{Nd} and XE_{Pr} are obtained using Eq. (4.26). Thus when a temporary value of [PrL] is given, [Pr] and [Nd] are

$$[\mathrm{Pr}] = XE_{\mathrm{Pr}} - [\mathrm{PrL}] \tag{4.30}$$

$$[\mathrm{Nd}] = XE_{\mathrm{Pr}} / (1 + K_{\mathrm{Nd}}[\mathrm{PrL}] / K_{\mathrm{Pr}}[\mathrm{Pr}]) \tag{4.31}$$

The appropriate [PrL] is obtained by trial–and–error to satisfy Eq. (4.32).

$$S\cdot[\mathrm{L}]_{\mathrm{f}} / (S + F) = [\mathrm{NdL}] + [\mathrm{PrL}] = XE_{\mathrm{Nd}} - [\mathrm{Nd}] + [\mathrm{PrL}] \tag{4.32}$$

Thus, the organic metal concentrations are

$$YE_{\mathrm{Nd}} = D_{0,\mathrm{Nd}}[\mathrm{Nd}], \quad YE_{\mathrm{Pr}} = D_{0,\mathrm{Pr}}[\mathrm{Pr}] \tag{4.33}$$

As for the material balance, Eq. (4.26) is also applicable. By use of these equations, metal concentrations in each stage are calculated as in the case of the TOMAN system and are shown in Fig. 4.9. Although ρ_{Pr} is reduced to 23.1% by addition of EDTA, ρ_{Nd} is further reduced to 0.764%; thus f increases to 30.2. On the other hand, the ratio of output metal concentration in the aqueous phase is reduced from 3.18 to 1.29 by addition of EDTA. The addition of EDTA to the

TOMAN system is effective in enhancing the purity of Pr.

The effect of flow rate ratio and EDTA concentration on ρ_{Pr} and f was studied and the results are shown in **Table 4.4.** Good separation and high Pr yield are achieved when the flow rate of scrubbing solution is relatively small. In some cases such as $F : E : S = 5 : 5 : 1$ and the amount of EDTA added is 70% of the feed elements, an unfamiliar $[\overline{Pr}]$ feature is seen in the scrubbing stage, as shown in **Fig. 4.11.** The organic Pr concentration is greater than the feed concentration (YS_0) in stages 1 ~ 4, which shows that Pr extraction occurs

Table 4.4. Effect of flow rate ratio, $F : E : S$ and EDTA concentration on overall fractional recovery of Nd and Pr, ρ_{Nd} and ρ_{Pr}, and on overall decontamination factor, f, in simulation of Nd / Pr separation by counter-current batteries of 10 extraction stages and 5 scrubbing stages. $[\overline{TOMAN}] = 0.1$ mol/l, $[NH_4NO_3] = 6$ mol/l and $[Nd]_f = [Pr]_f = 5 \times 10^{-3}$ mol/l.

run	$F:E:S$	$[EDTA]_f$ [mol/l]	ρ_{Nd} [%]	ρ_{Pr} [%]	f [–]
1	1 : 1 : 1	0	15.7	49.8	3.17
2	1 : 1 : 1	1.0×10^{-3}	7.00	41.5	5.93
3	1 : 1 : 1	2.5×10^{-3}	0.764	23.1	30.2
4	1 : 1 : 1	3.0×10^{-3}	0.278	15.2	54.7
5	2 : 2 : 1	0	36.9	76.8	2.08
6	2 : 2 : 1	8.0×10^{-3}	1.49	39.8	26.7
7	2 : 2 : 1	1.0×10^{-2}	0.319	23.6	74.0
8	3 : 3 : 1	0	50.7	88.1	1.74
9	3 : 3 : 1	1.5×10^{-2}	1.36	44.1	32.4
10	3 : 3 : 1	1.8×10^{-2}	0.323	27.8	86.1
11	3 : 3 : 1	2.0×10^{-2}	0.106	15.9	150
12	4 : 4 : 1	0	60.0	93.4	1.56
13	4 : 4 : 1	2.0×10^{-2}	2.91	55.2	19.0
14	4 : 4 : 1	2.5×10^{-2}	0.510	35.6	69.8
15	4 : 4 : 1	3.0×10^{-2}	0.0689	13.4	195
16	5 : 5 : 1	0	66.5	95.9	1.44
17	5 : 5 : 1	2.5×10^{-2}	4.60	61.6	13.4
18	5 : 5 : 1	3.0×10^{-2}	1.17	47.4	40.5
19	5 : 5 : 1	3.5×10^{-2}	0.296	30.5	103
20	5 : 5 : 1	4.0×10^{-2}	0.0550	12.3	224

in these stages, together with the scrubbing of Nd. This is caused by the high concentration of free Pr in the scrubbing solution in these stages, which moved from the organic phase in the 5th stage. In these cases, effective separation is chieved; the f value is more than 100.

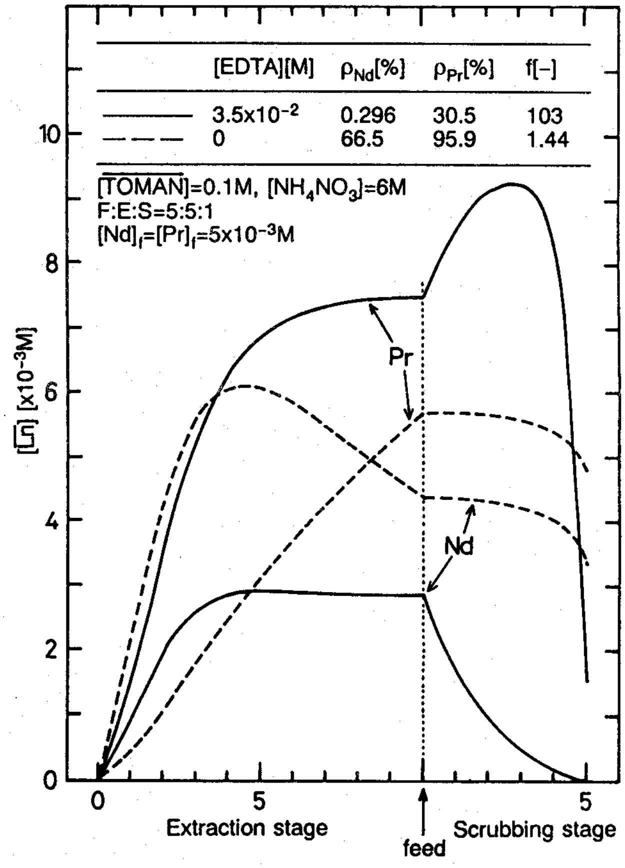

Fig. 4.11. Simulation of Nd / Pr separation by countercurrent batteries in the case of $F:E:S=5:5:1$.

4.5 Summary

The extraction and separation of rare–earth elements by tri–*n*–octylmethylammonium nitrate (TOMAN) and a β–diketone (α–acetyl–*m*–dodecylacetophenone : LIX54) in the presence of a water–soluble complexing agent such as ethylenediaminetetraacetic acid (EDTA) were studied, with the following results.

(1) All EDTA in the aqueous phase make 1 : 1 complex with rare earth, and only free rare–earth ions (not complexed with EDTA) can take part in the extraction.

(2) The effect of EDTA on the separation factor of the elements is predicted using the distribution ratio of each element in the absence of EDTA, stability constants of EDTA–element complexes and the feed concentrations of the species.

(3) Separation and recovery of rare–earth element from aqueous raffinate solution is feasible by use of tri–*n*–butylphosphate (TBP) as an extractant in acidic condition.

(4) In mixer–settler batteries of 10 stages of extraction followed by 5 stages of scrubbing, the output concentration ratio is calculated to be greater than 100 by addition of 70% as much EDTA as the feed elements.

General Conclusions

This thesis deals with the separation and purification of rare metals by combination of solvent extraction and chemical reactions. As the chemical reactions, (1) reduction of the target metal ions by adding reducing agent, by electroreduction or photoreduction, (2) modification of the metal ions by adding water–soluble complexing agent, and (3) modification of the organic–phase species by adding the second extractant have been used.

In chapter 1, the extraction mechanism of rare metals without chemical reactions has been studied as the basic studies, for the extraction systems used in the following chapters. The extraction mechanism of hydrochloric acid, cobalt and vanadium(V) by tri–*n*–octylmethylammonium chloride (TOMAC) from the acid solution was investigated. The simple extraction model was presented, assuming that TOMAC was tetramerized in benzene and dimerized in chloroform, and only the monomeric species of TOMAC could take part in the extraction of the acid and metals. The extraction was assumed to occur via replacement of water in the salt hydration sphere by hydrochloric acid, cobalt chloride or vanadyl chloride. The present extraction schemes could express the extraction of the acid and metals over a wide range of loading of the extractant in both diluent systems. The extraction of rare–earth elements by tri–*n*–octylmethylammonium nitrate (TOMAN) and ammonium nitrate as a salting–out agent was also described. The extraction schemes of the elements was described which expressed the extraction behavior for the whole range of the loadings of the extractant.

In chapter 2, it was shown that the chemical, electrochemical and photochemical reduction of the target metal enabled the selective stripping in the solvent extraction process. As the case studies, the separation of vanadium and molybdenum, and the separation of europium from samarium and gadolinium have been investigated. The pentavalent vanadyl anion was found to be extracted preferentially than hexavalent molybdate anion by TOMAC. It was shown that the extracted vanadyl anion in the organic phase was reduced to the form of tetra– and trivalent cations by contact with an aqueous solution containing L–ascorbic acid or by electroreduction using a platinum electrode, which enabled V to be stripped selectively with the Mo remaining in the organic phase. The separation efficiencies of 1.64 x 10^4 and 400 were obtained by the chemical–reductive stripping and by the electro–reductive stripping, respectively, for an aqueous solution containing initially equal concentrations of the two metals by single extraction followed by single selective stripping. In the case of Eu, Eu^{3+} was found to be reduced to Eu^{2+} by electrochemical or photochemical reduction method in $(NH_4)_2SO_4$ aqueous solution to make $EuSO_4$ precipitate selectively. In the two–phase systems consisted of di–5–methyl–2–(1–methylneohexyl) neodecanoyl phosphoric acid (DP–18)/xylene or bis(2–ethylhexyl)phosphoric acid (D2EHPA)/xylene containing Sm, Eu and Gd and $(NH_4)_2SO_4$ aqueous solutions, $EuSO_4$ precipitated selectively in the aqueous phase by electro– or photoreduction. The purity of Eu in the precipitate was more than 95% in both cases.

In chapter 3, it was shown that the extractability of the rare–earth elements increased with the atomic number series in the DP–18 system. In the DP–18–TOMAN system, enhancement of the extractability by synergistic effect was observed, and the degree of the enhancement was favored for middle rare–earth element such as Tb. A synergistic extraction scheme for the elements presented accurately expressed the extraction behaviors. The mechanism of synergistic extraction of the elements by combination of TOMAN and β–diketone, α–acetyl–*m*–dodecylacetophenone (LIX54) was also described.

In chapter 4, it was shown that the addition of a water–soluble complexing agent such as ethylenediaminetetraacetic acid (EDTA) enhanced the separation of the rare–earth elements in TOMAN and LIX54–TOMAN systems. The distribution ratio and separation factor of the elements could be predicted by the simple model that all EDTA in the aqueous phase made 1 : 1 complex with rare–earth ions and only free ions (not complexed) could take part in the extraction.

The simulation of Nd/Pr separation by continuous countercurrent batteries showed that Pr was highly purified by addition of EDTA in the aqueous phase.

Suggestions for Future Work

To extend the findings obtained in this work, the following studies are recommended.

(1) The target rare metals in this study were cobalt, vanadium, molybdenum and rare–earth elements. The study on the separation should be expanded to the other sets of rare metals, e.g. actinides.

(2) The use of the other chemical reaction may enhance the efficiency and selectivity of the separation. Oxidation of rare metals in the solvent extraction system may be effective for separation, since the extractability of the metal is increased by oxidation. For example, Ce^{4+} is extracted preferentially by tri–*n*–butylphosphate than Ce^{3+} or the other trivalent lanthanide ions. In the case of photochemical reaction, the use of laser as a light source may enhance the reaction rate and selectivity. The combination of the chemical reactions in the solvent extraction process should also be studied.

(3) To apply the present separation processes to the practical or industrial operation, the process should be examined from the standpoint of the kinetic behaviors.

Nomenclature

a, b, c = rare–earth element

a_H = mean ionic activity of hydrochloric acid [mol/l]

$a_{NO_3^-}$ = mean ionic activity of ammonium nitrate [mol/l]

a_W = activity of water in hydrochloric acid [mol/l]

C_N = feed concentration of TOMAC [mol/l]

D = distribution ratio of the metal [–]

D_0 = distribution ratio of rare–earth element in the absence of complexing agent [–]

E = potential of cathode vs. anode [V]

E = extraction percentage (in chapter 2) [%]

E = flow rate of organic phase (in chapter 4) [l/min]

f = overall decontamination factor [–]

F = flow rate of aqueous phase [l/min]

K = stability constant of rare–earth element–complexing agent complex [l/mol]

K_A = extraction equilibrium constant for hydrochloric acid

K_D = dimerization constant of TOMAC in chloroform [$(\text{mol}/l)^{-1}$]

K_T = tetramerization constant of TOMAN in xylene [$(\text{mol}/l)^{-3}$]

K_{ex} = extraction equilibrium constant for the metal

$K_{ex,1}$, $K_{ex,2}$ = extraction equilibrium constants for rare–earth element in DP–18 alone system

K_{105} , K_{205} = extraction equilibrium constants for rare–earth element in TOMAN alone system

K_{115}, K_{124}, K_{215}, K_{224}, K_{112} , K_{122} = extraction equilibrium constants for rare–earth element by synergistic adduct formation

K_S = extraction equilibrium constant of ammonium nitrate by TOMAN [$(\text{mol}/l)^{-5}$]

L = EDTA

Ln = rare–earth element
M = number of scrubbing stage
N = number of extraction stage
R = monomer of TOMAC (in chapter 1)
R = anion of LIX54 or DP–18 extractant (in chapter 3)
RH = LIX54 or DP–18 extractant
S = monomer of TOMAN
S_4 = tetramer of TOMAN
S = flow rate of scrubbing solution [l/min]
XE, XS = concentrations of rare–earth element in aqueous solution in the extraction and scrubbing stages respectively [mol/l]
YE, YS = concentrations of rare–earth element in organic solution in the extraction and scrubbing stages respectively [mol/l]
β = separation factor [–]
$\Delta[\mathrm{Cl}^-]$ = amount of chloride ion moved from organic phase to aqueous phase in the course of extraction [mol/l]
ρ = overall fractional recovery ($= E \cdot YS_M / F \cdot X_f$) [–]
[ ] = concentration of species in the brackets [mol/l]

<Subscripts>
aq = aqueous phase
eq = equilibrium value
f = feed or initial value
p = precipitate
S = extraction by synergistic adduct formation
0 = extraction by TOMAN alone
1 = extraction by DP–18 alone

<Superscript>
– = organic–phase species

Literature Cited

1) Aveston, J., E. W. Anacker and J. S. Johnson : *Inorg. Chem.*, **3**, 735 (1964).
2) Bard, A. J., R. Parsons and J. Jordan : "Standard Potentials in Aqueous Solutions", p. 462 and p. 516, Marcel Dekker, New York (1985).
3) Baumgartner, F. : *Chem. Ing. Tech.*, **49**, 795 (1977).
4) Baumgartner, F. and H. Schmieder : *Radiochim. Acta*, **25**, 191 (1978).
5) Bell, J. T. and L. M. Toth : *Radiochim. Acta*, **25**, 225 (1978).
6) Bell, J. T., L. M. Toth and H. A. Friedman : *ACS Symp. Ser.*, **216**, 263 (1983).
7) Benedict, M., T. H. Pigford and H. W. Levi : "Nuclear Chemical Engineering", p.157, McGraw–Hill, New York (1981).
8) Biswas, R. K., M. Wakihara and M. Taniguchi : *Hydrometallurgy*, **14**, 219 (1985).
9) Brucher, E. and G. Laurenczy : *J. Inorg. Nucl. Chem.*, **43**, 2097 (1981).
10) Daud, H. and R. W. Cattrall : *Aust. J. Chem.*, **35**, 1087 (1982).
11) Depoorter, G. L. and C. K. Rofer–Depoorter : *ACS Symp. Ser.*, **117**, 267 (1980).
12) Donohue, T. : *J. Chem. Phys.*, **67**, 5402 (1977).
13) Donohue, T. : *Opt. Eng.*, **18**, 181 (1979).
14) Enokida, Y. and A. Suzuki : *J. Nucl. Sci. Technol.*, **26**, 770 (1989).
15) Enokida, Y. and A. Suzuki : *Nucl. Technol.*, **88**, 47 (1989).
16) Feess, H. and H. Wendt : *Ger. Chem. Eng.*, **5**, 156 (1982).
17) Goldstein, M., J. J. Barker and T. Gangwer : *Nucl. Eng. Int.*, **22**, 69 (1977).
18) Good, M. L. and F. F. Holland Jr : *J. Inorg. Nucl. Chem.*, **26**, 321 (1964) and references contained therein.
19) Hoh, Y.–C., T.–Y. Wei, Y.–Y. Wang and T.–M. Chim : *Hydrometallurgy*, **19**, 209 (1987).
20) Hurst, F. J. and D. J. Crouse : *Hydrometallurgy*, **13**, 15 (1984).
21) Ishida, A. and S. Takamuku : *Chem. Lett.*, 1497 (1988).

22) Jeriazkowa, B. G., S. Nakamura and H. Fukutomi : *Bull. Chem. Soc. Japan*, **48**, 347 (1975).

23) Komasawa, I., N. Kurokawa, Y. Maekawa and T. Otake : *J. Chem. Eng. Japan*, **19**, 592 (1986).

24) Komasawa, I., Y. Maekawa and T. Otake : *J. Chem. Eng. Japan*, **20**, 41 (1987).

25) Komasawa, I. and T. Otake : *J. Chem. Eng. Japan*, **20**, 46 (1987).

26) Komasawa, I., H. Hosoba, N. Kurokawa and T. Otake : *J. Chem. Eng. Japan*, **20**, 176 and 183 (1987).

27) Komasawa, I., K. Hisada and M. Miyamura : *J. Chem. Eng. Japan*, **23**, 308 (1990).

28) Komasawa, I. and M. Miyamura : *J. Chem. Eng. Japan*, **24**, 306 (1991).

29) Kondo, K., K. Momota and F. Nakashio : *Solv. Extr. Ion Exch.*, **7**, 1027 (1989).

30) Lo, T. C., M. H. I. Baird and C. Hanson : "Handbook of Solvent Extraction", John Wiley & Sons, New York (1983).

31) Marcus, Y. and A. S. Kertes : "Solvent Extraction and Ion Exchange of Metal Complexes", p. 922 and p. 924, Wiley-Interscience, New York (1969).

32) Matsuyama, H., T. Okamoto, Y. Miyake and M. Teramoto : *J. Chem. Eng. Japan*, **22**, 627 (1989).

33) Minagawa, I., K. Kojima, T. Kaneko, Y. Yamaguchi and T. Miwa : Proceedings of Oslo Symposium '82, IV-1(1982).

34) Miyake, Y., T. Okamoto, K. Ichikawa and M. Teramoto : Proc. Symp. Solv. Extr. Japan, p.179 (1987).

35) Miyamura, M. : MSc thesis, Osaka Univ. (1990).

36) Peppard, D. F., G. W. Mason, J. L. Maier and W. J. Driscoll : *J. Inorg. Nucl. Chem.*, **4**, 334 (1957).

37) Peppard, D. F., J. R. Farrars and G. W. Mason : *J. Inorg. Nucl. Chem.*, **4**, 371 (1957) and **7**, 231 (1958).

38) Peppard, D. F., E. P. Horwitz and G. W. Mason : *J. Inorg. Nucl. Chem.*, **24**, 429 (1962).

39) Qiu, L.–F., X.–H. Kang and T.–S. Wang : *Sep. Sci. Technol.*, **26**, 199 (1991).
40) Ritcey, G. M. and A. W. Ashbrook : "Solvent Extraction, Principles and Applications to Process Metallurgy", Part I", Elsevier, Amsterdam (1984).
41) Ritcey, G. M. and A. W. Ashbrook : "Solvent Extraction, Principles and Applications to Process Metallurgy", Part II, p. 386, Elsevier, Amsterdam (1979).
42) Rofer–Depoorter, C. K. and G. L. Depoorter : *J. Inorg. Nucl. Chem.*, **39**, 631 (1977).
43) Rossotti, F. J. C. and H. Rossotti : *Acta Chem. Scand.*, **10**, 957 (1956).
44) Rydberg, J. : *J. Inorg. Nucl. Chem.*, **5**, 79 (1957).
45) Sanuki, S., T. Izaki and H. Majima : *J. Japan Inst. Metals*, **47**, 832 and 838 (1983).
46) Sato, T. and H. Watanabe : *Anal. Chim. Acta*, **49**, 463 (1970).
47) Sato, T., S. Ikoma and T. Nakamura : *J. Inorg. Nucl. Chem.*, **39**, 395 (1977).
48) Sato, T., T. Shimomura, S. Murakami, T. Maeda and T. Nakamura : *Hydrometallurgy*, **12**, 245 (1984) and references contained therein.
49) Sato, T., Y. Takeuchi and K. Sato : Proc. Symp. Solv. Extr. Japan, p.63 (1987).
50) Shibata, J., M. Sano, A. Okada and S. Nishimura : Proc. Symp. Solv. Extr. Japan, p.137 (1986).
51) Tedesco, P. H. and V. B. de Rumi : *J. Inorg. Nucl. Chem.*, **42**, 269 (1980).
52) Toth, L. M., J. T. Bell and H. A. Friedman : *ACS Symp. Ser.*, **117**, 253 (1980).
53) Tsujino, T., T. Aochi and T. Hoshino : *J. Nucl. Sci. Tech.*, **13**, 321 (1976).
54) Vieux, A. S., K. Bibombe and M. Nsele : *Hydrometallurgy*, **6**, 35 (1980).
55) Warf, J. C. : *J. Am. Chem. Soc.*, **71**, 3257 (1949).
56) Wheelwright, E. J., F. H. Spedding and G. Schwarzenbach : *J. Am. Chem. Soc.*, **75**, 4196 (1953).

List of Publications

Papers:

1. Separation and Purification of Vanadium and Molybdenum by Solvent Extraction Followed by Reductive Stripping
   T. Hirai and I. Komasawa, *J. Chem. Eng. Japan*, **23**, 208–213 (1990).

2. Mechanism of Extraction of Cobalt from Hydrochloric Acid by Tri-*n*-octylmethylammonium Chloride
   T. Hirai and I. Komasawa, *J. Chem. Eng. Japan*, **24**, 58–62 (1991).

3. Electro-reductive Stripping of Vanadium in Solvent Extraction Process for Separation of Vanadium and Molybdenum
   T. Hirai and I. Komasawa, *J. Chem. Eng. Japan*, **24**, 124–125 (1991).

4. Extraction of Vanadium(V) from Hydrochloric Acid by Tri-*n*-octylmethylammonium Chloride
   T. Hirai and I. Komasawa, *J. Chem. Eng. Japan*, **24**, 301–305 (1991).

5. Extraction and Separation of Rare-Earth Elements by Tri-*n*-octylmethylammonium Nitrate and β-Diketone Using Water-soluble Complexing Agent
   T. Hirai and I. Komasawa, *J. Chem. Eng. Japan*, **24**, 731–736 (1991).

6. Synergistic Extraction of Rare-Earth Elements by Alkyl Phosphoric Acid and Tri-*n*-octylmethylammonium Nitrate
   T. Hirai and I. Komasawa, *J. Chem. Eng. Japan*, **25**, 218–220 (1992).

7. Electro-reductive Stripping of Vanadium in Solvent Extraction Process for Separation of Vanadium and Molybdenum using Tri-*n*-octylmethylammonium Chloride
   T. Hirai and I. Komasawa, *Hydrometallurgy*, in press.

8. Separation of Europium from Samarium and Gadolinium by Combination of Electrochemical Reduction and Solvent Extraction Techniques
   T. Hirai and I. Komasawa, *J. Chem. Eng. Japan*, submitted.

9. Separation of Europium from Samarium and Gadolinium by Combination of Photochemical Reduction and Solvent Extraction Techniques
   T. Hirai, N. Onoe and I. Komasawa, *J. Chem. Eng. Japan*, submitted.

Proceedings:

1. Extraction and Separation of Vanadium and Molybdenum by Quaternary Ammonium Chloride
   T. Hirai and I. Komasawa, *Proc. Symp. Solv. Extr.*, 193–196 (1988).

2. Effect of Functional Chemical Reactions on Solvent Extraction Process for Separation and Purification of Rare–Metals
   T. Hirai and I. Komasawa, *Proc. Symp. Solv. Extr.*, 331–338 (1991).

3. Separation and Purification of Vanadium and Molybdenum by Solvent Extraction and Subsequent Reductive Stripping
   T. Hirai and I. Komasawa, *Solv. Extr. 1990, T. Sekine (Editor) (Proc. Int. Solv. Extr. '90)*, 1015–1020, Elsevier (1992).

Acknowledgment

The work of this dissertation was carried out under the guidance of Professor Isao Komasawa at Department of Chemical Engineering, Faculty of Engineering Science, Osaka University.

The author would like to express his grateful acknowledgment to Professor Dr. Isao Komasawa for his continuous guidance and encouragement throughout this work.

The author is also indebted to Professor Dr. Setsuji Tone, Professor Dr. Hiroshi Yoneyama and Professor Dr. Yoshihiro Nakato for their valuable comments and suggestions.

The author is so much obliged to Associate Professor Dr. Ryoichi Kuboi and Dr. Izumi Tsuboi in Osaka University for their helpful discussion and encouragement.

Thanks are given to the author's co-workers, Mr. Hodaka Norimatsu, Mr. Makoto Miyamura, Mr. Nobuyoshi Sasaki, Mr. Naohisa Onoe, and all the other members of Komasawa Laboratory for their collaboration.

Finally, the author wishes to thank his parents Taketsugu Hirai and Akiko Hirai for their continuous and hearty encouragement.